Universitat Politècnica de Catalunya

Ph.D in Environmental Engineering

Evaluating the impact of urban mobility policies on the air quality levels of Barcelona by means of an integrated modelling system

Author:
Daniel Rodriguez Rey

Advisors:
Dr. Marc Guevara Vilardell
Dr. Josep Casanovas Garcia

Barcelona, November 2021

UNIVERSITAT POLITÈCNICA DE CATALUNYA BARCELONATECH

Barcelona Supercomputing Center
Centro Nacional de Supercomputación

inLab FIB talent & tech

Acknowledgements

It is hard to acknowledge everybody involved in a project of more than four years. But before anything else, I want to thank my director Marc Guevara, for his constant guidance through this long work, his patience, effort and for sharing his knowledge. Sharing this responsibility with Marc, I want to thank to M$^{\underline{a}}$ Paz Linares from the inLab-FIB. For selflessly introducing me to the unknown and amazing world of traffic simulation, always finding a spot in an always full agenda, despite all professional and personal matters. Guiding the personal part of this thesis and connecting the BSC and the inLab-FIB I also want to thank to Josep Casanovas, who maintained up the project during its hardest moments.

Caring about the project networking, communication and giving a vision with more perspective I cannot forget Albert Soret, who I have to thank since the early beginning of this work, being the person who actually convinced me to get into this project. Then, providing both a casual and essential technical knowledge I want to thank Jaime Benavides and Jan Mateu Armengol, with who between urban dispersion models we could also share some beers and guitar concerts.

The quality of this work has been undoubtedly increased by the contribution and lead of Oriol Jorba and Carlos Pérez García-Pando, specially during the manuscripts development. I also want to thank Miriam Olid and Carles Tena from the BSC and Juan Salmerón from the inLab-FIB for their support and patience in the models run, development and adaptation to the project needs. They are just a part of the BSC Earth Sciences and inLab-FIB crew with who I really enjoyed working and made all this way lighter. Contributing to the special working atmosphere I have to thank to Paco Doblas and again Josep Casanovas as directors of the BSC Earth Sciences department and inLab-FIB, respectively.

I also want to acknowledge CARNET-The Future Mobility Research HUB to allow the usage and work on the BCN-VML network, as well as PTV-VISUM and AIMSUN for the traffic software licenses. I thankfully acknowledge the computer resources at MareNostrum and the technical support provided by the BSC.

Finally, I could not have done this project without the assistance and care of my parents, Mercedes and Jose Antonio and my siblings, Mauro and Elena, who patiently kept in asking when I will defend since a year ago. Also, helping me to disconnect from traffic and emissions I want to thank all my friends and the people who come and go. All collaborated in different ways, specially the design work of Isaac Claramunt who helped me with the main thesis cover.

You are all, in a way or another, part of this thesis.

Funding sources

This research has been funded by the grant BES-2016-078116 from the FPI program by the Spanish Ministry of Economy and Competitivenes as well as the VITALISE project (PID2019-108086RA-I00 / AEI / 10.13039/501100011033) from the Agencia Estatal de Investigacion (AEI).

Publications

International Journals Included in the Science Citation Index (SCI)

1. Rodriguez-Rey, D., Guevara, M., Linares, Mª P., Casanovas, J., Salmerón, J., Soret, A., Jorba, O., Tena, C., Pérez García-Pando, C., (2021). A coupled macroscopic traffic and pollutant emission modelling system for Barcelona. Transportation Research Part D: Transport and Environment. 92. 102725. doi: https://doi.org/10.1016/j.trd.2021.10272

2. Benavides, J., Guevara, M., Snyder, M. G., Rodriguez-Rey, D., Soret, A., Pérez García-Pando, C., Jorba, O., (2021). On the impact of excess diesel NOx emissions upon NO_2 pollution in a compact city. Environmental Research Letters. 2021. 16, 2. doi: https://doi.org/10.1088/1748-9326/abd5dd

3. Rodriguez-Rey, D., Guevara, M., Linares, Mª P., Casanovas, J., Armengol, J. M., Benavides, J., Soret, A., Jorba, O., Tena, C., Pérez García-Pando, C., (2022). To what extent the traffic restriction policies applied in Barcelona city can improve its air quality?. Science of The Total Environment, Volume 807, Part 2, 150743, ISSN 0048-9697,
doi: https://doi.org/10.1016/j.scitotenv.2021.150743.

Proceedings of International Congresses

1. Daniel Rodríguez Rey, Marc Guevara, Mari Paz Linares, Josep Casanovas, Jaime Benavides, Jan Mateu, Oriol Jorba, Albert Soret, Carlos Pérez García-Pando. A multi-scale approach to evaluate the impact of urban mobility policies in emission and air quality in Barcelona. 2021 POLIS Annual Conference: Innovation in transport for sustainable cities and regions, Gothenburg, Sweden, 1-2 December 2021.

2. Daniel Rodríguez Rey, Marc Guevara, Josep Casanovas Mª Paz Linares, J.M Armengol, J. Benavides, C. Pérez García-Pando, O. Jorba, A. Soret. Modelling the impact of urban traffic management strategies on emissions and

air quality levels in Barcelona (Spain). 38^{th} International Technical Meeting (ITM), Barcelona, Spain, 18-22 October 2021. (poster)

3. Daniel Rodríguez Rey, Marc Guevara, Josep Casanovas Mª Paz Linares, J.M Armengol, J. Benavides, C. Pérez García-Pando, O. Jorba, A. Soret. Modelling the impact of urban traffic management strategies on emissions and air quality levels in Barcelona (Spain). 16^{th} IGAC Scientific Conference, Online, 13-17 September 2021. Best poster award in MAP-AQ section.

4. Daniel Rodríguez Rey, Marc Guevara, Mari Paz Linares, Josep Casanovas, Jaime Benavides, Jan Mateu, Oriol Jorba, Albert Soret, Carlos Pérez García-Pando. A multi-scale approach to evaluate the impact of urban mobility policies in emission and air quality in Barcelona. 20^{th} International Conference on Harmonisation within Atmospheric Dispersion Modelling for Regulatory Purposes, Tartu, Estonia, 14-18 June 2021.

5. Jan Mateu Armengol, Daniel Rodríguez Rey, Marc Guevara, J. Benavides, O. Jorba, A. Soret, Carlos Pérez García-Pando. Advances on urban air quality modeling: bias correction approach for estimated annual NO_2 levels and macroscopic traffic simulators for scenario planning. EGU General Assembly 2021, Online, 19-30 April 2021.

6. Jaime Benavides, Michelle Snyder, Jan Mateu Armengol, Daniel Rodríguez Rey, O. Jorba, Marc Guevara, Carlos Pérez García-Pando, Albert Soret. Impact of excess diesel NO_x emisions upon NO_2 pollution in a compact city: the role of model resolution. EGU General Assembly 2021, Online, 19-30 April 2021.

7. Daniel Rodríguez Rey, Marc Guevara, Mari Paz Linares, Josep Casanovas, Jaime Benavides, Oriol Jorba, Albert Soret, Carlos Pérez García-Pando. An integrated system to evaluate the impact of urban mobility policies on air pollution in Barcelona. 23^{rd} Euro Working Group on Transportation EWGT 2020. Paphos, Ciprus, 16-18 September 2020.

8. Daniel Rodríguez Rey, Marc Guevara, Josep Casanovas, Mª Paz Linares, A. Soret, Juan Salmerón, Oriol Jorba. Coupling between traffic and emission models for the evaluation of mobility plans. FAIRMODE technical meeting. Madrid, Spain, 7-9 October 2019.

9. Daniel Rodríguez Rey, Marc Guevara, Josep Casanovas Mª Paz Linares, A. Soret. Evaluation of traffic emission models coupled with a microscopic traffic simulator and real driving measures. 11^{th} International Conference on Air Quality – Science and Application. Barcelona, Spain, 12-16 March 2018. (poster)

Summary

The excessive accumulation of air pollutants is a source of different environmental, economical and health-related issues. As a consequence, different intercontinental and European legislation regulate emissions and set atmospheric pollutant concentration limits that should not be over-passed. In urban areas, these limits are often overpassed due to their population density, their high traffic load and their urban build. Particularly, in the city of Barcelona (Spain) the two traffic air quality monitoring stations persistently exceed the NO_2 concentration limit value imposed by the European Union. Considering this, local policy makers are forced to develop air quality plans which often go hand in hand with the development of mobility policies or traffic management strategies (TMS) which aim to reduce the vehicle activity within the city and their emission levels. In order to quantify and evaluate the level of effectiveness of the applied air quality plans, air quality modelling is presented as a necessary tool to complement the information provided by the air quality monitoring stations. For the specific case of traffic management strategies evaluation (e.g., removal of urban vehicle space) the application of integrated traffic-emission-air quality models is crucial to first simulate the new vehicle routes generated as a consequence of the traffic restrictions, second to estimate the induced emissions from the previously generated traffic activity and third to compute the dispersion and chemical transformation of the estimated traffic emissions considering the urban meteorology and background pollutant levels.

In this sense, the present thesis evaluates the impact that the different TMS have on the resulting NO_x emissions and NO_2 concentration levels in Barcelona. To accomplish that, we developed an integrated air quality system composed by the traffic simulator BCN-VML, the emission model HERMESv3 and the street-scale dispersion model CALIOPE-Urban, which integrates the mesoscale CALIOPE air quality forecast system and the Gaussian dispersion model R-LINE. The BCN-VML was developed by the inLab-FIB laboratory within the framework of the Cooperative Automotive Re-search Network (CARNET) initiative while the HERMESv3 and CALIOPE-Urban are state-of-the-art modelling frameworks developed

by the Earth Science department of the Barcelona Supercomputing Center - Centro Nacional de Supercomputación (BSC-CNS). The collaboration between the BSC and the inLab-FIB allowed to combine the knowledge in traffic simulation and atmospheric modelling that gave fruit to the resulting integrated system used in this thesis.

The TMS studied are the current measures applied or planned to be applied by the Barcelona city hall, gathered from the last Urban Mobility Plan 2018-2024. These measures try to reduce and renew the number of circulating vehicles in the city by two lines of action: On the one hand, (i) they reduce urban vehicle space by removing vehicle lanes from major urban corridors by the so called Tactical Urban Planing and (ii) they implement traffic calming measures in particular areas of the city -Superblocks- and, on the other hand, they apply a Low Emission Zone to exclude the most polluting vehicles from the city.

In order to understand the fundamentals of the different traffic, emission and air quality models, this work initially presents an overview of their workflow and main characteristics. This is followed by a discussion of the appropriate level of detail needed to simulate a desired working domain according to the project goal, data and computational resources available. Also, different state-of-the-art traffic and emission models are presented, with a deeper description of the tools selected for this work according to the characteristics discussed.

In the first work of the thesis, we explain the traffic-emission models coupling process and the calibration procedure followed to correct some of the limitations associated to the macroscopic approach followed in this work. In order to validate the NO_x and PM_{10} annual emission estimates of the developed tool, we performed an emission simulation of 2017 and compared the obtained NO_x and PM_{10} emission values against two other emission inventories of the city. The computed annual NO_x emission results are in agreement with the other inventories (range of -5% and +9%) but higher discrepancies are found regarding PM_{10} emission estimates (+18% and +105%). These are believed to be caused by the inclusion of resuspension in the HERMESv3 emission model, which were not included in the other two reports. Additionally, to have a better understanding of the spatio-temporal emission distribution across the city, we also performed an spatial and temporal

analysis of the obtained emission results. The spatial analysis shows that a particular central area of Barcelona -the Eixample district- holds the largest emission density (291 kg·day^{-1}·km^{-2}) which contrasts with the 144 kg·day^{-1}·km^{-2} from a neighboring area. From the emission temporal profile we observe that traffic emission values follow a steady pattern during the daylight hours (7:00h to 18:00h) and during weekdays for most of the year.

The first work of the thesis concludes with an emission sensitivity analysis of typically high uncertainty emission features. This section aims to guide the modeller into the parameters that require more detailed data due to their high impact on the estimated emissions. In this sense, different approaches in regard of vehicle fleet composition, public bus transport implementation, temperature effect or the application of non-exhaust PM sources are analysed. The main findings show important street gradient differences between the different vehicle fleet compositions used (up to +788% in NO_x) and with the implementation of public bus transport routes (up to +300% in NO_x). Homogeneous increases of +19% in NO_x and +410% in PM are observed at the city level when considering the temperature-dependent processes and non-exhaust PM sources, respectively.

The second work of the thesis explores the limitations of the developed macroscopic system by comparing it with a microscopic approach composed by the microscopic traffic simulator Aimsun Next and the PHEMLight instantaneous vehicle emission model, also developed during this thesis. To do so, we quantified the emission discrepancies between both modelling approaches in a limited but representative area of Barcelona (0.4 km^2). This area contains three urban corridors representative of different traffic states (free-flow, normal flow and congestion) that allowed us to observe the influence of the vehicle-to-vehicle microscopic vehicle dynamics and the computed instantaneous vehicle emissions on the total estimated values. The results of this comparison show discrepancies during congested traffic conditions (up to +65% in NO_x emissions for the microscopic approach) but similar results during free and normal flow (-12% and +16% in NO_x for the microscopic approach). Additionally, to compute the impact of another variable which is not often considered in traffic emission studies, this chapter also analyses the road gradient effect in emissions for three different vehicle groups (Passenger Car, HDV and Bus) at the three different corridor types of the study domain. The

observed results show (i) a balance between the extra emissions from the positive road gradient and the negative one (+14% and -12%), that (ii) vehicle weight increases the road gradient impact (+20% and +14% for HDV and passenger car, respectively) and that (iii) the level of congestion decreases road gradient impact (+20% at free-flow vs a +10% in congested situation).

During the third work of the thesis we quantified the impact at the NO_x emissions and the NO_2 concentration levels of the different TMS adopted or planned to be adopted in Barcelona during the last 4 years: The previously commented Tactical Urban Planing, Superblocks and Low Emission Zone measures. To do so, we coupled the VML-HERMESv3 macroscopic traffic-emission system to the street-scale CALIOPE-Urban and the mesoscale CALIOPE air quality systems to also expose the differences between a street-scale and a mesoscale simulating approach. To quantify their specific effects, these were applied to the BCN-VML network in an individual and combined basis over different simulated scenarios. Results show that when only implementing measures related to the reduction of private transport space (Tactical Urban Planning and Superblocks) overall NO_x emission changes at city level are negligible (+0.1%). However, important street-level gradients that can reach up to ±17% in NO_x and ±5 µg/m^3 in NO_2 are generated as a consequence of the traffic re-routing and the newly congested areas. The Low Emission Zone appears as the measure with higher impacts at city level with reductions of -13% in NO_x emissions and -10 µg/m^3 in the daily NO_2 mean. Another scenario combines all the above-mentioned measures in a demand-reduction case, where traffic activity is reduced by a -25%. This is the scenario showing higher air quality improvements with overall NO_x reductions of -30% and daily mean NO_2 reductions of -25 µg/m^3 that can go up to -70 µg/m^3. The mesoscale approach shows that despite presenting consistent results, it is not capable of modelling the strong street gradients and associated NO_2 concentration changes induced by the mobility restrictions. Considering the obtained results, although the applied traffic management strategies lead to significant emissions and air quality improvements, the reductions achieved are insufficient to ensure compliant air quality levels, and are very far from reaching the new WHO air quality guideline values. These strategies must be accompanied by a larger decrease in the total number of circulating vehicles throughout the city which could be achieved, for instance, by the applica-

tion of a congestion charge in the city, or the implementation of local zero emission zones similar to the ones that are currently being deployed in the city of London.

The thesis manuscript finishes with the conclusions and most important results of the work, as well as future works and model improvements section, followed by some final remarks about urban mobility in the XXI century.

Resumen

La acumulación excesiva de contaminantes atmosféricos es una fuente de diferentes problemáticas ambientales, cuestiones económicas y de salud. Como consecuencia, diferentes leyes intercontinentales y europeas regulan las emisiones y establecen límites de concentración máxima que no deben sobrepasarse. Estos límites a menudo se exceden en áreas urbanas debido a su densidad de población, la alta carga de tráfico y la edificación urbana. Particularmente, en Barcelona (España) las dos estaciones de monitoreo de calidad del aire referentes a tráfico exceden de forma continua los límites de NO_2 impuestos por la Unión Europea. Considerando lo anterior, los responsables políticos locales se ven forzados a desarrollar planes de calidad del aire que a menudo van de la mano del desarrollo de políticas de movilidad o estrategias de restricción al tráfico enfocadas a reducir la actividad vehicular y sus niveles de emisión en la ciudad. Para cuantificar y evaluar el nivel de eficiencia de los planes de calidad del aire aplicados, la modelización de calidad del aire se presenta como una herramienta necesaria para complementar la información dada por las estaciones de monitorización de calidad del aire. Para la evaluación específica de estrategias de restricción de tráfico (e.g., reducción del espacio del vehículo privado) la aplicación de sistemas integrales de modelización de tráfico-emisión-calidad del aire es esencial para primero simular las nuevas rutas de vehículos generadas como consecuencia de las restricciones al tráfico, segundo para estimar las emisiones inducidas de la actividad vehicular previamente generada y tercero para computar la dispersión y transformaciones químicas de las emisiones de tráfico estimadas considerando la meteorología urbana y los niveles de contaminación de fondo.

En este sentido, la presente tesis evalúa el impacto que diferentes planes de restricción al tráfico tienen en los niveles resultantes de emisión de NO_x y de concentración de NO_2 en Barcelona. Para ello, hemos desarrollado un sistema integral de calidad del aire compuesto por el simulador de tráfico BCN-VML, el modelo de emisiones HERMESv3 y el modelo de dispersión a nivel de calle CALIOPE-Urban, que integra el modelo mesoescalar de predicción de calidad del aire CALIOPE y

el modelo Gaussiano de dispersión R-LINE. El BCN-VML fue desarrollado por el laboratorio inLab-FIB en el marco de la iniciativa del Cooperative Automotive Research Network (CARNET) mientras que HERMESv3 y CALIOPE-Urban son marcos de modelización del estado del arte desarrollados por el departamento de Ciencias de la Tierra del Barcelona Supercomputing Center - Centro Nacional de Supercomputación (BSC-CNS). La colaboración entre ambos centros de investigación ha permitido combinar el conocimiento en simulación de tráfico y modelización atmosférica dando como fruto el sistema integral de calidad del aire usado en esta tesis.

Las medidas de restricción al tráfico estudiadas estan ya aplicadas o en ejecución, recogidas en el último plan de movilidad urbana de Barcelona 2018-2024. Estas medidas buscan una reducción y renovación del número de vehículos circulantes en la ciudad mediante dos líneas de acción: Por una parte, (i) reducen el espacio que tiene el vehículo mediante la reducción de carriles de circulación en los principales corredores de la ciudad por las llamadas medidas de urbanismo táctico y (ii) implementan medidas de pacificación de tráfico en areas específicas de la ciudad -Supermanzanas- y, por otra parte, aplican una zona de bajas emisiones para restringir la entrada a los vehículos mas contaminantes.

Para entender los principios fundamentales de los diferentes simuladores de tráfico, emisión y calidad del aire, este trabajo presenta inicialmente un resumen de su metodología de trabajo y características principales. A esto le sigue una discusión del nivel de detalle apropiado para simular un dominio deseado de acuerdo al objetivo del proyecto, datos y recursos computacionales disponibles. Además, se presentan diferentes modelos de tráfico y de emisión en el estado del arte, con una descripción más profunda de las herramientas seleccionadas para este trabajo de acuerdo a las características mencionadas.

En el primer trabajo de la tesis, explicamos el proceso de acoplamiento de los modelos de tráfico y emisiones y el proceso de calibración seguido para corregir algunas de las limitaciones asociadas a la metodología macroscópica seguida en este trabajo. Para validar las emisiones anuales de NO_x y PM_{10} estimadas por la herramienta desarrollada, realizamos una simulación de 2017 y comparamos los valores de NO_x y PM_{10} obtenidos con otros dos inventarios de emisión de la ciu-

dad. Los resultados de emisión anual de NO_x computados están en el orden de los otros inventarios (rango de -5% y +9%) pero se observan mayores discrepancias en referencia a las emisiones de PM_{10} estimadas (+18% y +105%). Creemos que estas discrepancias se deben a que el modelo de emisión HERMESv3 considera la resuspensión, no incluida en los otros dos inventarios. Adicionalmente, para tener un mayor conocimiento de la distribución espacio-temporal de las emisiones en la ciudad, también hemos realizado un análisis temporal y espacial de los resultados de emisión obtenidos. El análisis espacial muestra que una zona particular de Barcelona -el distrito Eixample- tiene la mayor densidad de emisiones (291 kg·dia^{-1} ·km^{-2}) que contrasta con los 144 kg·dia^{-1} ·km^{-2} de un área colindante. Del perfil temporal de emisión podemos observar que los valores de emisión de tráfico siguen un patrón estable durante las horas diurnas (7:00h a 18:00h) y durante los laborables durante la mayoría del año.

El primer trabajo de esta tesis concluye con un análisis de sensibilidad de diferentes factores de emisión que usualmente presentan una alta incertidumbre. Esta sección pretende guiar al modelizador en los parámetros que requieren datos más detallados dado su alto impacto en la estimación de emisiones. En este sentido, se analizan diferentes propuestas en cuanto a composición vehicular, implementación del sistema público de transporte de bus, el efecto de la temperatura o la consideración de emisiones que no salen de los gases de escape.

El segundo trabajo de la tesis explora las limitaciones del sistema macroscópico desarrollado mediante una comparación con un sistema microscópico compuesto por el simulador de tráfico microscópico Aimsun Next y el modelo instantáneo de emisiones PHEMLight, también desarrollado en esta tesis. Para ello, cuantificamos las discrepancias de emisión entre las dos formas de modelización abordadas en una zona limitada pero representativa de Barcelona (0.4 km^2). Esta zona contiene tres corredores urbanos representativos de diferentes estados de tráfico (libre, normal y congestión) que nos permitieron observar la influencia de las dinámicas de vehículo a vehículo microscópicas y de las misiones instantáneas computadas en el total de emisiones estimadas. Los resultados de esta comparativa muestran discrepancias durante el estado de congestión (hasta un +65% en emisiones de NO_x para el modelo microscópico). Adicionalmente, para computar el impacto de otra variable que no se considera de forma habitual en estudios de emisiones de tráfico,

este capítulo también analiza el efecto de la pendiente de calle en las emisiones para tres tipologías de vehículo diferentes (turismo, vehículo pesado y bus) en los tres tipos de corredores del dominio de estudio. Los resultados obtenidos muestran (i) un equilibrio entre las emisiones extra de la pendiente positiva y la negativa (+14% y -12%), que (ii) el peso del vehículo aumenta el impacto de la pendiente (+20% y +14% para vehículos pesados y turismos, respectivamente) y que (iii) el nivel de congestión disminuye el impacto de la pendiente (+20% en estado libre vs un +10% en estado de congestión).

Durante el tercer trabajo de la tesis hemos cuantificado el impacto en las emisiones NO_x y los niveles de concentración de NO_2 de las diferentes restricciones al tráfico adoptadas en Barcelona durante los últimos 4 años: Las antes comentadas medidas de urbanismo tactico, Supermanzanas y la zona de bajas emisiones. Para ello, hemos acoplado el sistema de tráfico-emisión macroscópico VML-HERMESv3 al sistema de dispersión a escala de calle CALIOPE-Urban y al sistema de calidad del aire mesoescalar CALIOPE para exponer también las diferencias entre la escala de calle y la mesoescalar. Para cuantificar sus efectos específicos, las medidas se aplicaron a la red BCN-VML de manera individual y combinada sobre diferentes escenarios de simulación. Los resultados muestran que cuando solo se implementan medidas relacionadas con la reducción del espacio del transporte privado (medidas de urbanismo táctico y las Supermanzanas) los cambios en las emisiones globales de la ciudad son negligibles (+0.1%). Sin embargo, importantes gradientes a nivel de calle que pueden llegar a ±17% en NO_x y ±5 µg/m^3 en NO_2 se generan como consecuencia de la redistribución de tráfico y de las nuevas zonas de congestión. La Zona de Bajas Emisiones aparece como como la medida con mayor impacto a nivel de ciudad, con reducciones del -13% en las emisiones de NO_x y de -10 µg/m^3 en la media diaria de NO_2. Otro escenario combina todas las medidas antes descritas en un caso de reducción de demanda, donde la actividad del tráfico se reduce un 25%. Este es el escenario que muestra mayores mejoras en la calidad del aire con reducciones globales de NO_x del -30% i reducciones de la media diaria de NO_2 de -25 µg/m^3 que puede llegar a -70 µg/m^3. El sistema mesoescalar muestra que, a pesar de presentar resultados consistentes, no es capaz de modelizar los gradientes a nivel de calle y los cambios en las concentraciones de NO_2 asociados a las restricciones de movilidad. Considerando los resultados obtenidos, aunque las restricciones de tráfico aplicadas llevan a reducciones en emisiones y mejoras en la

calidad del aire, las reducciones obtenidas son insuficientes para asegurar niveles de calidad del aire conforme a la legalidad europea. Estas estrategias deben ir acompañadas por una disminución aun mayor en el número total de vehículos circulando por la ciudad, que se podría conseguir, por ejemplo, con la aplicación de un peaje de congestión en la ciudad.

El manuscrito de la tesis finaliza con las conclusiones i los resultados más importantes del trabajo, así como un apartado de trabajos futuros y mejoras del modelo, seguido por unos apuntes finales sobre la movilidad urbana en el siglo XXI.

Contents

List of Figures

List of Tables

Acronyms

AQD Air Quality Directive.

AQG Air Quality Guidelines.

AQMS Air Quality Modelling Systems.

CTM Chemical Transport Model.

DTA Dynamic Traffic Assignment.

HDV Heavy Duty Vehicle.

LDV Light Duty Vehicles.

LEZ Low Emission Zone.

OD Origin-Destination.

PC Passenger Car.

PM Particular Matter.

STA Static Traffic Assignment.

TMS Traffic Management Strategies.

TUP Tactical Urban Planning.

VdF Volume delay Function.

VKT Vehicle Kilometers Travelled.

VOCs Volatile Organic Compounds.

VSP Vehicle Specific Power.

WHO World Health Organisation.

1. Introduction

The excessive accumulation of air pollutants can lead to severe environmental, economical and health-related issues. These are particularly accentuated in urban areas due to their population density, the high traffic load and the urban build, among other urban characteristics. This chapter provides an overview of the air pollutant health effects, their classification and sources with a deeper description for the traffic-related air pollutants. Furthermore, the chapter comments the air quality situation in Europe and Spain, and the regulations that currently exist to reduce the release of air pollutants and improve air quality. This chapter also performs a review of the current regulations at urban level which are mostly focused in the road transport sector and studies the particular air quality situation of Barcelona. The present Ph.D Thesis is developed at the Earth-Sciences department of the Barcelona Supercomputing Center - Centro Naconal de Supercomputación (BSC-CNS) in collaboration with the inLab-FIB laboratory from the UPC. Therefore, a description of both research groups is also provided.

1.1. Air quality and health effects

The number of people living in urban areas has increased from 751 million in 1950 (30%) to 4.2 billion in 2018 (55%) and by 2050 2.5 more billion people are expected (United Nations, 2018). The rapid growth and densification of urban areas has largely increased urban emissions and the amount of population exposed to bad air quality. According to the World Health Organisation (WHO), 9 out of 10 people around the world breathe highly polluted air. The persistent exposure to it can be the cause of stroke, ischemic heart disease, chronic obstructive pulmonary disease, lung cancer, lower respiratory infections and diabetes (WHO, 2018) (Fig. 1.1). As a consequence, air pollution has become the largest single environmental risk factor, and the cause of 4 million premature deaths every year (WHO, 2018).

Urban areas are more subject to present excessive air pollution levels due to their extension, complex geometry, meteorological patterns, the local emission den-

sity and the temporal pattern in the releases dominated by the traffic rush hours (Hertel et al., 2009). The constant increase of traffic combined with bad infrastructure planning and insufficient public transport policies has led to severe traffic problems in most of the cities around the globe, carrying with it the noise and the vehicle emissions associated. Road transport sector produce tailpipe emissions (e.g., particulate matter, nitrogen oxides), evaporative emissions, resuspension of road dust, and particles from brake and tyre wear. The release of these pollutants is of special concern since they are emitted near pedestrians and are particularly toxic. In 2012 the World Health Organisation (WHO) classified engine exhaust gases as carcinogenic to humans (Group 1) together with several components from the air pollution mixture and Particular Matter (PM) (Silverman et al. (2012); WHO (2013)). PM, specially the fine fraction ($PM_{2.5}$) and O_3 are a source of breathing problems, cardiovascular disease, and shortened lives, while NO_2 causes irritation of eyes, nose, and throat (Gilda et al., 2013). In 2015, global vehicle exhaust PM emissions and traffic attributable ozone were responsible of 385.000 premature deaths. This values do not consider other road transport emissions such as non-exhaust PM sources (e.g., resuspension), evaporative emissions and other attributable health impacts such as noise, physical activity effects, road injuries or fuel life-cycle emissions (Anenberg et al., 2019).

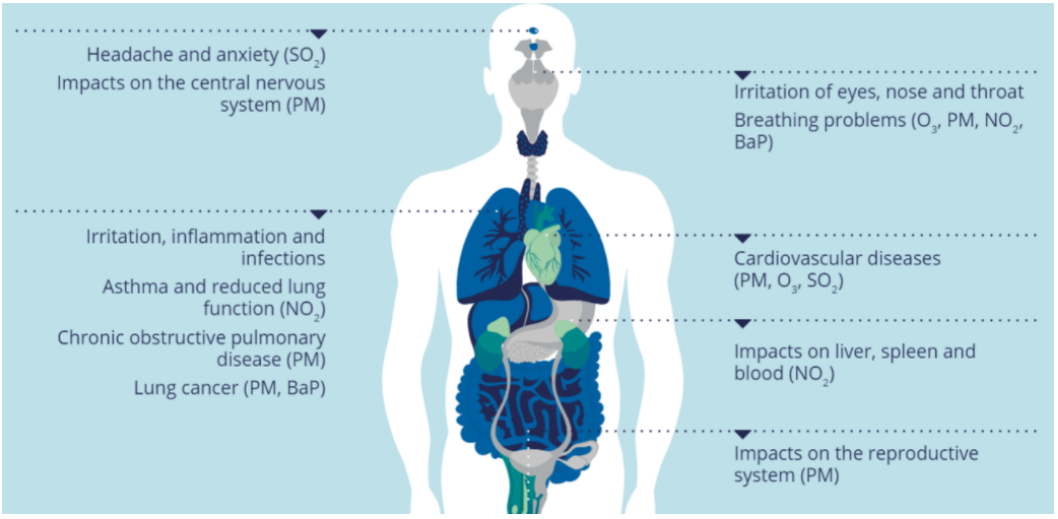

Figure 1.1: Potential human health impacts of different ambient air pollutants (EEA, 2019).

1.1.1 Air pollutants

Air pollution occurs when air pollutants are present at higher concentrations than their normal levels, capable of producing adverse effects on humans, animals, vegetation or materials (Seinfeld and Pandis, 2016). Air pollutants can be emitted by human activity (anthropogenic) or by natural activity (biogenic). Besides the adverse health effects that air pollution have on humans, air pollution has indeed a direct effect on vegetation and the quality of water and soil that support the ecosystems (EEA/EMEP, 2017). Forests and plants growth, acidification or eutrophication, are some examples of the effects that air pollution has on ecosystems. Moreover, the damage that they cause to materials and buildings degrade monuments and cultural heritage. In overall, it leads to a large economic cost together with the loss of labor productivity and additional health expenditure which underscores the need for strong policy action (EEA/EMEP, 2017). Air pollution is in many ways also related to climate change as several air pollutants are also climate warming forcers, like O_3 or black carbon (Williams, 2009). However, in many cases air pollution relation with global warming is opposite. There are some antagonist factors, like a majority of aerosols (e.g., nitrate, sulfate, or organic carbon) that have a cooling effect (Williams, 2009), the use of diesel against petrol vehicles or the usage of biofuels and biomass (e.g., pellets) for home heating.

Classification of air pollutants: Gaseous and particles

There are two types of air pollutants: particles (solid or liquid) and gaseous. Gaseous pollutants can be classified as primary (i.e., directly emitted from sources) or secondary (i.e. formed in the atmosphere from primary precursors). Among the firsts, the most common ones by historical importance and their effect on humans health are sulphur dioxide (SO_2), oxides of nitrogen (NO_x = NO + NO_2), and carbon monoxide (CO) (Tiwary and Colls, 2009). SO_2 has largely been controlled in Europe after the introduction of FGD (Flue Gas Desulphurization) abatement technologies into power station exhaust gasses stacks, and its concentration is within the legislation limits (Fig. 1.2) (Hertel et al., 2009). NO_x gasses are produced in high-temperature processes during the oxidation of the N_2 present in the air. Such processes occur in boilers and the internal combustion engines equipped in vehicles. CO is produced during incomplete combustion processes, very com-

mon on domestic appliances. Its presence in vehicles exhaust gasses has been controlled by the application of catalytic converters. The Volatile Organic Compounds (VOCs) are other common pollutants in urban areas. These denote the vapor phase of atmospheric organic compounds (e.g., alkanes, alkenes and aromatics) that come from the evaporation of organic compounds such as gasoline and solvents or the vehicles exhaust gasses due to unburned vehicle's fuel during combustion. Although most of the anthropogenic pollutant sources come from industry or transport sectors, agricultural activities are often an important source to take into account. The atmospheric ammonia which volatilizes from animal waste and synthetic fertilizers have a notable effect during the formation of secondary particulate matter, commented below. From the secondary pollutants the most common one in urban locations is the tropospheric ozone (O_3). This pollutant is generated during the decomposition of NO_2 catalysed by sun radiation and has adverse health effects on human health and ecosystems. It usually reaches its higher levels during the summer season in areas downwind from large urban locations that generate the primary NO_2 needed for its composition.

Pollutants in the form of particles -Particulate Matter (PM)- is the term used to describe a mixture of both, solid particles and liquid droplets (aerosols). They have different sizes and compositions and can be primary or secondary (commented later) (Guevara, 2016). Primary PM is mostly composed of a complex mixture of soot (also referred as black carbon or BC), organic carbon or organic matter (OC or OM), inorganic materials (e.g., SO_4^{2-}, NO_3^-) and sea salt (EEA, 2008). They are classified according to the aerodynamic diameter of the particle as follows: Up to 10 µm (PM_{10}), 2.5 µm ($PM_{2.5}$), 0.1 µm ($PM_{0.1}$) and 0.05 µm ($PM_{0.05}$). Primary PM can be emitted from both, natural and anthropogenic sources, most of the lasts originated during combustion (i.e., vehicle engines) and high-temperature processes. The incomplete combustion of these generates BC and OC, producing the smallest and most toxic particles, the fine and ultrafine particles ($PM_{2.5}$ and $PM_{0.1}$ respectively). The combination of BC or OC with other gaseous compounds (e.g., NH_3, NO_x, SO_x, or VOC) during condensation or gas to particle conversion processes can generate secondary organic or inorganic aerosols (SOA or SIA, respectively) (Guevara, 2016). Secondary organic compounds can contribute to a great proportion to the total PM registered, being often a significant participant of the PM registered levels.

1.2. Air quality in Europe

During the last decades the EU has been working to improve air quality by emission controls, improving fuel quality and integrating environmental protection requirements into the transport, industry and energy sectors. As a consequence, primary emissions and precursors contributing to PM_{10}, O_3 and NO_2 concentrations have decreased over the last 20 years despite the Gross Domestic Product (GDP) increase (Fig. 1.2). This was in part led by the decrease on road transport emissions (Fig. 1.3), which is the sector with higher contribution to NO_x emissions (39% in the EU-28) and a considerable contributor of PM_{10} and $PM_{2.5}$ (10% in the EU-28), black carbon (26% in the EU-28) and CO emissions (20% in the EU-28) (Fig. 1.4) (EEA, 2020). Despite the general trend in emission reduction, several European locations persistently present exceendaces for PM_{10} and NO_2 (Fig. 1.5). In 2018, sixteen of the EU Member States had at least one station with NO_2 values above the annual limit (EEA, 2020). It is important to note that none of the stations exceeding NO_2 values was rural background, and the highest values, as well as 95% of the total exceedances were observed in traffic stations. The same year in Spain, Madrid exceeded 33 times the hourly limit value of NO_2 (200 µg/m^3), while Granada, Madrid capital, Corredor del Henares (Madrid) and Barcelona exceeded the average annual value (40 µg/m^3) with values of 46, 55, 41 and 54 µg/m^3 respectively (Fig. 1.5) (MITECO, 2019). Twenty member states (19% of reporting stations) reported PM daily limit exceedances, the majority of which are also found in urban (89% of all exceedances) and suburban (8% of all exceedances) stations (EEA, 2020). The annual limit value was exceeded in ten member states (6% of reporting stations) while the most restrictive WHO Air Quality Guidelines (AQG) annual limit value for PM was exceeded at 53% of all reporting stations (2006 WHO AQG value). In Spain, the daily limit value for PM was exceeded in Jaén (Andalucía) while there were no exceendaces of the annual limit value (MITECO, 2019). In the view of this results, the reduction of traffic emissions becomes one of the main priorities and challenges in the EU to improve urban air quality.

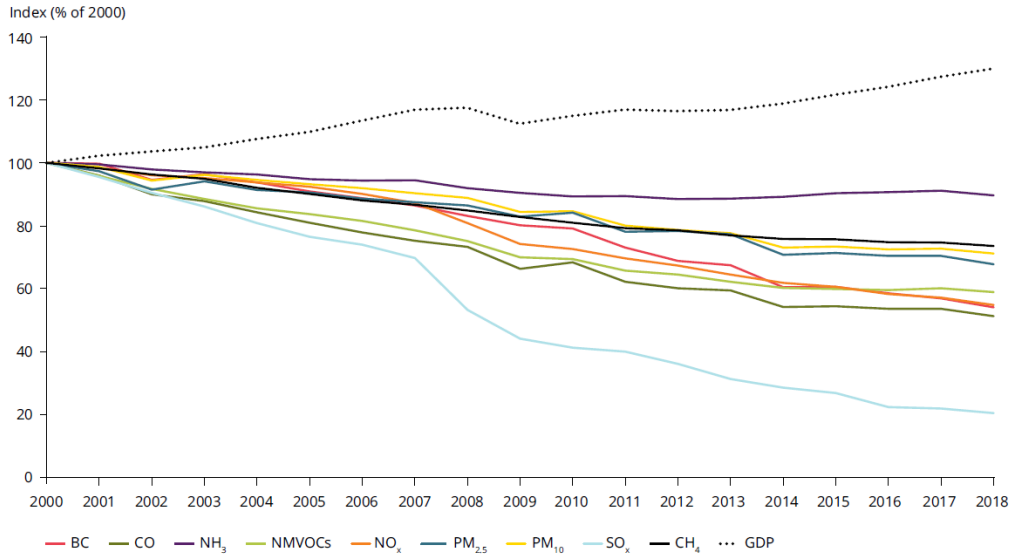

Figure 1.2: Development in EU-28 GDP and emissions from the main source sectors of NO_x, PM_{10}, $PM_{2.5}$, SO_x, NMVOC, NH_3, BC, CO and CH_4 between 2000 and 2018 (% 2000 levels) (EEA, 2020).

1.3. Traffic emissions

As above-mentioned, the traffic sector is responsible for a large part of the registered NO_2 and PM levels in urban locations. It is then important to understand the reasons and processes behind the traffic emissions. These are produced during engine combustion but also from evaporative and non-exhaust processes. In this sense, vehicle emissions are divided in: (I) Exhaust, which consider all tailpipe exhaust gases and are classified into hot and cold-start emissions, (II) non-exhaust, which consider wear processes such as brake, tyre and road wear, as well as the road resuspension, and (III) evaporative emissions, which consider the non-exhaust volatile organic components (VOCs) that escape through the vehicle's fuel tank.

Exhaust emissions are the direct gases emitted as a consequence of the fuel combustion. These are formed by CO_2, CO, H_2O, PM, HC, NO and NO_2 (NO_x) and SO_2. Since the combustion process is less efficient while the engine is cold and vehicle catalysts are not yet at their best performance temperature, the emissions during the vehicle "cold-phase" are higher, and are referred as cold-start emissions. Non-exhaust emissions are the PM emissions resulting from the mechanical

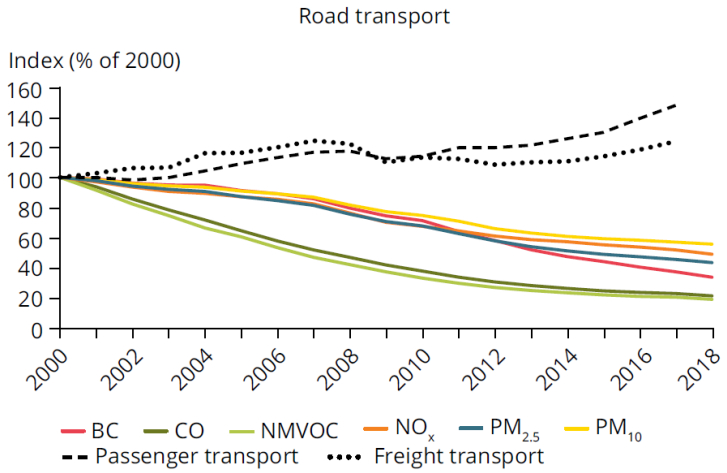

Figure 1.3: Development in EU-28 emissions from the road transport of NO_x, PM_{10}, $PM_{2.5}$, SO_x, NMVOC, NH_3, BC, CO and CH_4 between 2000 and 2018 (% 2000 levels). For comparison, key EU-28 sector's activity statistics are shown (% 2000 levels, except waste (kg per capita)) (EEA, 2020).

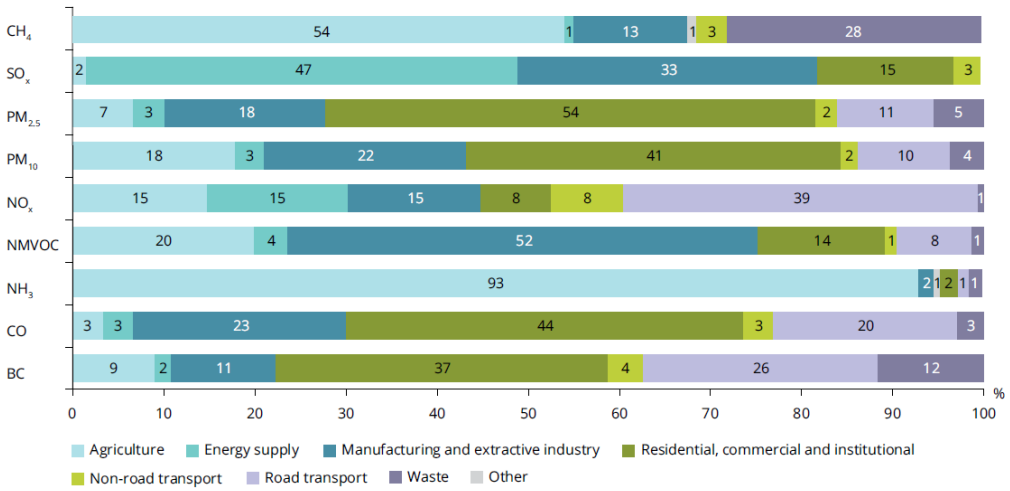

Figure 1.4: Contribution to EU-28 emissions from the main source sectors in 2018 of CH_4, SO_x, NO_x, primary PM_{10}, primary $PM_{2.5}$, NMVOCs, CO and BC (EEA, 2020).

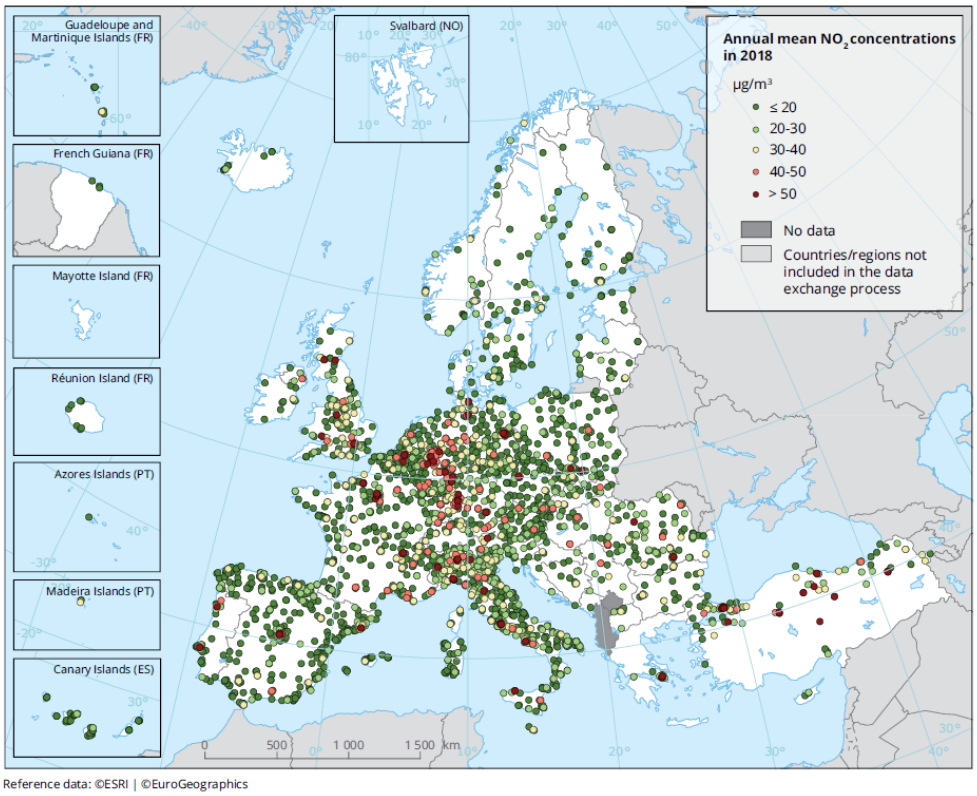

Figure 1.5: NO_2 concentrations in 2018 (EEA, 2020).

abrasion of the vehicle tyres, brakes and road surface wear and the resuspension. The last is generated by the vehicle circulation over the pavement where PM has already been deposited. The surface turbulence generated by the vehicle pass re-emit the deposited material, adding the resuspension emissions to the total vehicle emissions. Non-exhaust emissions are currently the main challenge in reducing road-transport PM emissions, since these already represent between 50 to 85% (Amato et al., 2014) of the total traffic PM_{10} and are expected to keep increasing over the next years as cleaner vehicle technologies are introduced to reduce exhaust PM emissions (Guevara, 2016). Finally, evaporative emissions are the result of the non-exhaust VOC escapes of the vehicle fuel tank and unburned fuel. As previously mentioned, these contribute to the Secondary Organic Aerosols generation, which is another source of atmospheric PM formation.

1.4. Legal Framework: Air quality targets

On the basis of scientific assessment of pollution effects and abatement options, in 1979 at the Convention on Long-Range Transboundary Air Pollution (LRTAP) (LRTAP, 1979) came the first multilateral agreement addressing transboundary air pollution. This was applicable to Europe, North America and Russia. The LRTAP protocol began to tackle acid rain, although over the years the number of substances covered by the Convention was extended. In the 1990s it was recognised that the pollutant interaction in the atmosphere lead to combined impacts which were often caused by the same sources. This was the reason to develop a so-called multi-pollutant-multi-effect approach, which was first applied on the 1999 Gothenburg Protocol to abate acidification, eutrophication and ground-level ozone (UNECE, 1999). This protocol set national emission ceilings for 2010 up to 2020 for SO_2, NO_x, VOCs and NH_3. In the European Union, the reductions of the Gothenburg Protocol are transposed by the new National Emission reduction Commitements (NEC) Directive (2016/2284/EU) (EEA, 2016) which entered into force on 31 December 2016. The NEC presents the more ambitious reduction commitments agreed for 2030 and replaces the earlier National Emission Ceiling Directive (NECD) (2001/81/EC) (European Commission, 2001). The NEC also requires Member States to come up with National Air Pollution Control Programmes that should contribute to the implementation of air quality plans established under the EU's Air Quality Directive (AQD) 2008/50/EC (European Parliament, 2008) which provides the current framework for the control of ambient concentrations of air pollution in the EU. The emission control of mobile sources include the air quality standards which set limit values for ambient air pollutant concentrations that must not be over-passed. Where levels are above the limit values, the Member States should prepare an air quality plan to address the responsible sources and to ensure compliance with the limit value. These values are based on the WHO AQG, which establish short and long-term exposure concentration levels for the main pollutants that should not be over-passed (WHO, 2021). These guidelines have been recently updated with more stringent values that in some cases have suffered a drastic reduction (e.g., annual NO_2 mean has gone from 40 to 10 $\mu g/m^3$). A summary and comparison between the updated WHO guidelines and the EU AQD limits is shown in Table 1.1.

Table 1.1: WHO air quality guidelines (WHO, 2021) and European air quality standards (European Parliament, 2008) to human health protection.

	WHO guidelines		European Union Standards		
	Concentration [μg/m^3]	Averaging period	Concentration [μg/m^3]	Averaging period	Permitted exceedances each year
NO_2	25	24 hour	200	1 hour	18
	10	1 year	40	1 year	n/a
O_3	60	8 hour mean peak season	120	Maximum daily 8 hour mean	25 days averaged over 3 years
	100	8 hour mean			
PM_{10}	45	24 hours	50	24 hours	35
	15	1 year	40	1 Year	n/a
$PM_{2.5}$	15	24 hours	25	1 Year	n/a
	5	1 year			
SO_2	40	24 hours	350	1 hour	24
			125	24 hours	3
CO	$4{\cdot}10^3$	24 hours	$1\cdot10^3$	Maximum daily 8 hour mean	n/a
Lead	n/a		0.5	1 year	n/a
Nickel	n/a		20	1 year	n/a
Benzene	n/a		5	1 year	n/a
Arsenic	n/a		$6{\cdot}10^{-3}$	1 year	n/a
Cadmium	n/a		$5{\cdot}10^{-3}$	1 year	n/a
BαP	n/a		$1{\cdot}10^{-3}$	1 year	n/a

For a direct control over vehicle emissions, the EU established emission standards over the exhaust vehicle emissions. These consist on a series of directives based on different amendments to the 1970 Directive 70/220/EEC (European Economic Community, 1970) which are updated with more restrictive values over time. The updates for each amendment are known as the Euro norms (i.e., Euro 1, Euro 2, ...). Currently, the latest Euro group for Passenger Car (PC) corresponds to Euro 6, and the next Euro 7 will probably come into force in 2025. Table 1.2 shows a list of the standards for each Euro group for PC, although these apply to all vehicle categories (e.g., HDV, motorbikes, ...).

The tests to measure the vehicle emission values were performed by standardised measurements in laboratories, where the vehicle was tested over a predefined driving cycle: the "New European Drive Cycle" -NEDC-. Nevertheless, since September 2017 -due to the Dieselgate scandal (Carslaw et al., 2011)- new car models have to pass a test in real driving conditions (Real Driving Emissions - RDE test) and an improved laboratory test, the "World Harmonised Light Vehicle Test Procedure" -WLTP-. The RDE procedure is based on the portable emission measuring system (PEMS). A system which measures real time exhaust emissions by a small lab attached to the car while real driving. This test complements the WLTP, which is a globally harmonised test procedure which replaces the former laboratory test, defeated by several vehicle manufacturers during the known as "Dieselgate" scandal (European Commission, 2017).

Table 1.2: European emission standards for passenger cars (g/km).

Euro Classification		CO (g/km)		HC+NO_x (g/km)		NO_x (g/km)		PM (g/km)	
	Date	Diesel	Petrol	Diesel	Petrol	Diesel	Petrol	Diesel	Petrol
Euro 1	07-1992	2.72	2.72	0.97	0.97	-	-	0.14	-
Euro 2	01-1996	1	2.2	0.7	0.5	-	-	0.08	-
Euro 3	01-2000	0.66	2.3	0.56	-	0.5	0.15	0.05	-
Euro 4	01-2005	0.5	1	0.3	-	0.25	0.08	0.025	-
Euro 5	09-2009	0.5	1	0.23	-	0.18	0.06	0.005	0.005
Euro 6	09-2014	0.5	1	0.17	-	0.08	0.06	0.005	0.005

1.4.1 "Dieselgate" scandal: The new EU vehicle emission compliance tests

The Dieselgate is a scandal related with the NO_x emissions of the Volkswagen (VW) group between 2009 and 2015, although not only VW vehicles were implicated. Later on, in the European Union it became clear that most, if not all diesel car manufacturers were employing some type of defeat device (Bernard et al., 2019). The NO_x emissions from the vehicles involved showed values that could reach up to 40 times more than the permitted limits for their Euro category, with average NO_x emission values that sometimes were higher than their previous Euro category (e.g. Euro 4 to Euro 5, Fig. 1.6). The fraud was done by the application of defeat devices during the NEDC test. The software could detect when the vehicle was passing the NEDC test and activate the emission control devices, while these remained deactivated under real driving conditions. The Dieselgate was a breakdown for the EU driving emission tests. It became the main reason why the EU road vehicle emission legislation changed in a direction towards capturing conditions more representative of real driving with the implementation of the above mentioned RDE and WLTP tests.

The excess NO_x emissions from the defeated vehicles became the cause of health and legislation compliance issues. Only in Europe, Anenberg et al. (2017) estimated about 6,800 premature deaths every year due to excess NO_x from cars and vans which could have been avoided if on-road diesel vehicles performed in the real world within the limits defined in vehicle emissions regulation. In terms of the AQD compliance, the excess Diesel NO_x emissions were an important reason for the bad performance of the implemented Low Emission Zones whose effect was far less than expected, as commented in section 1.5.1. In Berlin, von Schneidemesser et al. (2017) estimated the impact of the excess NO_x emissions upon the NO_2 levels at 16 measurement sites. They found that potential reductions up to 22 $\mu g/m^3$ at the roadsite stations could be achieved with NO_x emission compliance vehicles. This would reduce the registered NO_2 values by a -52% to a -36%, depending on the measuring site. In Barcelona, Benavides et al. (2021a) found that around a 20% of the NO_2 levels in the city were associated with the excess NO_x diesel emissions. The Dieselgate is the reason behind several economic, health and

legislation compliance issues and the trigger of a different view in the automotive industry, legislative tests and air quality management policies.

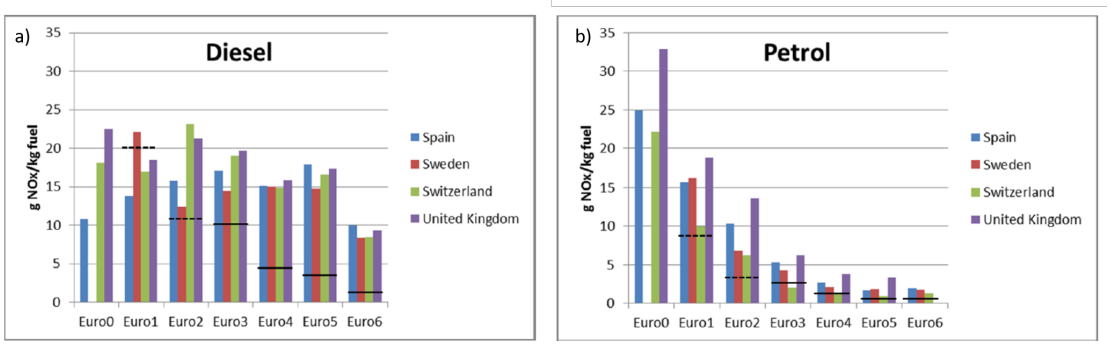

Figure 1.6: Average NO_x emissions (in g/kg fuel burned) by Euro standard and country for diesel (a) and petrol (b) passenger cars as measured by remote sensing. Black lines indicate the emission limit (Sjodin et al., 2018).

1.5. Urban air quality management

According to the above-mentioned, air pollution presents serious health issues on population above certain concentration levels. For the zones and agglomerations where the concentration of pollutants exceed the EU limits, the EU Ambient Air Quality Directives (European Parliament, 2008) obliges national and local authorities to develop and implement air quality plans and measures. Urban conurbations are areas that often overpass these levels due to the particular urban conditions and the near-the-source vehicle emissions to the traffic AQ monitoring stations. Considering this, the development of urban air quality plans go hand in hand with the development of mobility policies or Traffic Management Strategies (TMS). These are primarily focused in two areas of operation; at the technological level reducing emission rates by the renewal of the circulating vehicle fleet, and by the reduction of vehicles Vehicle Kilometers Travelled (VKT). The first is affected by the vehicle technology, fuel type and speed modifications. The Low Emission Zone (explained below) or the 30 km/h speed limit are examples of such policies. Measures affecting VKT go through the reduction of travel activity (e.g., teleworking) and modal choice (e.g. change to public or active ways of transport). The reduction of vehicle emission factors and the total amount of kilometers driven can have a noticeable effect on emissions which depending on their temporal and spatial distribution will

have a higher or lower impact at the urban air quality and population exposure.

Due to the high pollutant levels and their relation to the traffic sector, several cities in Europe are implementing a set of different traffic management strategies within their air quality plans to limit pollutant concentration values within the EU regulations (Fig. 1.7).

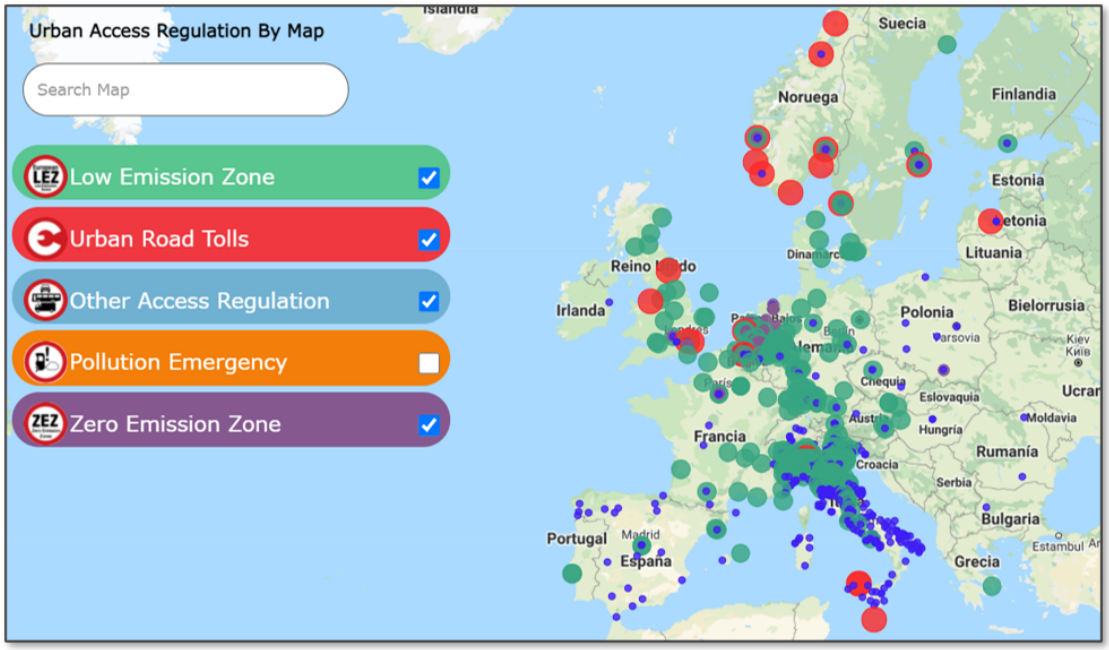

Figure 1.7: Distribution of the different traffic management strategies along Europe (European Comission, 2021).

1.5.1 Renewal of the circulating vehicle fleet: The Low Emission Zone

The Low Emission Zone (LEZ) area is one of the most common measures applied in large cities to reduce traffic emissions (Fig. 1.7). They go back to 1996 where the idea first appeared in Sweden; in Stockholm, Gothenburg, and Malmo (Holman et al., 2015). After Sweden, in Europe, Germany, Italy, Greece, Portugal, France and Spain among others, have implemented a LEZ (Table 1.3). They consist of the entrance restriction of vehicles according to their category (e.g., such as HDV or cars) and Euro classification in a certain urban area. The time of application goes from 24h seven days a week, to only weekdays or several hours a day.

However, their effectiveness is directly related with the efficacy of the Euro vehicle emission limits to reduce vehicle exhaust emissions. Since these have been proven to be inefficient for NO_x exhaust emissions due to the Dieselgate (section 1.4.1), the expected outcomes of the applied LEZ could have been too optimistic. Although the LEZ is globally a common measure (257 LEZs only in Europe), not many studies have deeply revised their air quality impact. Those who have generally coincide that the LEZ effect on air quality is moderate or limited, specially in European cities (Holman et al. (2015), Huang et al. (2021), Bigazzi and Rouleau (2017)). Most European cities report insignificant reductions (Boogaard et al. (2012), Ellison et al. (2013)) while NO_2 reductions of 19% (Huang et al., 2021) or NO_x and BC reductions of 13% and 10% (Tartakovsky et al., 2020) are observed in Haifa and Hong Kong, respectively. The studies also coincide that the effects of their application are hard to estimate since other factors such as meteorology, the changing nature of vehicle fleets or the particular design of the LEZ (area of action, vehicles restricted, ...) greatly influence the pollutants concentration and emissions (Lurkin et al., 2021).

1.5.2 License plate restrictions

Another applicable measure which does not need of the appliance of infrastructure for its integration is the license-plate based driving restriction, which became very popular in Latin American countries (Cantillo and Ortuzar, 2014) and China (Huang et al., 2016). The vehicles circulation is restricted according to the last number of their plate number and the day of the week. The application varies across cities, but most of them restrict vehicles from driving once or twice during weekdays. One of the cities that first applied this policy in order to reduce air pollutants is Mexico City. In there, drivers are not allowed to drive one weekday per week according to their license-plate last digit, where every weekday corresponds to certain numbers (e.g., Mondays “1” and “2”) (Davis, 2017). Although the measure has been applied since 1989, the research studies performed after its application show disappointing results. No evidence proves that air quality had initially improved after the restrictions. Moreover, air pollution had increased 12 to 24 months after the restrictions were imposed (Davis, 2008). The main suggested reasons state that drivers use taxis or get rides from other drivers whose car

Table 1.3: European Low Emission Zones. Adapted from Lurkin et al. (2021)

Country	Nº of LEZs	National LEZ framework
Austria	7	Yes
Belgium	3	No
Czech Republic	2*	Yes
Denmark	4	Yes
Finland	1	Yes
France	5	Yes
Germany	82	Yes
Greece	1	No
Italy	107**	No
Netherlands	14***	Yes
Norway	2	Yes
Poland	1	No
Portugal	1	No
Spain	3****	Yes
Sweden	8	Yes
UK	15*****	Yes
Total	257	

* incl. Prague - Access Regulation - Lorry LEZ.

*** incl. A12 Motorway (Tirol) LEZ.

**** incl. Rotterdam Dock - AR/LEZ LEZ.

***** incl. Madrid - LEZ Parking LEZ.

****** incl. London Clean Bus Zones LEZ.

is not banned, or even buy a second vehicle to be able to drive every day, which is often older and hence more polluting than the main one. An extension of the measure in 2008, also banning one Saturday per month to all drivers does not show air quality improvements either. Results of the Saturday restriction show that the public transport usage has not increased, while people's activity has not decreased, nor the gasoline consumption or new vehicle's registrations (Davis, 2017). Similar results occurred in Medellin (Colombia) and Lanzhou (China) after the application of license-plate restrictions. After an initial improvement on air pollutant levels the public's behavioral adaptation or the purchase of a new car made the driving restrictions ineffective (Huang et al. (2016); Ramos et al. (2017)). In a review study of this policy in several places Cantillo and Ortuzar (2014) concludes with quite a pessimistic point of view, stating the necessity of implementing measures which have been proved to work, like the congestion charge. On a similar direction, Huang proposes its combination with incentive-based demand-side policies like the parking fee, which has been found to discourage the use of a private transport or the already mentioned congestion charge (explained next). It is essential though to provide an integrated network of public transport services, at an affordable price and with a competent speed to provide a competitive alternative to private transport.

1.5.3 Congestion Charge Scheme (CCS)

The Congestion Charghing Scheme (CCS), or congestion charge is one of the measures which has proved to be more efficient (Johansson et al., 2009). It consists on the application of a toll to dissuade vehicles from entering a certain urban area by increasing the travel cost in comparison with other travel modes. The largest European cities with CCS are London (since 2003), Stockholm (since 2007) and Milan (since 2008). The singular effect of this measure on air quality improvements is hard to estimate since it is normally combined with other measures. In London the CCS came with the implementation of new bus lanes, the renewal of the bus fleet with new particle filters, increased bus frequency and changes on the traffic light phases (Atkinson et al., 2009). All these measures brought reductions of -4.4% and -9.4% in NO_x and NO together with NO_2 and PM_{10} increases of 3.7% and 2.5%, respectively. In Stockholm after the CCS trial year, the daily mean ve-

hicles reduction crossing the charge cordon was of -22%. The traffic reduction lead to a decrease in annual NO_x concentration of around -11% and a -7% for PM_{10} (Johansson et al., 2009). The Milan CCS, named "Area C" was a success with a traffic flow reduction of -30%, and an increase in public transport of 12.5% which lead to a -18% reduction in PM_{10} emissions after the first year (Croci (2016); Selmoune et al. (2020)). Although the improvements in traffic congestion and emission reductions cannot be directly associated to the application of the CCS, currently the CCS is the measure with best results in improving urban air quality. The combination of this measure with the improvement of other competing ways of transport (e.g. public transport) can generate even greater revenues.

1.6. The case of Barcelona

In Barcelona there are 10 air quality monitoring stations, 3 representative of a traffic site, 6 representative of urban background and 1 representative of suburban background site. From these stations 7 measure NO_2 values (Fig. 1.8). The two traffic air quality monitoring stations that measure NO_2 (Eixample and Gràcia - St.Gervasi) persistently exceed the EU AQD for NO_2 and the WHO AQG for PM (Fig. 1.9). This is a consequence of Barcelona's orography, meteorology and the activities in the city combined with the highest vehicle density in Europe (6,000 vehicles/km^2) (Ajuntament de Barcelona, 2020a).

Barcelona is settled at the northeast of the Iberian Peninsula, in the subtropics. All along the Mediterranean coast, large mesosocale circulations with strong diurnal cycles occur due to the thermal lows that originate over the peninsula (Millán et al., 2002). The thermal low leaves a space that is filled with air from the sea breezes, generating an air circulation. This circulation is favored by the chimney effect originated by the heating of the east and south-facing slopes of the high coastal mountains surrounding the sea (Fig. 1.10). The generated circulation helps to the development of a closed air flow cell, which creates a situation analogue to be "locked in a closed room within a fan running" (Lyons and Olsson, 1973) that difficult the dispersion of air pollutants.

Figure 1.8: Location of the official air quality monitoring network in Barcelona. The map represents traffic (red), suburban background (orange) and urban background (green) stations. The boxes in purple represent the stations that measure NO_2. Adapted from ASPB (2020).

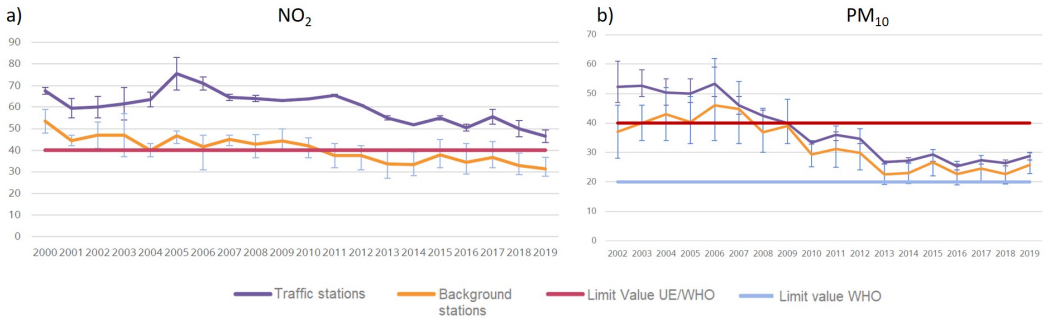

Figure 1.9: Historical evolution of the a) measured NO_2 and b) PM_{10} annual mean ($\mu g/m^3$) for the traffic (purple) and background (orange) monitoring stations between 2000 to 2019. The red line determines the EU Limit value, while the blue line determines the former WHO limit value (ASPB, 2020).

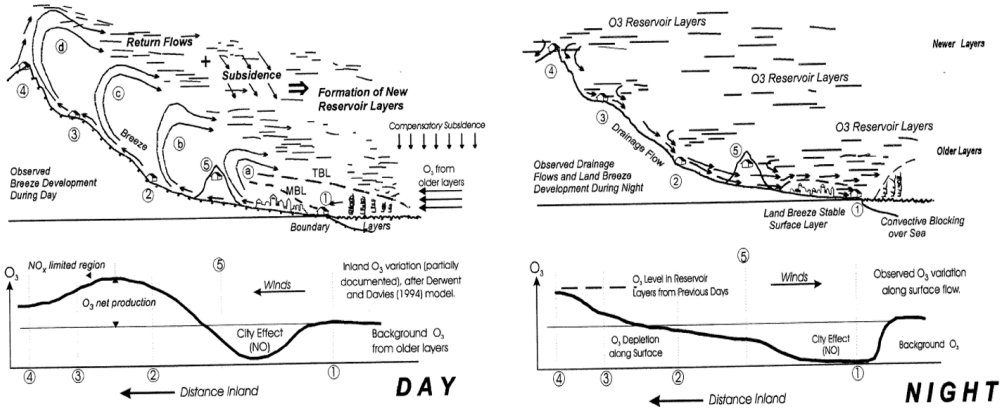

Figure 1.10: Day (a) and night (b) perpendicular circulations along the Mediterranean coasts in summer (Millán et al., 2000).

The particular meteorology and orography of the city would not lead to air quality issues without large emission sources. Barcelona holds one of the largest ports in the Mediterrenean sea which contributes to the 46% and 52% in NO_x and anthropogenic PM_{10} emissions respectively. The city also holds an elevated traffic activity of 6,000 cars/km^2 (that is the double of Madrid and the triple of London) which accounts for the 33.5% in NO_x and 37% in anthropogenic PM_{10} emissions (Ajuntament de Barcelona, 2015).

The combination of these factors contributes to the bad urban air quality of the city, which fails to pass the NO_2 EU AQD at the traffic sites (Fig. 1.9a). Due to the technological improvements in vehicle emissions and to the local measures applied, during the last years the historical record of annual mean NO_2 concentration values registered at the city shows a smooth decline with values of almost 70 µg/m^3 in 1996 to 48 µg/m^3 in 2019 for the traffic stations (Fig. 1.9a). The decreasing trend is more accentuated for PM_{10}, which goes from 53 µg/m^3 in 2002 to 29 µg/m^3 in 2019, complying with the EU AQD ($\leq$ 40 µg/m^3) but not with the former WHO AQG ($\leq$ 20 µg/m^3) (Fig. 1.9b). Despite the positive trend, it is still necessary to keep applying structural measures to maintain the trend towards satisfactory pollutant levels.

On the view of the results, during the last years Barcelona has been applying a series of structural policies regarding traffic control in order to comply with the EU regulations. The first measures that were applied in the city and its surroundings aimed at reducing vehicle emission rates by decreasing the speed

limit. In 2007, the Zone 30 was applied in several streets of the city followed in 2008 by the 80 km/h speed limit in the motorways heading to the city. A modeling study performed by Baldasano et al. (2011) showed a reduction of 4% in traffic emissions, which supposed an average reduction level of 5 to 7% of primary pollutants over the area. Another study performed by Bel and Rosell (2013) showed empirical results with NO_x and PM_{10} increases up to 3.2% and 5.9% respectively. The measure was then updated to a variable speed limit, which according to the same study was more successful in reducing NO_x and PM_{10} with reductions up to -17.1% and -17.3% respectively. Also in 2007, the city implemented the public bike system, *Bicing*, aimed to encourage active transport. But it was on the two last Urban Mobility Plans - years 2014-2018 (Ajuntament de Barcelona, 2014) and 2019-2024 (Ajuntament de Barcelona, 2020d) - where the main target was to reduce the usage of private transport, while enhancing active ways of transport (e.g., cycling) and public transport. In this direction, Barcelona has increased the total kilometers of bike lanes (from 105 km in 2013 to 230 in 2020, (Ajuntament de Barcelona, 2020d)), it has implemented a new bus network based on orthogonal lines and has approved the construction of a new tram line. These measures go in hand with the implementation of the park and ride (parking lots on train stations to encourage its use) and the application in 2017 of a Low Emission Zone during pollution episodes, that became permanent in 2020 (Fig. 1.11). Two of the main actions appearing in the lasts urban mobility plans to reduce private vehicle space are the Superblocks and a series of Tactical Urban Planning (TUP) measures which reduced vehicle lanes on several urban corridors in the city. Superblocks began as a pilot project in 2016, and currently more than 8 are implemented or planned to be implemented in the city. The Superblock idea consist on the traffic pacification of several streets within an area comprised by several blocks. The traffic pacification measures performed within the Superblock comprise a reduced speed limit (10 km/h), the usage of urban furniture to hassle traffic -such as urban vegetation, bollards or speed humps- and the introduction of mandatory turnings that throw out the incoming vehicles. The goal of the Superblock is to provide a traffic-pacified interior area accessible primarily to active transport (e.g., cycling) and secondarily to residents and services, diverging through traffic and gaining space for leisure activities (Fig. 1.12a) (Rueda, 2019). On the other hand, the measures performed by tactical urbanism are low-cost and scalable elements such as strips of

colours, urban furniture or moveable plant beds to transform the urban space. In the case of Barcelona, the introduction of these elements allowed reducing traffic lanes dedicated to private vehicles from major urban corridors in the city, and gaining pedestrian and public transport space. The importance of this measure lies in the streets that have been affected, which are the principal corridors used by residents to quickly cross the city that in some cases have gone from 6 to 4 vehicle lanes (Fig. 1.12b).

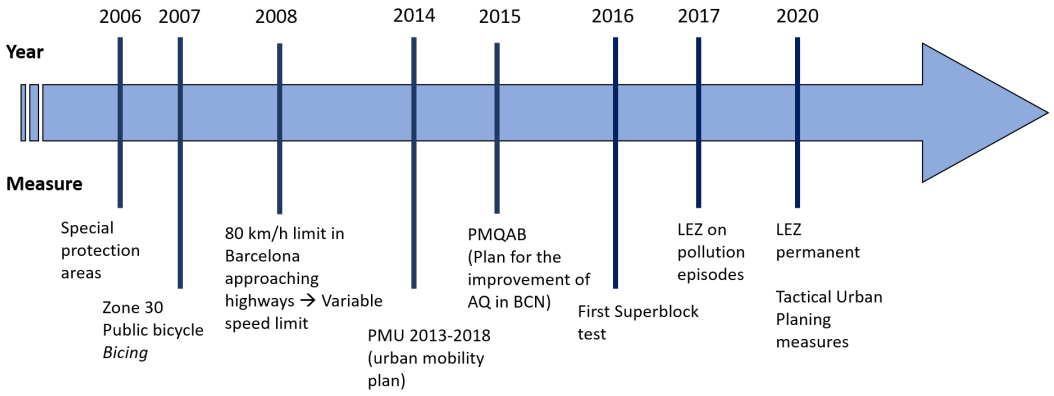

Figure 1.11: Timeline of the applied mobility measures related to vehicle emissions in Barcelona.

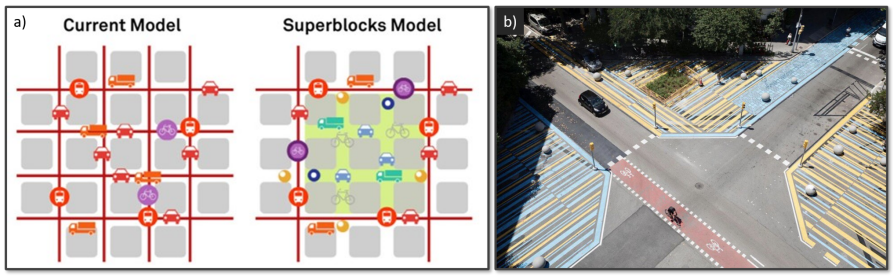

Figure 1.12: a) Scheme of the superblock concept (Ajuntament de Barcelona, 2014) and b) example of a tactical urbanism action.

1.6.1 Mobility patterns

An understanding of the mobility patterns that occur in the Barcelona area is essential to apply the adequate set of traffic management strategies and reduce the traffic circulation within the city. It is particularly important to reduce the connection traffic (i.e., with origin or destination outside of Barcelona) since a large part of the elevated traffic activity in the city comes or goes to the surrounding cities of the region. In Fig. 1.13 we can observe the total inner (circled arrows)

and connection trips (vertical arrows) between the different areas of the Barcelona region. The total displacements done within Barcelona city are the largest (4.4M), but only a 14.7% of them are done by private transport (660,000 trips). On the other hand, the city hosts 744,200 connection trips done by private transport, which represents a 54.3% of the total connection trips (ATM, 2020) (Table 1.4). This data does not count freight transport, adding an additional 490,000 trips (66% of which with origin or destination outside of Barcelona) (Ajuntament de Barcelona, 2020d). These values are a direct consequence of the public investments in transport infrastructure done during the last decades. While the population outside of Barcelona has been increasing during the last years (Fig. 1.14), so did the construction of highways (e.g., C-32, C-16, B-24, A-2 or C-60) and the ring-roads for Barcelona. Yet, the promotion of private transport was in detriment of the public, which remains practically the same since its creation in the 90s. It is then expected to see that from 1986 to 2014 there has been an increase of 116% in commuting by private transport and a 38% increase when it refers to the public (AMB, 2014). However, this situation reverses when it refers to Barcelona city. Opposite to what has been done outside the city, in Barcelona the public transport infrastructure has been constantly updated. New and longer metro lines, the creation of a tram and the optimization of bus lines are some examples of public transport infrastructures that lead to the low proportion of private transport users within the city.

On the view of this, measures aiming at reducing the incoming vehicles to the city combined with an adequate public transport network able to absorb part of the daily commuting to or from Barcelona seem essential to notable reduce the

Table 1.4: Modal distribution of the trips inside Barcelona and the connection trips between Barcelona and its surrounding areas.

	Private transport	Public transport	Active mobility	Total	%
Barcelona inner displacements	14.7% (660,000)	17.3% (789,000)	67.7% (3E+06)	4.4E+06	76%
Conection trips in/out Barcelona	54.3% (744,000)	39% (527,000)	7.3% (100,000)	1.4E+06	24%
Total	1.4E+06	1.3E+06	3.1E+06	5.8E+06	100%
%	24%	23%	53%	100%	

total traffic activity in the city.

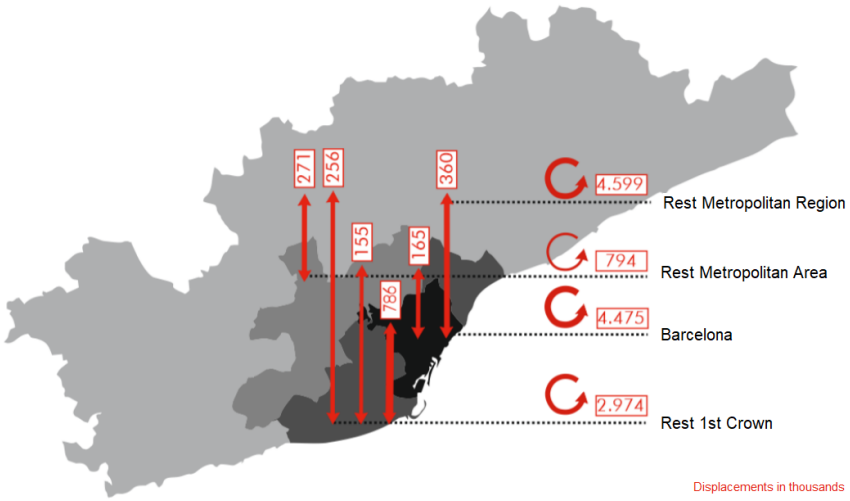

Figure 1.13: Origin-destination fluxes done in the Barcelona region. Circled arrows represent displacements done within the area while vertical arrows represent fluxes between areas (ATM, 2020)

1.6.2 Previous studies in Barcelona

Due to the persistent air quality issues in Barcelona, during the last years several studies were performed at the city to give some insights about possible benefits of air quality policies (Table 1.5). Soret et al. (2014) estimated the air quality improvements of 3 different electrification scenarios at a resolution of 1km × 1km. With the most ambitious scenario (40% fleet electrification) reductions in NO_x emissions of 11% were estimated, with maximum NO_2 hourly reductions of 16%. Mueller et al. (2020) estimated the health impacts of the complete implementation of the superblock plan, which comprises a total of 503 Superblocks in the city. They estimated how traffic demand would be affected, the gains related to physical activity, changes in NO_2 emissions, the new green spaces and reduced heat island effect. Results expected that 667 premature annual deaths could be prevented, where the greatest number of preventable deaths are attributed to NO_2 reductions (291) due to the estimated decrease in traffic activity (-19%). Based on a Remote Sensing Device study -which reads instantaneous vehicle emissions-, the AMB and RACC studied the real circulating vehicle fleet on the city and their emission factors. They found large differences with the censed vehicle fleet, specially for

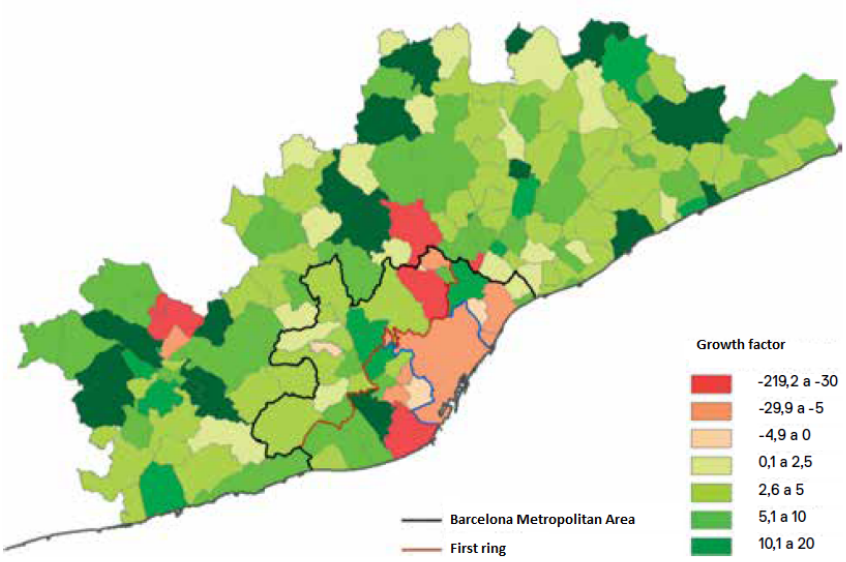

Figure 1.14: Mobility growth relative to population growth (AMB, 2014).

Light Duty Vehicles (LDV) which was in average 7.2 years newer, and the passenger cars (-4.3 years). In agreement with other studies regarding vehicle emissions, they also found large differences between the real exhaust emissions and the Euro limits, specially for Diesel vehicles. Due to this gap between regulated and current diesel vehicle emissions, Benavides et al. (2021a) analysed the impact of excessive LDV emissions upon NO_2 levels in Barcelona at a mesoscale (1km $\times$ 1km) and street-scale (20m x 20m) resolution. With the street-scale approach, they found that the excess NO_x emissions were associated with about a 20% of the NO_2 registered levels in the city. The mesoscale approach could not properly capture these gradients and largely underestimated the impact of diesel excess NO_x emissions upon NO_2 by a 38% to 48%.

1.7. Framework of the thesis at BSC

The present Ph.D thesis follows the research line of the Earch Sciences Department of the Barcelona Supercomputing Center - Centro Nacional de Supercomputación (BSC-CNS). The group directed by Dr. Francisco J. Doblas Reyes was initiated at the Environmental Modelling Laboratory of the Technical University of Catalonia

Table 1.5: Review of different studies of the applied policies in Barcelona.

Measure	Year of application	Relevant studies
Settling of Bicing, bike shared system	2007	Short-term planning and policy interventions to promote cycling in urban centers: Findings from a commute mode choice analysis in Barcelona, Spain (Braun et al., 2016).
80 km/h speed limit on motorways	2008	Air pollution impacts of speed limitation measures in large cities: The need for improving traffic data in a metropolitan area (Baldasano et al., 2011).
Superblocks	2016	Estimation of future emission scenarios for analyzing the impact of traffic mobility on a large Mediterranean conurbation in the Barcelona Metropolitan Area (Spain) (Soret et al., 2011)
	2019	Changing the urban design of cities for health: The superblock model (Mueller et al., 2020)
Implementation of the Low Emissions Zone.	2017	Informe de resultats de la ZBE (Barcelona Regional, 2019)
Excess NOx from diesel vehicles	2021	On the impact of excess diesel NO_x emissions upon NO_2 pollution in a compact city (Benavides et al., 2021a)

(LMA-UPC) directed by Dr. José María Baldasano. The main research lines of the group lie in Earth system modelling, with the following main research topics: atmospheric modelling, air quality modelling, mineral dust modelling and climate modeling. Particularly, the air quality research is focused in understanding the air pollution dynamics focused in the relationship between emissions, atmospheric transport, chemistry and deposition and obtain an air quality estimation through the development and implementation of high resolution modelling. A review about the most relevant works at the department in emission and air quality modelling can be found in Table 1.6.

Table 1.6: List of relevant publications in international journals related to AQM from the former Environmental Modelling Laboratory of the Technical University of Catalonia and the Earth Science department of the BSC-CNS

Reference	Topic	Domain
Costa and Baldasano (1996)	Development of the EMITEMA-EIM athmospheric emission model for Barcelona over 1990	Barcelona
Gomez and Baldasano (1999)	Development of a biogenic VOC emission inventory for Catalonia	Catalonia
Delgado et al. (2000)	Development of a high-resolution vehicle emission model	Catalonia
Parra et al. (2006)	Development of the EMICAT2000 high-resolution emission model for Catalonia 2000	Catalonia
Baldasano et al. (2008a)	Development of the HERMES04 high-resolution emission model for Spain 2004	Spain
Pay et al. (2010)	Evaluation CALIOPE AQMS over Europe for 2004	Europe
Badia et al. (2017)	Evaluation of the Multiscale Online Nonhydrostatic AtmospheRe CHemistry model (NMMB-MONARCH) version 1.0	Global
Guevara et al. (2019) Guevara et al. (2020)	Development of the HERMESv3 high-resolution emission model Part I and Part II	Global
Benavides et al. (2019)	Development of CALIOPE-Urban v1.0: coupling R-line with a mesoscale air quality modelling system	Barcelona

One of the firsts attempts to describe and quantify the the emission sources of Barcelona was the EMITEMA-EIM athmospheric emission model. It was developed between the years 1994 and 1996 and it could estimate CO, SO_x, NO, NO_2, CH_4, NMVOC and PM hourly emissions in a 1.5 km^2 area. Air pollutants were estimated from both anthropogenic and biogenic sources by a bottom up (i.e. road-traffic, industrial activities, air traffic, gas stations and biogenical sources) and top-down approaches (i.e. domestic heating) using the CORINAIR methodologies and emission factors (Eggleston et al., 1989). Following this work, Gomez and Baldasano (1999) presented an emission inventory for vegetation in Catalonia for the year 1992 and Delgado et al. (2000) extended the EMITEMA-EIM for Catalonia and performed an estimation of on-road traffic emissions during the year 1994.

These works were the basis for the development of EMICAT2000 emission model (Parra et al., 2006) which estimated emissions for Catalonia with the year 2000 as reference. The model included the most important primary air pollutants (NO_x, NMVOCs, CO, SO_x and TSP), integrating hourly, daily, monthly and yearly emissions and providing information both for environmental management and photochemical modelling. Finally, following the work on emission modelling of the previous studies, during the years 2005 and 2006 the BSC-CNS developed the - High-Elective-Resolution Modelling Emission System (HERMES04) - with the objective of generating an anthropogenic and biogenic emission inventory for Spain with a temporal and spatial resolution of 1 h and up to 1 km^2 (Baldasano et al., 2008a). The initial version of HERMES was then updated by the following works within the framework of another Ph.D thesis (Guevara et al., 2013) up to the current version used in this thesis, HERMESv3 (Guevara et al. (2019); Guevara et al. (2020)). The HERMES emission system is the emission core of the CALIdad del aire Operacional Para España air quality forecast system (CALIOPE-AQFS). The CALIOPE-AQFS established an air quality forecast system for Spain to increase knowledge on transport and dynamics of pollutants (Baldasano et al., 2008b). The CALIOPE-AQFS is a state-of-the-art modelling framework which works with a temporal resolution of 1 hour and a horizontal resolution that varies with the working domain: from 12km $\times$ 12km for Europe, to 1km $\times$ 1km for Madrid and Catalonia. The system estimates the concentration values of NO_2, CO, SO_2, O_3,

C_6H_6 PM_{10} and $PM_{2.5}$ (http://www.bsc.es/caliope/es). It is integrated by the Weather Research and Forecasting (WRF) model version 3.5.1 with WPS version 3.9.1 (Skamarock and Klemp, 2008), the Community Multiscale Air Quality Modelling System version 5.0.2 (CMAQ) (Byun and Schere, 2005), the mineral Dust REgional Atmospheric Model (BSC-DREAM8b) (Basart et al., 2012) and the above-mentioned HERMES emission model. The implementation of CALIOPE-AQFS was possible thanks to the previous works of the group (Baldasano et al. (2008b); Baldasano et al. (2011); Pay et al. (2010)) also about meteorological modelling (Soriano et al. (2001); Pérez et al. (2004)), emission modelling (Costa and Baldasano (1996); Parra et al. (2006); Baldasano et al. (2008b); Guevara et al. (2013)) and air quality modelling (Costa and Baldasano (1996); Jiménez et al. (2005)).

Concerning air quality management at urban scales, the CALIOPE-AQFS has been used in the framework of other Ph.D thesis for air quality evaluation and epidemiological studies, and air quality environmental impact studies of particular installation impacts (e.g., power plants, biomass plants) (Baldasano et al., 2014). To increase the resolution to street-level modelling, Benavides et al. (2019) performed a downscaling exercise with the implementation of the gaussian dispersion model RLine to the CALIOPE-AQFS, achieving a street scale resolution tool able to estimate pollutant concentration values at a resolution of few meters. This tool, named CALIOPE-Urban, has already been used to estimate the NO_2 increases in Barcelona as a consequence of the excess diesel NO_x emissions in light duty vehicles (Benavides et al., 2021a) and it is the main air quality tool used in this thesis.

1.8. Collaboration with the inLab-FIB UPC

The thesis has been developed at the Earth Sciences department of the BSC, but in close collaboration with the inLab-FIB laboratory of the Universitat Politècnica de Catalunya (UPC). The inLab-FIB is a research and innovation laboratory of the Barcelona School of Informatics at UPC, specialized in applications and services based on the latest ICT technologies such as data science, smart mobility and modeling, simulation and optimisation. In this sense, they have done projects related

to systems and processes improvement through the use of modeling, simulation and optimization techniques applied to transport, manufacturing, logistics, industrial processes or emergency systems. Within the transport modelisation field, they developed the first detailed multi-modal model of the First Crown of the Metropolitan Area of Barcelona -the BCN-VML network- that has been used in this thesis after a calibration and validation process, described in detail in sections 2.2.3 and 3.2.1.

1.9. Objectives

Considering that: (i) excessive tropospheric pollutant levels are dangerous to human health and these often occur in urban environments to a large extent due to traffic near-pedestrian emissions (sections 1.1 and 1.3), (ii) to address this, Europe has applied air quality regulations which set limit values that have to be accomplished by the implementation of air quality plans (sections 1.2 and 1.4), (iii) these often go in hand with the implementation of traffic management strategies (section 1.5) and (iv) Barcelona overpass the EU limit values and it is currently applying different traffic management strategies to tackle air pollution by the reduction of private vehicle space in the city (section 1.6), the main objective of this Ph.D thesis is **to quantify the impact of Barcelona's traffic management strategies upon local emission and air quality levels by using a multi-scale modelling approach**.

In order to achieve this objective, the following specific objectives need to be accomplished:

- Development and calibration of a coupled traffic-emission modelling system for Barcelona. Analysis and validation of the NO_x and PM_{10} obtained emission results.
- Coupling of the traffic-emission model developed to the Gaussian street-scale dispersion model CALIOPE-Urban and the mesoscale air quality model CALIOPE.
- Validation of the air quality results from the integrated air quality modelling system.

– Assessment of the individual and combined impacts on NO_x and PM_{10} emissions and NO_2 air quality levels of the different traffic management strategies applied.

1.10. Organisation of the manuscript

This manuscript has the following organisation: Chapter 2 provides a literature review of some of the traffic, emission and air quality modelling tools and states the fundamentals of their workflow. Chapter 3 presents the coupled traffic-emission system: VML-HERMESv3. It describes the coupling procedure, the calibration process and a comparison with other emission inventories. The chapter finally presents a sensitivity analysis with different key emission input parameters. Chapter 4 provides a comparison between the previously mentioned macroscopic coupled system with a microscopic traffic-emission system to observe the possible discrepancies between both modelling approaches. Chapter 5 integrates the VML-HERMESv3 system into CALIOPE and CALIOPE-Urban air quality modelling tools to estimate the NO_2 air quality impacts of the different traffic restrictions applied in Barcelona and to observe the differences between the mesoscale and street-scale modelling approaches. Finally, Chapter 6 presents the main conclusions of the work, the future works and the final remarks of the thesis.

2. MODELLING TOOLS

Modelling tools, together with observations, are the current methodology recommended by the Air Quality Directive of the European Commission to assess and evaluate air quality plans. When these comprise large urban modifications through the application of traffic management strategies, the air quality modelling process has to be preceded by a traffic estimation done by a traffic simulator, to be then followed by a vehicle emission estimation integrated in an air quality model. This chapter introduces and describes the workflow of a traffic simulator, a vehicle emission model and the fundamentals of an air quality modelling system. Furthermore, this chapter presents a literature review of the current state of the art of traffic simulators and vehicle emission models that can be used for vehicle emission estimation, as well as the specific modelling tools used in this Ph.D thesis for the evaluation of traffic management strategies in Barcelona. Finally, the chapter includes a review of different air quality modelling studies using the tools and models previously described.

2.1. Introduction

The current methods to characterise pollutant concentration values are based on modelling tools or by observations measured at ground level in urban, sub-urban and and rural locations. Air pollution measurements give quantitative information about ambient concentrations and deposition, but this is limited to specific locations and times (Daly and Zannetti, 2007). In Barcelona there are 10 air quality monitoring stations, 3 representative of a traffic site, 6 representative of urban background and 1 representative of suburban background site. However, as stated by Duyzer et al. (2015), these are insufficient to properly characterise population exposure. The spatial representativiness of the observational network can be extended for specific time periods by passive dosimeters to measure a certain pollutant, which allows to cover a wider area at a lower cost than the installation of full monitoring stations but with the time coverage limitation. On the other hand,

air pollution modelling tools can give a more complete deterministic description of the air quality problem; including an analysis of factors and causes such as emission sources, meteorological processes or physical and chemical changes (Daly and Zannetti, 2007). However, modelled results come with an associated uncertainty level that cannot be avoided. In this sense, it is crucial to work with the most detailed data available, specially concerning the emission estimation (Kryza et al., 2015). More accurate and realistic assumptions of the input parameters may result in emission levels being significantly higher or lower than the current consideration leading to a better planning, modelling and policy making (Dey et al. (2019); Dias et al. (2018)).

In this context, modelling tools complement observational methods by offering an insight of exposure levels in a quantitative continuous map of the area of study at any time in the past, present or future by preventing local authorities from pollution episodes or for scenario modelling. For the analysis of traffic management strategies, modelling tools can estimate the induced new vehicle routes and possible rebound effects that might occur and, if necessary, apply the corresponding modifications on the planned strategies. In this sense, air quality models should be used for both assessment and planing; but to do so, the modelling chain has to be fit-for-purpose and properly checked and verified with the available observational data. In the framework of this Ph.D thesis, the modelling chain needed to analyse the air quality impact of different TMS includes the following modelling tools (Fig. 2.1).

- A traffic simulator, which contains the road network data, including specific characteristics of each link (i.e., street segment), the vehicle generation centroids, the traffic demand generation and attraction areas, the traffic activity between the specific areas (i.e., number of trips) and mobility patterns (see section 2.2).

- An emission model, which describes the spatio-temporal distribution of all emission sources, natural and anthropogenic. For the scope of the thesis we focus on the emissions associated to the road traffic sector, explained in section 2.3.

- A meteorological model, able to characterise the state and evolution of the

atmosphere where emissions occur. The atmosphere state takes an important role in the chemical and physical interactions between pollutants and the dispersion processes, which are characterised by the last component, the Chemical Transport Model (CTM).

– A chemical transport model, which characterise the physical and chemical transformations that occur to the emitted pollutants in the atmosphere according to the specific meteorological conditions estimated by the meteorological model. A more detailed explanation can be found in section 2.4.

The variables and parameters involved in the modelling system differ between the level of detail desired and the study domain. An air quality assessment can go from a hot-spot (street, roundabout) to an entire city, or region. In this sense, it is important to acknowledge the available data, the computational resources and simulation time in order to select the tools and their level of detail according to the above-mentioned factors. In the next sections we will expose the parameters to take into account in order to choose the appropriate tools for the desired simulation.

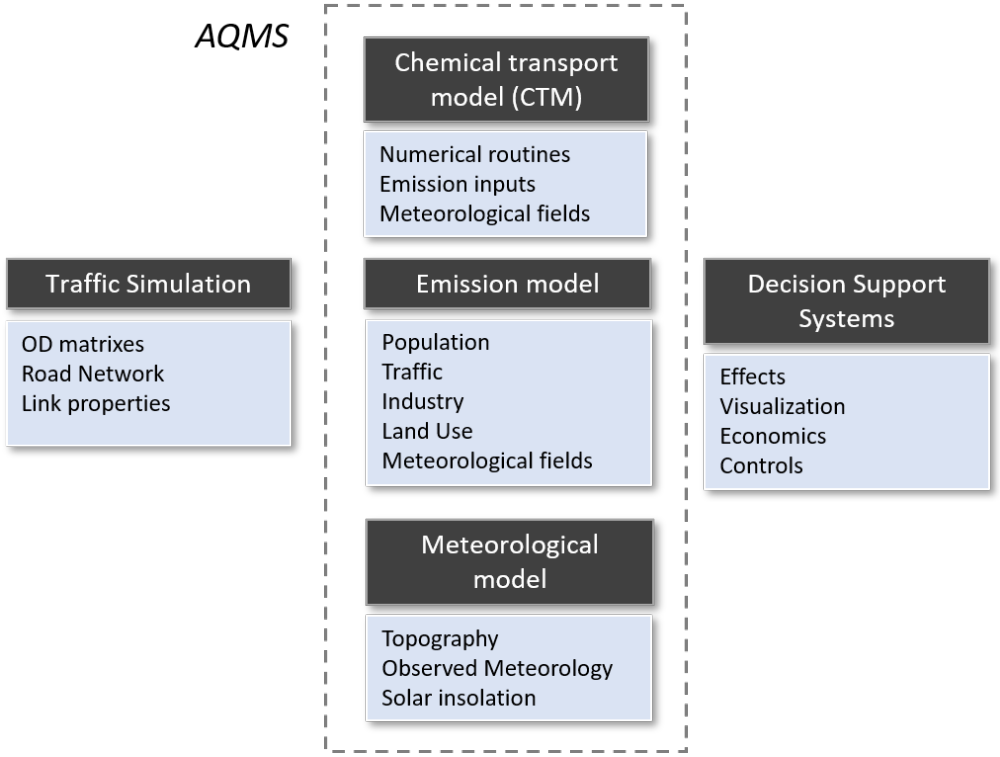

Figure 2.1: Interaction between the different modelling tools used in an air quality modelling system. Adapted from Russel and Denis 2000.

2.2. Traffic simulation

A traffic simulation model is composed by three main components: (i) the transport demand model, (ii) the supply model and (iii) the traffic assignment method. The transport demand model gives the magnitude of the total travel demand on the network. It establishes how many trips originate in a certain -previously defined- transport zone and arrive at another zone based on the Origin-Destination (OD) matrices. The defined transport zones will eventually generate and attract trips that will propagate flow along the available network entities (e.g., links, nodes), according to specific attributes and parameters (e.g., link capacity, number of lanes, the volume-delay function, ...) which limits the flow movement. This is done by the traffic assignment method during the (i) route-choice and (ii) network loading processes (Fig. 2.2). The route-choice defines which routes will be considered by each OD pair, or in other words: define how travellers choose their routes. The most common hypothesis used in transport modeling is the user equilibrium based on the Wardrop's first principle (Wardrop and Whitehead, 1952). This hypothesis assumes that every traveler chooses the route that is faster for him considering the current traffic conditions, regardless of the system optimum (Barceló, 2010).

Based on the routes selected by the route-choice, the traffic assignment loads the demand model (i.e., the OD pairs) and computes the traffic flow over the different network links (network loading process). This is done by computing the *cost* of each possible route. The cost is a unit that gives a common value to the distance, price (i.e., the economic value) and the time of each route so they can be compared. The distance and price are already defined by the total kilometers or the possible tolls on the way. But the time is flow dependent (i.e., a user will take more time to cross a congested street). The traffic flow-time dependence is defined by the route impedance parameters or capacity restraints. The impedance warranties that an increased flow in a link will end up with an increased travel time (i.e., cost). In macroscopic simulation, the two most important capacity restraints are the link capacity and the Volume delay Function (VdF). These express travel time T as function of flow q. The *Bureau of Public Roads* (BPR) power function shown in equation 2.1 and Fig. 2.3 is one of the most popular VdF functions and the one used in the BCN-VML model of this thesis (Maerivoet and De Moor,

2005).

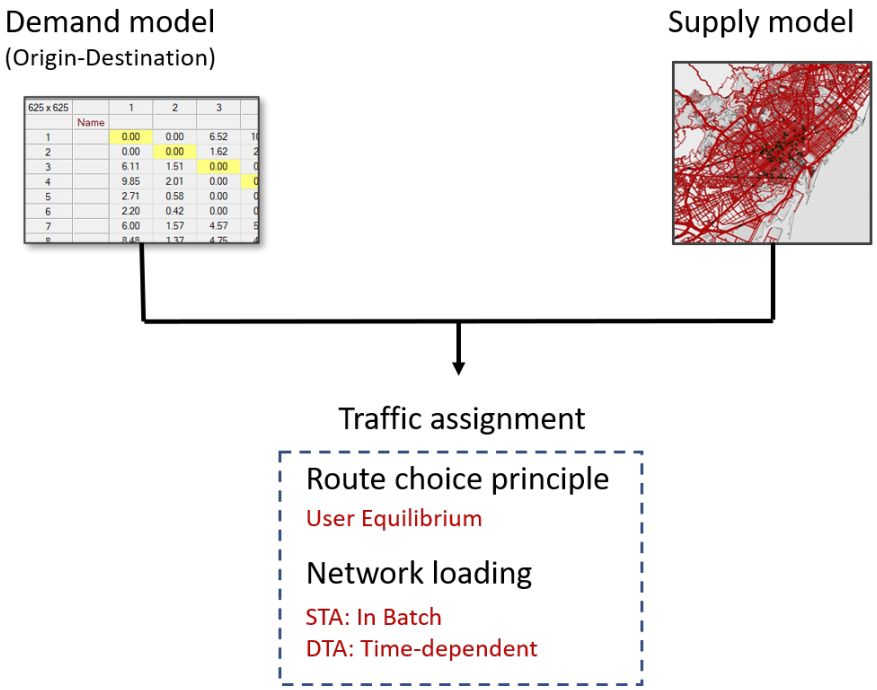

Figure 2.2: Scheme of a traffic model parts

$$T = T_{ff}\left(1 + \alpha\left(\frac{q}{q_{pc}}\right)^{\beta}\right) \tag{2.1}$$

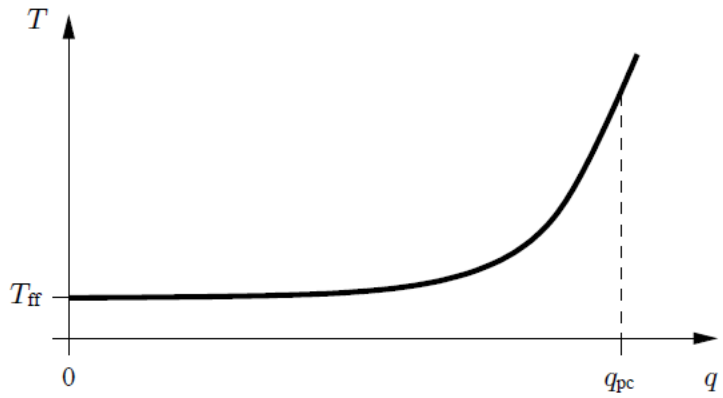

Figure 2.3: The Bureau of Public Roads function, relating travel time to traffic flow. It is based on the travel time at free flow conditions T_{ff} and the saturation capacity q_{pc} of the link (Maerivoet and De Moor, 2005). The function expresses how the travel time does not increase with traffic flow while the link is at free-flow conditions. When higher flows occur at the link (i.e., congestion situation) the coefficient β determines the threshold at which the BPR function rises until it reaches the link saturation capacity q_{pc}

Once the total route costs are defined, the network is loaded in an iterative process where all the demand is launched in a batch exercise per iteration. For each iteration, traffic flow is assigned and redistributed to all available routes and, if necessary, new routes are considered until all traffic routes are in equilibrium (i.e., same cost for all). This occurs in a steady-state or stationary condition known as the Static Traffic Assignment (STA). A more detailed and complex modelling methodology considering traffic time dependencies also exists, the Dynamic Traffic Assignment (DTA).

The DTA algorithm is time dependent, it considers the paths and the demand proportion loaded in the network for each time period (based on time dependent OD matrices). During the network loading process, the DTA describes how flow propagates with time along the network within the previously selected routes. This process is computationally more expensive and data demanding than the STA, so it is usually used for medium to small domains. When a DTA method is based on the user equilibrium principle, it is known as a Dynamic User Equilibrium (DUE), a very common algorithm in traffic modelling systems.

2.2.1 Computation of vehicle dynamics in traffic simulation

How vehicle dynamics are computed responds to the level of aggregation of link-level vehicle data. In this sense, there are three standardised levels from lower to higher level of detail: Macroscopic, mesoscopic or microscopic. Macroscopic traffic models describe traffic in an aggregate manner at link level, such an homogeneous fluid (e.g. average speed and flow per link), able to simulate road speeds and flows by physical concepts or analytical methods, but unable to predict single vehicle speed and behavior. The mesoscopic simulators combine elements from the microscopic and macroscopic approaches. These simulators have different approximations; generally, they represent the paths and interactions of each vehicle with less detail, but enough to characterize some traffic dynamics essentials (e.g., nº of stops per link). Finally, microscopic traffic models simulate all dynamical parameters of each vehicle on the network (i.e., acceleration, deceleration, lane changes...) at a very high temporal resolution (in the order of seconds, or less) as a response with its needs and the surrounding traffic, assisted by some behavioral models such as car following, lane change, merging and yielding (Linares, 2014). These models can provide the drive cycle of each vehicle (e.g., instantaneous speed curves) which is needed to estimate instantaneous vehicle emissions, explained on section 2.3. The computational load and data required to simulate such level of detail for each vehicle on the network limits the application of microscopic traffic simulators to specific areas of the city or hot spots. Note that although the traffic assignment methodology (STA/DTA) is independent to this level of vehicle-data aggregation, due to the shared data and computational requirements usually DTA go in hand with microscopic and mesoscopic models, while STA is used for macroscopic approaches in large scale networks.

2.2.2 Review of traffic simulators

On this section, we give a brief description of the most important traffic simulators (summarised in Table 2.1) followed by the description of the traffic modelling tool used in this Ph.D thesis.

VISUM

Visum is a GIS-based macroscopic multi-modal model developed by PTV able to simulate public and private transport travel demand (PTV Group, 2019). Visum is mostly used for transport planning in large transport networks, to estimate travel demand, transit changes and public transport services. The model integrates several impact inner models to to analyse and evaluate the transport system. These includes a user model, able to estimate travel behaviour of public transport passengers and car drivers (e.g., traffic volume, number of transfers, service frequency, etc), an operator model which determines operational indicators of a public transport service (e.g., revenues, number of kilometers) and an environmental impact model. All the input data needed by the model is defined in the network and the demand model. The first is composed by the nodes -which represent intersections or public transport stops-, the links and their attributes (e.g., link capacity, VdF), the turnings and their attributes (e.g., turning penalties) and the public transport lines. The demand model is composed by the Origin Destination matrices (OD) and the logit model choice which splits the trip chain into specific modes of transport (Friedrich, 1999).

TRANSYT

TRANSYT (TRAffic Network StudY Tool) model was developed at the Transport Research Laboratory (TRL) in Britain. TRANSYT is a macroscopic deterministic simulation and optimisation model that simulates traffic as cycle flow profiles (CFP) and traces the flow of the CFP from link to link along the network. It considers traffic signals by the systematic changes to the offset, their phase split and cycle length. The associated traffic conditions are estimated through a performance index (PI) which is a linear combination of the vehicle delay and the number of vehicle stops (Ratrout et al., 2009).

Vissim

Vissim is a microscopic time-step and behavior-based traffic simulation system developed by PTV that models both motorway and urban traffic operations. It can estimate private and public transport mobility but indeed it simulates particular pedestrian movements and their different usage of public transport. The model is divided into three blocks plus one more for the output data storage. The first

block contains all the infrastructure data, including sign posts, parking facilities and road and railway infrastructures. The second block contains all technical features of a vehicle, traffic flow specifications and routing, public transport lines are also defined within this block. Finally, the third block contains all traffic control elements, not-signalized intersection rules and traffic signs are contained within this block. During simulation, the three independent blocks are constantly activated and interacting with each other (Barceló, 2010). The traffic simulator included in Vissim is a microscopic traffic flow simulation model which includes car following -based on the Wiedemann model- and lane change logic (CHEN and YU, 2007).

Paramics

Paramics is a DTA microscopic model developed in 1997 by SIAS Ltd. and Quadstone Ltd. of Scotland. It incorporates a car following and lane-changing model based on parameters representing the driver's behavior and a generalized cost equation to estimate the route choice (Misra et al., 2013). Paramics is designed for a wide range of applications where traffic congestion is the predominant one, with visual capabilities and good simulation performance. It can be used for a wide range of network sizes, including national scenarios. Vehicle to vehicle interactions are based on vehicle following, gap acceptance, and vehicle kinematics while the traffic demand is generated from an origin-destination matrix (OD_t) (Krogscheepers and Kacir, 2001). Besides the most normal traffic simulation applications, Paramics can also draw roundabouts, public transportation plans, car parking or different incidents that might occur.

MATSim

MATSim (Multi-Agent Transport Simulation) is an open-source microscopic traffic simulation model. The framework of MATSim is designed for large-scale scenarios, with a network loading implementation based on queue model instead of the more complex and computationally expensive car-following model, which is more common among microscopic traffic simulation models. The route-choice process is done by an inner-model, the MobSim (mobility simulator) whose process is similar to a DTA: It considers time, mode or destination choice into the iterative loop. At

every iteration, each agent memorizes the cost of the route they took, and for the next one, the agent selects a route choice from its memory. The iteration is finally completed by evaluating the agent's experiences by the calculated day routes and finished when the average population cost stabilizes (Horni et al., 2016). Besides MobSim, in MATSim two other mobility simulators can be plugged in, or the user could plug external ones, which confers the model good flexibility.

Aimsun Next

Aimsun microsimulator prototype was originally developed by members of the former LIOS (Simulation and Operations Research Laboratory) at the Polytechnic University of Catalonia (UPC). It later became Aimsun Next, a fully integrated application that fuses travel demand modeling, macroscopic functionalities and the mesoscopic-microscopic hybrid simulator (Aimsun S.L., 2019). The microscopic level is composed of several sub-models which make up the core of AIMSUN behavior, to mention as the most important: lane changing, gap acceptance for lane changing and yielding, overtaking and car following (Anya et al., 2014). This last one, based on the safety distance model proposed by Gipps (Gipps, 1981), is the major internal behavior model, which depends on vehicle dynamics (Madi, 2016). AIMSUN can also evaluate Intelligent Transportation Systems measures like variable speed policies and the application of a toll and road pricing.

2.2.3 The BCN-VML traffic model

The traffic model used in this thesis is based on the detailed multimodal transport model Barcelona Virtual Mobility Lab (BCN-VML), which uses the PTV Visum platform (Montero et al., 2018). The BCN-VML was developed within the framework of the Cooperative Automotive Research Network (CARNET) initiative (CARNET, 2017), a knowledge hub for automotive science and technology, in collaboration with SEAT, PTV IBERIA, Volkswagen Group Research and the Universitat Politècnica de Catalunya (UPC).

The BCN-VML road network was built based on geographical maps from HERE (Here, 2020), with manual edition for specific areas. It has a hierarchy of 10 different link types which hold different road capacities, speed limit and Volume

Table 2.1: Comparative analysis of currently used microscopic and macroscopic traffic simulation software. Adapted from Ratrout et al. (2009).

Model Name	Scale	Main Features	Reference
Visum	Macro	GIS-based, large-scale networks, public-transport, intermodal, user operator and environmental impact models	PTV Group (2019)
TRANSYT	Macro	Traffic simulated as traffic flow profiles (CFP), traffic signal, traffic conditions	of Florida (2021)
Vissim	Micro	Surface streets, freeways, ramp metering, pedestrians, transit operations, 3-D animation	PTV AG, 2011
Paramics	Micro	Surface streets, freeways, transit operations, 3-D animation, roundabouts, congested networks.	Paramics (2021)
MATSim	Micro	Open-source, large scale scenarios, network loading based on model queue, route choice by MobSim	MATSim (2021)
Aimsun Next	Micro	Surface streets, freeways, actuated signals, dynamic traffic assignment, variable message signs, 3-D animation, telematics.	Aimsun S.L. (2019)

Delay Function parameters according to vehicles ease to cross the link (e.g., due to a green wave traffic light, street with pedestrian's priority) (Table 2.2). The VdF used is the BPR function previously described (slightly adapted in equation 2.2), with a modification to further increase the link impedance when saturation is achieved (i.e., sat ≥ 1) referred as BPR2 (equation 2.3). The demand model is based on OD matrices, whose data was obtained from mobile phone KINEO (Kineo, 2017) from March 2017. The original KINEO matrices were treated and fused with the EMEF public survey (ATM et al., 2015) as described in (Montero et al., 2019) in order to obtain the daily private transport OD matrix used in this work. In order to disagregate the obtained 24h private transport matrix into hourly matrices, we used hourly traffic flow profiles obtained from local traffic loop detectors. Public transport (bus line routes, stops and frequencies) were built according to the public transport data of the Metropolitan Area of Barcelona (TMB, 2019).

BPR

$$T = T_{ff}(1 + a \times sat^b) \tag{2.2}$$

Table 2.2: Specification of the different link types and their impedance variables: maximum speed (km/h), lane capacity (nº vehicles), volume delay function and its parameters (a, b, b', c).

Road name	max speed [km/h]	lane capacity	VdF	a	b	b'	c
Highway	120	1500	BPR2	3	5.7	6	1
Ronda	80	1200	BPR2	2	4.6	5	1
Road	80	800	BPR2	2	4.6	5	1
Priority urban corridor	50	900	BPR2	1	3.2	4.16	1
Urban corridor	50	650	BPR2	1	4.6	6.18	1
Priority urban street	50	840	BPR2	1.72	1.06	5.26	0.98
Urban street	50	500	BPR2	1.72	1.06	5.26	0.98
Zone 30	30	300	BPR	1	0	-	1
Superblock	10	300	BPR	1	0	-	1
Rural road	30	100	BPR2	1.72	1.06	5.26	0.98

BPR2

$$T = \begin{cases} T_{ff}(1 + a \times sat^{b}) & \text{if } sat \leq 1 \\ T_{ff}(1 + a \times sat^{b'}) & \text{if } sat > 1 \end{cases} \text{ where } sat = \frac{q}{q_{max} \times c} \tag{2.3}$$

The BCN-VML working domain comprises the First Crown of the Metropolitan Area of Barcelona plus a large extension including its access highways (Fig. 2.4 a,b). The demand model of BCN-VML is composed of almost 4 million trips, distributed in a network of 265,000 links and 625 zones. Figure 2.5 shows part of the 625 zones defined in the VML network, and part of the OD matrix used (625 × 625). As observed, the areas with higher population density (mainly in Barcelona) have smaller OD zones for a better OD pair distribution, while the cities around Barcelona are composed of larger OD zones. For computational time optimisation, two working domains with different levels of detail are used. The first one covers a large area of around 6,000km^2. This domain is less detailed and is mostly focused on highways and national roads (Fig. 2.4a,b). The second domain, which is the area studied on the thesis, comprises a detailed build of Barcelona and 17 municipalities surrounding the city, gathering a population of more than two million inhabitants (Institut d'Estadística de Catalunya, 2019) (Fig. 2.4c). The wider domain allows the BCN-VML to properly diverge the traffic into the different accesses of the city. In this way we avoid forcing the entrance through

a particular city access according to its adjacent outflow zone, without adding an excessive load to the simulation. As seen on section 1.6.1, this is relevant due to the high connection traffic associated to the inner city.

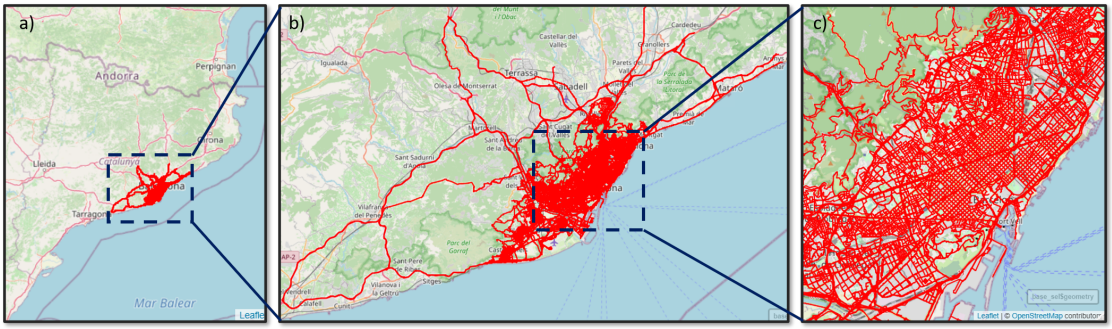

Figure 2.4: VML network within a) the region of Catalonia, b) the largest domain including highways and all access roads and c) the most detailed domain where the thesis analysis take place.

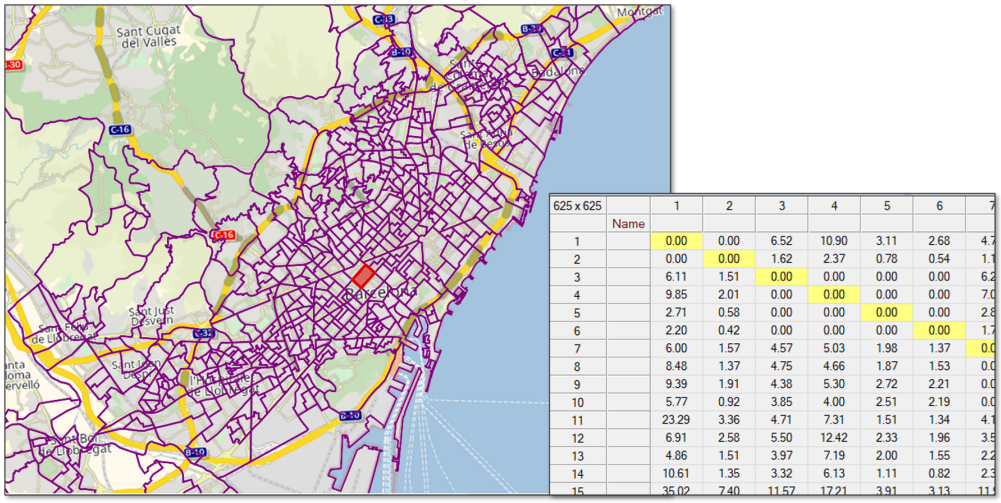

Figure 2.5: Representation of the VML zones (purple areas) and part of the origin-destination (OD) matrix.

2.3. Vehicle emission modelling

Vehicle emission models were developed to analyse the efficacy of transport policies and traffic management strategies in reducing vehicle emissions. After a pollution episode in California (Moore and Moore, 1976) it was necessary to have an emission inventory to estimate the pollutant sources. From this situation one of the first vehicle emission models came, the EMFAC (California Air Resources Board, 2021).

As commented on section 1.3, the vehicle's engines generate a set of various pollutants (e.g., CO, HC, NO_x, PM, CO_2,...) which can come from different sources associated to vehicle's emissions: hot and cold-start exhaust, evaporative and PM from wear processes and resuspension (more details of these emission processes can be found in section 1.3). In a vehicle emission model, the associated emissions of these processes are parametrized by different equations according to the level of aggregation of vehicle dynamics and the methodology followed. The level of aggregation of vehicle dynamics goes from an average vehicle speed and total traffic flow per segment for macroscopic models to instantaneous speed per vehicle for microscopic models. Macroscopic vehicle emission models usually require the average speed over time, the vehicle flow per road segment and a vehicle fleet composition, which may include: Vehicle type, age, engine fuel and power and/or the emission technology. These models estimate emissions adopting emission factors which correlate the grams per kilometer of pollutant with the speed for each specific vehicle class. Examples of this type of models include COPERT (EEA/EMEP, 2017) and MOBILE (U.S. EPA, 2003). Mesoscopic modelling approaches are also based on emission factors that depend on vehicle speed, but they also include the traffic state in the emission estimation process. To properly classify the traffic state, these models require qualitative variables such as congestion level, road type or the number of stops. According to this data, they assign the link segment to a particular (and already pre-defined) traffic state which has specific emission factors. As a consequence, the average emission rates used are not only speed-dependant but also traffic-condition dependant. This is the case of traffic-situation models like HBEFA (Matzer et al., 2019), which use different driving operating modes besides the average speed to determine emissions. Finally, microscopic emission models consider instantaneous speed profiles (i.e. drive cycle) of each vehicle. These consider second-by-second speed, acceleration, deceleration, idling and cruising, with different approaches depending on the model. For instance, Versit + works with driving cycle variables (e.g. idle time, average speed, kinetic energy) (Smit et al., 2007). However, other models such as PHEM (Hausberger et al., 2009a), PHEM-Light or CMEM (An et al., 1997b) work with the Vehicle Specific Power (VSP) over time. Under this approach emission factors are dependent on the estimated instantaneous power performed at each second (Song et al., 2012) which is computed with specific vehicle data (e.g. vehicle weight, gear intervals) and the drive

cycles. Since microscopic emission models consider instantaneous vehicle dynamics, they are sensitive to the different transient operations and provide a higher temporal resolution for the emission estimation. This is particularly important to reproduce emission peaks during rush hours due to the start-stop occurring during congestion events, where the emission factors are the highest, as shown in Fig. 2.6.

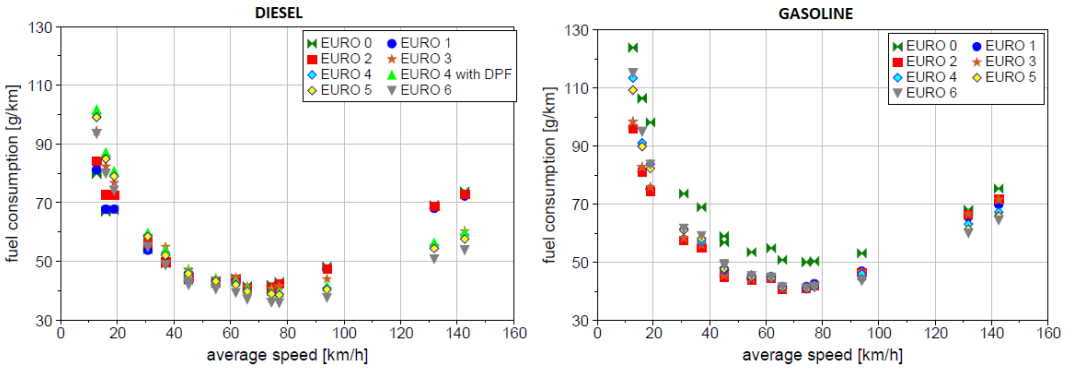

Figure 2.6: Specific fuel consumption for a selected set of cycles for passenger cars (Hausberger et al., 2009b)

2.3.1 Review of vehicle emission models

On this section, we give a brief description of the most important vehicle emission models (summarised in Table 2.3) followed by the description of the vehicle emission model used in this Ph.D thesis.

MOVES

MOVES, Multi-scale mOtor Vehicle & Equipment Emissions System is a modal emission model developed by the EPA that estimates traffic states, emission factors and inventories based on historical data of the EPA. The user defines the type of vehicles, the period, the vehicle engine characteristics, the road type, the geographical area and the pollutants. The model already contains a database with five main operating modes (idle, acceleration, cruise, deceleration and cold-start) that become 23 when it considers the different engine size and fuel use. MOVES assigns the emission factor per vehicle type under a specific operating mode (Zhang and Ioannou, 2016). The workflow of MOVES is useful when the user wants to estimate the vehicle emissions in a certain area of the US, as the model takes the

average behavior of a certain vehicle type in the county or the entire US registers.

COPERT

The COmputer Program to calculate Emissions from Road Transport is an average speed vehicle emission model integrated into the EMEPE/EEA methodology for emissions computation. The database of vehicle categorisation in COPERT is composed of more than 400 vehicles, including passenger cars, light duty vehicles, heavy duty vehicles (with busses), mopeds and motorcycles. The methodology followed by COPERT allows the estimation of vehicle fleet emissions at regional level, without the need of an extensive and detailed traffic data. COPERT estimates hot and cold-start exhaust, PM wear and evaporative emissions (EEA/EMEP, 2017). The emission factors algorithms calculated by COPERT are expressed as non-linear and continuous functions of the mean travelling speed over a complete drive cycle, specific for every vehicle type, Euro class, fuel usage, or engine capacity classes.

PHEM and PHEMLight

PHEM, Passenger car and Heavy duty Emission Model, is a microscopic modal emission model which generates instantaneous fuel consumption and emission factors based on the vehicle engine power. This is calculated from the driving resistances and the losses in the transmission system and several other longitudinal dynamics of the vehicle. PHEM contains an internal database with more than 1000 measures of vehicles for different drive cycles (Tielert et al., 2010) in both laboratory and on road tests from the ERMES group (European Research for Mobile Emission Sources). As model inputs PHEM needs the vehicles drive-cycle, the road grade, the fleet composition and the cold-start coefficients. From the vehicle drive-cycles, PHEM computes the actual engine power demand based upon the driving resistances and losses, the engine speed and transmission ratios from the gearshift model. With the engine power and speed it calculates the emissions and fuel consumption based on steady-state engine maps (Boulter et al., 2007). PHEM also has a cold-start tool based on heat balances and emission maps for cold-start extra emissions and a SCR module to correctly simulate NO_x emissions of vehicles equipped with SCR after treatment system (Hausberger et al., 2009b).

PHEMlight is a simplified version of PHEM developed to work with SUMO, a microscopic traffic simulator developed in the framework of the COLOMBO's project (Hausberger and Krajzewicz, 2009). PHEMLight simplifies the transient dynamic corrections, the temperature influence on the after-treatment-systems and the gear shift model that computes engine speeds that the full version of PHEM offers. The rest of the vehicle emission calculation is done exactly as PHEM: estimating the engine power using the driving cycle, road grade and vehicle fleet (Fig. 2.7).

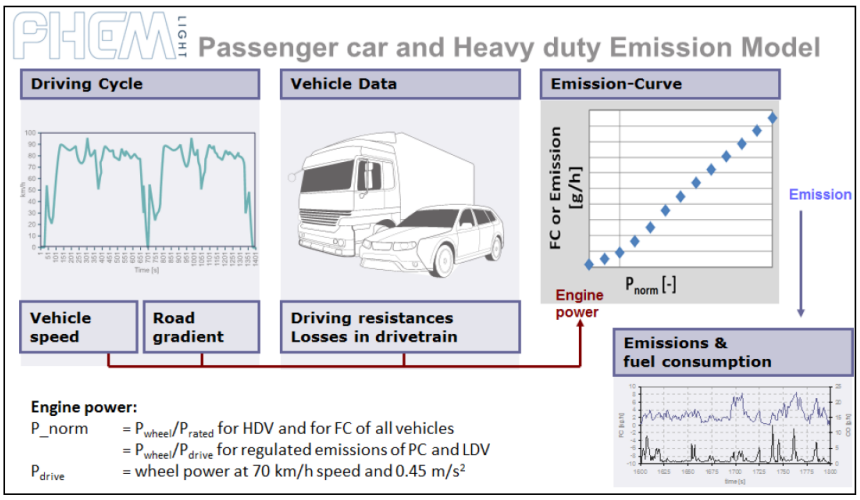

Figure 2.7: PHEMLight schematic workflow (Hausberger et al., 2009b)

Versit+

Versit+ is a microscopic cycle-variable model, developed in the Netherlands by TNO. It computes vehicle emissions by multivariate regression functions based on a large amount of vehicles in different driving cycles and traffic conditions (Ligterink, 2009). Versit+ contains a database of 246 vehicle categories that are used with the driving cycles provided to define a model class (Smit et al., 2007). The model uses the different parameters of each driving cycle (e.g., speed, acceleration, maximum speed, etc) and the generated model classes to predict by a statistical optimisation software the average emission values of the different driving cycles for each vehicle category and pollutant.

Table 2.3: Summary and characteristics of different traffic emission models

Model Name	Scale	Model type	Pollutants evaluated	Reference
Versit+	Micro/ meso	Cycle-Variable	CO, HC, NO_x, PM, FC, CO_2	Smit et al. (2007)
MOVES	Meso	Data-driven	CO_2, NO_x, PM, CO, HC, PM	U.S. EPA (2014)
CMEM	Micro	Modal emissions	CO, CO_2,NO_x, HC, FC, PM	An et al. (1997a)
PHEM	Micro	Modal emissions	CO, CO_2, NO_x, NO,HC, FC, PM	Hausberger et al. (2009a)
PHEMlight	Micro	Modal emissions	CO, CO_2,NO_x, NO,HC, FC, PM	Hausberger and Krajzewicz (2009)
HBEFA	Meso	Traffic situation	CO, CO_2,NO_x, NO,HC, FC, PM	UT Graz (2019)
PAP	Micro	Power based	FC, CO_2, NO_x	Smit (2014)
VeTess	Micro	Power based	FC, CO, CO_2, HC, NO_x, PM	Beckx et al. (2007)
VT-Micro	Micro	Regression	FC, CO, CO_2, HC, NO_x, PM	Rakha et al. (2004)
COPERT	Macro-Meso	Average speed	FC, CO, CO_2, HC, NO_x, PM,	EMISIA (2016)

2.3.2 The HERMESv3 emission model

The emission model used to compute emissions from all natural and anthropogenic sources in this work is the High-Elective Resolution Modelling Emission System version 3 (HERMESv3) developed at the Barcelona Supercomputing Center (Guevara et al., 2020).

For the Iberian Península and Catalonia region HERMESv3 estimates anthropogenic emissions at high spatial (e.g. road link level) and temporal (hourly) resolution using state-of-the-art and bottom-up calculation methods that combine local activity and emission factors along with meteorological data following the Selected Nomenclature for Air Pollution (SNAP) with 2010 as the reference period (Guevara et al., 2019). At the European domain, anthropogenic emissions are estimated using two regional emission inventories, TNO-MACC_III (Kuenen et al., 2014) and the EMEP (EMEP, 2021). The emission data library comprises gaseous (NO_x; CO; non-methane volatile organic compounds, NMVOC; SO_x ; NH_3) and particulate (PM_{10}; $PM_{2.5}$; black carbon, BC; organic carbon, OC) air pollutant

emissions (Guevara et al., 2019). The model output consists of hourly, gridded and speciated emissions according to the CB05 chemical mechanism used by the CMAQ chemical transport model of CALIOPE.

For the road transport sector, HERMESv3 behaves as a macroscopic average speed vehicle emission model which computes hourly exhaust (hot and cold-start), and non-exhaust emissions (tire, road and brake wear and resuspension) per vehicle category and road link for all criteria pollutants. A total of 491 vehicle categories are considered, discriminated by vehicle and fuel type, Euro category, engine power and gross weight class. Hourly emissions are computed through the application of temporal profiles (i.e., daily, weekly, monthly) to the estimated emissions. Exhaust and wear emissions are computed using the vehicle and speed dependent emission factors reported by the Computer Program to calculate Emissions from Road Transport version V (COPERT V) (EMISIA, 2016), which are included in the tier 3 approach of the European emission inventory guidelines EMEP/EEA (EEA/EMEP, 2017). Emissions from resuspension processes are estimated using vehicle type dependent emission factors (i.e. motorcycles, passenger cars, light duty vehicles, heavy duty vehicles), which were derived from a measurement campaign performed in Barcelona (Amato et al., 2012). The temperature effect on emissions considered by the cold-start is based on the hourly temperature data from the Copernicus ERA5 dataset (C3S, 2017). Finally, The fleet composition profiles used by HERMESv3 for Barcelona are derived from a remote-sensing campaign performed in Barcelona in 2017 (AMB and RACC, 2017)) and information provided by the Barcelona's Port Authority (Port de Barcelona, 2017).

With the objective of assessing the performance of the emission model, we compared the COPERT V NO_x emission factors used in HERMESv3 against measured-based NO_x emission factors derived from a Remote Sensing Device campaign performed in Barcelona in 2017 (AMB and RACC (2017)). The results of this comparison are shown in Fig. 2.8 and show a good agreement between the modelled and measured emission factors for all diesel vehicles, while it underestimate by more than half in some cases for the petrol vehicles. Yet, the absolute apportionment of NO_x emissions from petrol vehicles is between four and five times lower than for Diesel.

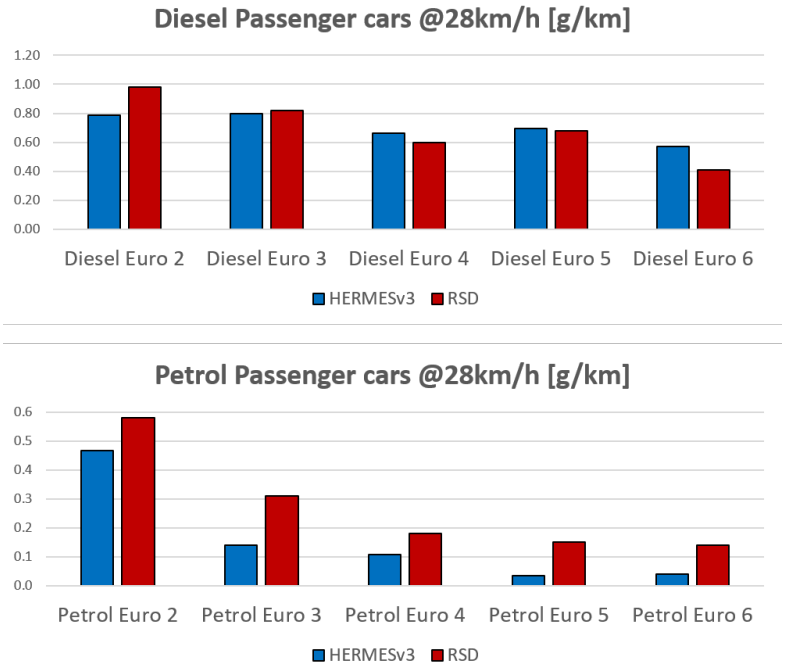

Figure 2.8: Comparison of the NO_x emission factors from HERMESv3 and the measured during the 2017 remote sensing device campaign in Barcelona. The emission factors are obtained from a representative urban drive cycle at an average speed of 28km/h.

2.4. Air quality modelling

Air Quality Modelling Systems (AQMS) compute primary and secondary pollutant concentration values at a given location and time by estimating the formation, accumulation, transport and removal of air pollutants between the emission sources and the receptors (Fallah Shorshani et al., 2015b). To do so, an AQMS is composed by (i) an emission model which describes the temporal behaviour and spatial variability of the sources generating air pollutants; by (ii) a meteorological model which characterise the atmospheric conditions at which air pollutant dispersion occurs; and by (iii) a chemical transport model (CTM) that computes the physical and chemical transformations that occur to the emitted pollutants under the specific estimated meteorological conditions (Fig 2.1). CTMs are the core of the emission interaction with the atmosphere, a crucial component in the AQMS process which define the final output resolution. CTMs can be approached by different methodologies according to the spatial and temporal resolution, available data and computational resources: from a lower to a higher complexity and resolution there

are the box models, Lagrangian models, Eulerian models, Gaussian models and Computational Fluid Dynamics models.

Box, Lagrangian and Eulerian modelling approaches

In this sense, the simplest CTM approximation is by a Box model, where concentration values are considered as homogeneous within the modelling domain (i.e., the box). The emission, chemical and physical processes occur within the domain based on the conservation of mass. To work with larger domains while following pollutants trajectory over time, Lagrangian and Eulerian models are the most common approaches. Lagrangian models work with the same methodology as the the Box model, but the computational process considers the trajectory of the Box as it moves downwind. Eulerian models study the pollutant flow as an homogeneous element of volume going through a 3D gridded mesh. Mass conservation equations are solved in an iterative way for each grid cell as the flow volume moves downwind, taking as input the meteorological variables previously calculated by a meteorological model. These type of models can deal with a large number of sources due to the fixed gridded 3D system and the iterative solving process (Fallah Shorshani et al., 2015b).

Gaussian modelling approaches

In a higher level of detail, the near-source dispersion models use Gaussian distributions in the vertical and horizontal directions under steady-state conditions (Holmes and Morawska, 2006). This approach is based on the assumption that without the presence of obstacles and under stationary atmospheric conditions, the Gaussian distribution is a good approximation of the atmospheric dispersion processes. However, since Gaussian equations assume a constant meteorology, their application is limited to distances of less than some tens of kilometers from the source and time intervals of less than one hour. Partly due to their spatial limitation, Gaussian models are often nested with Lagrangian and Eulerian models for large domain representation. If a finer horizontal resolution is needed, Gaussian models can also be applied to urban environments with different approximations to deal with atmospheric dispersion around buildings. Yet, the approximation presents several limitations in intersections and buildings recirculation (Holmes and Morawska, 2006).

Computational Fluid Dynamics modelling approaches

Finally, the Computational Fluid Dynamics (CFD) models are the ones with finer resolution, which makes them ideal for urban environments. Yet, the high computational load that they require limits their application to small areas such a particular street, or a single stack plume. CFD models handle turbulence by the mass and momentum conservation Navier-Stokes equations in three dimensions. These can be solved by three different approaches: (i) Direclty (Direcy Numerical Simulations (DNS)), which requires a fine grid resolution and hence it is a very time consuming approach. By (ii) the Large-eddy Simulation (LES) approach, which separates turbulence into large and small eddies. LES is a simplified and faster approach than DNS, but it is still a slow methodology for air quality assessments. Finally, the fastest CFD approach is the (iii) Reynolds-Averaged Navier-Stokes (RANS), a time-average proxy to simplify turbulent flow. Since it is based in CFD it is still a time consuming CTM but its simplifications make it viable for air quality studies in small areas (e.g., Borge et al. (2018)).

The horizontal resolution that the CTM is able to achieve is essential when working at urban scales. As mentioned in Pay et al. (2014), a subgrid air quality variability -even at high resolution 1km scales- is not adequate in urban environments since emissions are artificially diluted over the gridded area. This assumption ignores the building canalization effect and the particular wind conditions along the streets. As a consequence, street gradient variations along the urban network are lost, and possible pollutant concentration peaks might be missed. Street-scale AQMS are then needed when modelling air quality values at urban locations. These models take as input local emission sources (e.g., traffic activity), meterologocial conditions (e.g., wind speed and direction from a urban meteorological station) and urban morphology (i.e., buildings ground plan and height) to compute street-scale air quality pollutant values. The finest CTM methodologies able to estimate street-scale dispersion are the Computational Fluid Dynamics (CFD) models and the Gaussian plume and street-canyon models previously commented.

2.4.1 CALIOPE and CALIOPE-Urban

CALIOPE

For the present work, we use the mesoscale CALIOPE-AQMS and the street-scale system CALIOPE-Urban. CALIOPE is an AQMS developed and mantained at the Barcelona Supercomputing Center (http://www.bsc.es/caliope/en?language=en) which provides a 48h high-resolution mesoscale air quality forecast over Spain for nitrogen dioxide (NO_2), sulphur dioxide, carbon monoxide, ammonia and total suspended particles (PM_{10} and $PM_{2.5}$ fractions). It works at a 12km horizontal resolution over Europe, 4km resolution over the Iberian Peninsula and a 1km resolution over Catalonia (Fig. 2.9a,b,c). CALIOPE is composed of the Weather Research and Forecasting (WRF) model version 3.5.1 with WPS version 3.9.1 (Skamarock and Klemp, 2008) as meteorological model, combined with the above mentioned HERMESv3 (Guevara et al. (2019); Guevara et al. (2020)) and the mineral Dust REgional Atmospheric Model BSC-DREAM8b (Basart et al., 2012) as the emission models and the Community Multiscale Air Quality Modelling System version 5.0.2 (CMAQ) as the CTM (Byun and Schere, 2005). CMAQ follows an Eulerian approach using the CB05 gas-phase chemical mechanism, the

AERO5 aerosol scheme, and an in-line photolysis calculation. The system has been applied in several works over Spain to better understand air quality dynamics and to estimate the pollution impacts of different air quality measures (Baldasano et al. (2011); Soret et al. (2014); Pay et al. (2014); Pay et al. (2019)).

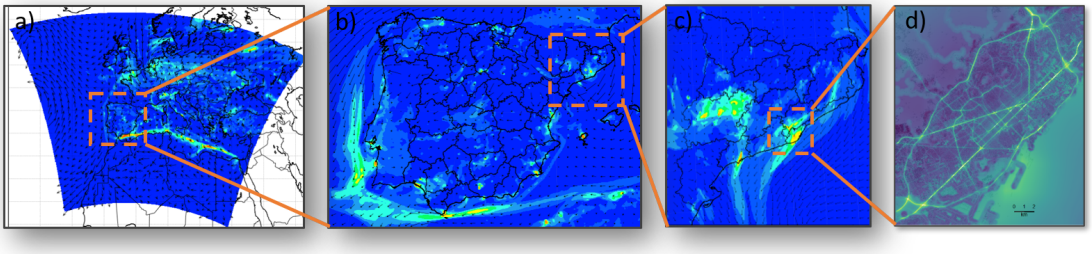

Figure 2.9: Different simulation domains of CALIOPE in a) Europe 12km, b) Iberian Peninsula 4km and c) Catalonia region 1km. In d) a CALIOPE-Urban simulation over the Barcelona domain at 20m resolution.

CALIOPE-Urban

CALIOPE-Urban is a street-scale dispersion model which allows to estimate local traffic dispersion driven by channelled street winds and vertical mixing considering background NO_2 and O_3 concentrations, atmospheric stability, and street morphology (Fig. 2.9d). This is done by coupling the CALIOPE mesoscale AQMS -which provides background concentrations and meteorological data- with the near-road Gaussian dispersion model R-LINE adapted to street canyons (Fig. 2.10) (Benavides et al., 2019). The model resolves the contribution of different point sources along a street segment (Snyder and Heist, 2013). To estimate NO_2 concentrations R-LINE applies the Generic Reaction Set (GRS) to resolve simple NO to NO_2 chemistry (Valencia et al., 2018). CALIOPE-Urban has already been applied to estimate the impact of excessive diesel NO_2 in Barcelona by Benavides et al. (2021a), and its results validated elsewhere (e.g., Benavides et al. (2019)).

2.5. Review of air quality modelling studies

The coupling of traffic-emission and dispersion models has already been applied to estimate the impact of traffic management strategies on emissions and air quality levels (Table 2.4). Borge et al. (2018) estimated the impact of the Madrid

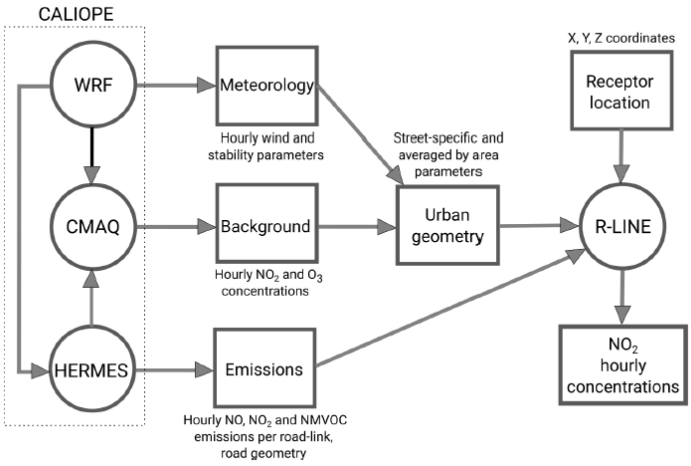

Figure 2.10: CALIOPE-Urban workflow. Models are represented by circles and data by boxes (Benavides et al., 2019).

NO_2 protocol using a multi-scale air quality model with a mesoscale approach ($1km^2$) for the citywide, and a street-level approach for one of the main streets in the city. Using different estimated traffic demand scenarios, their results showed that only the most restrictive measure would produce a noticeable air quality improvement (-25% in NO_x emissions). For the same pollution episode in Madrid, San Jose et al. (2018) performed a health impact assessment of the different traffic restrictions that came with the episode protocol. They used the microscopic traffic simulator SUMO together with the EMINO (emissions) and the WRF/Chem air quality modelling system at a horizontal resolution of 1 km. Although they expected traffic reductions up to -20% (-10% in NO_x) the health benefits found were marginal. Jensen et al. (2017) estimated the NO_2 concentration values in Denmark using a multi-scale air quality modelling approach. In this case, they combined the Danish Transport Model and GPS vehicle readings to estimate traffic volume and speed, respectively. This data was used by AirGis (Jensen et al., 2001) to estimate NO_2 concentration values at different resolutions with values that ranged between -27% and +12% from observations. The usage of traffic-emission models is also very common in the analysis of intersection configurations. In this sense, Qiu and Li (2015) analized the $PM_{2.5}$ exposure under three different intersection configurations using the AERMOD dispersion model. This was fed by the traffic emissions estimated by the MOVES model from USEPA. This model allows to estimate different geometric configurations without the need of

a traffic simulation since the model already contains standard American vehicle dynamics on its database. At a microscopic level, Stevanovic et al. (2015) combined the PTV-Visim traffic model with CMEM for signal timing optimisation in a 1.5-mile section. In this case, the microscopic approach was needed to play with different signal timings and observe their impacts on queue lengths, turnings and acceleration peaks. The study aimed at optimising mobility, with the safest and environmental-friendly configuration. Their results show that timings to improve safety and emission reductions coincide, but contradict mobility. Gori et al. (2015) used a mesoscale DTA traffic model -DYNAMEQ- in Brindisi (Italy) a town of 90,000 inhabitants, to obtain the link average speed, traffic flow, queue length, the free-flow speed and the link length. By a post-process of the DTA simulation data they divided each link in two segments: the free-flow part and the queued vehicles. The average speed of each segment was then passed to the emission factors provided by COPERT to obtain vehicle emissions under different scenarios. This methodology is able to differentiate the congested and non-congested parts of a link and assign the appropriate emission factors without adding much work-load to the system. Although the method still miss the acceleration peaks that occur during congestion (and its associated emissions), it is able to simulate different traffic management strategies and differentiate congested areas in a medium sized city using an average speed vehicle emission model. Another interesting simplification of DTA and microscopic traffic models is used by Zhou et al. (2015). He uses a lighter DTA model (DTAlite) where the linear car following model is simplified. This reduces computational time and allows the usage of a DTA in larger networks. The traffic data is used by a simplified version of MOVES emission model -MOVESlite- which considers a limited amount of vehicle types. Since the internal vehicle operating modes database that MOVES contains is reduced, MOVESLite reduces the emission rate search time in which the model is based and improves its efficiency. The applied simplifications allow to simulate different demand scenarios for a network of 20,200 links with a mesoscopic approach. In Barcelona, Rojas-Rueda et al. (2012) estimated the health effects of different modal shift scenarios were private transport users were shifting to public transport and cycling. For that study they did not perform a traffic simulation, emissions and air quality values were estimated with the Barcelona vehicle emission inventory and with the ADMS-Urban model to estimate pollutant dispersion. The higher health benefits

were found with the increase in physical activity, followed by the reduction of air pollution. Also in Barcelona, Mueller et al. (2020) studied the health impacts of the complete implementation of the Superblock idea on the city (500 Superblocks). They used the Street 5.2 air quality model (Kunz, 2005) estimating a reduction of 24% in the NO_2 concentration values assuming a 19% reduction in the private transport. They estimated 291 premature deaths due to NO_2 following a linear exposure-response function (Atkinson et al., 2018). Since the study followed a macroscopic approach obtaining the results at the city level, the most affected areas or streets as well as possible rebound effects were not identified.

The previous commented studies show different methodologies which combine the application of traffic simulators with emission models to estimate the impacts of different traffic restrictions or urban modifications. Although some of these studies use a higher level of detail in vehicle dynamics and emissions (e.g., DTA approaches, simplifications to reproduce congestion effect on emissions) they are however applied at street-scale level in small areas (e.g., specific sections or small cities) or they do not cover street-level resolution for the complete domain. The novelty of the work presented in this thesis lies in the large domain covered providing vehicle information, NO_x emissions and NO_2 levels at a street-scale level. This is achieved by decreasing the complexity of the traffic assignment by omitting individual vehicle dynamics, using an average vehicle emission model and a Gaussian street scale dispersion model instead of CFD. Over the next chapters we will provide details about the methodologies and the quality of the data used.

Table 2.4: List of relevant publications in international journals related to assess the air quality impacts of different traffic management strategies.

Topic	Modelling method	Reference
Madrid NO_2 protocol evaluation	Multi-scale: VISUM-COPERT-SMOKE Mesoscopic: Eulerian WRF-CMAQ Microscopic: RANS-CFD	Borge et al. (2018)
Health impact of Madrid protocol	EMINO WRF/Chem	San Jose et al. (2018)
Modelisation of NO_2 values in Denmark	Multi-scale: Local inventory-AirGis	Jensen et al. (2017) Jensen et al. (2001)
PM2.5 exposure at intersection	MOVES-AERMOD	Qiu and Li (2015)
Signal timing optimisation	VISIM - CMEM	Stevanovic et al. (2015)
Evaluation of traffic management strategies	DYNAMEQ-COPERT	Gori et al. (2015)
Health effects of modal shift	Local emission inventory ADMS-Urban	Rojas-Rueda et al. (2012)
Health impact of Superblock model	Local emission inventory Street 5.2 AQM	Mueller et al. (2020)

3. VML-HERMESv3: Developement of a coupled macroscopic traffic-emission system for Barcelona

This chapter is based on the following publications

D. Rodriguez-Rey, M. Guevara, M. P. Linares, J. Casanovas, J. Salmerón, A. Soret, O. Jorba, C. Tena, and C. Pérez García-Pando, (2021). A coupled macroscopic traffic and pollutant emission modelling system for Barcelona. Transportation Research Part D: Transport and Environment, 92:102725. ISSN 1361-9209. doi: https://doi.org/10.1016/j.trd.2021.102725.

D. Rodríguez-Rey, M. Guevara, M. P. Linares, J. Casanovas, O. Jorba, A. Soret, C. Pérez García-Pando. An integrated system to evaluate the impact of urban mobility -policies on air pollution in Barcelona. Euro Working Group on Transportation meeting, Paphos, Cyprus. 16-18 September 2020.

3.1. Introduction

Since the Ambient Air Quality Directive 2008/50/EC from the European Parliament was stablished, most of the European larger cities struggle to meet the AQD for NO_2 and PM (explained in detail in section 1.2). For the areas exceeding the AQD, it is mandatory to develop an Air Quality plan which establishes the steps to follow to reduce the pollutant levels and comply with the limit values. In the city of Barcelona, chronic nitrogen dioxides (NO_2) and fine particular matter ($PM_{2.5}$) concentrations exceed both the AQD limit values and the World Health Organization air quality guidelines (ASPB, 2020). Consequently, Barcelona and other large urban conurbations have been forced to apply action plans to improve their air quality by reducing traffic activity and emissions. Since the AQD encourages the use of numerical models in the evaluation of such air quality plans, the combination of traffic and vehicle emission models has become an extended practice to generate emission modelling inputs and derive traffic emissions at different scales (i.e macroscopic, mesoscopic and microscopic). While the precise definition of scales differs for traffic and vehicle emission models, in both cases they are related to the resolution of the vehicle dynamics, rather than to the spatial or temporal resolution (see sections 2.2 and 2.3).

Table 3.1 shows part of the extensive literature with case studies using a coupled traffic-emission system at different scales. It is generally accepted that traffic emissions derived from microscopic approaches using DTA are more accurate than those estimated with a macroscopic system, due to a better vehicle dynamics estimation, smaller time-step and ability to capture congestion behaviour. Some examples of the better performance of microscopic approaches compared to macroscopic can be found in Quaassdorff et al. (2016), Tu et al. (2018), Zhang et al. (2011) and Lejri et al. (2018). However, in contrast to the macroscopic approach, microscopic simulations are typically limited to very localized sites due to the detailed data needed by the traffic model and the high computational load required (Fallah Shorshani et al. (2015a); Tu et al. (2018); Lejri et al. (2018)), which hampers its applicability for traffic emissions evaluation at city or metropolitan level.

Table 3.1: Studies of vehicle emission models coupled with traffic simulators

Emission Model	Traffic coupling	Publications	
Versit+	VISSIM	Csikós and Varga (2012) - Comparison Versit+ with COPERT in a motorway. Madrid.	Quaassdorff et al. (2016) - Comparison COPERT with Versit+ in a roundabout. Madrid
	Paramics	Madireddy et al. (2011) - Speed limit reduction and traffic signal coordination	
MOVES	VISSIM	Abou-Senna et al. (2013) - Different approaches to capture environmental impacts (AVG, LDS, OPMODE).	Zhang and Ioannou (2016) - Environmental impact of variable speed limit. MOVES vs CMEM
	Paramics	Chamberlin et al. (2010) - Emissions from intersection control change. MOVES vs CMEM	Bartin et al. (2007) - Electronic toll collection
CMEM	VISSIM	Stevanovic et al. (2009) - Optimization traffic control.	Zhang and Ioannou (2016) - Environmental impact of variable speed limit. MOVES vs CMEM
	Paramics	Amirjamshidi et al. (2013) - Pollutants dispersion and population exposure.	Misra et al. (2013) - Air quality modelling morning peak emissions downtown Toronto
PHEM	VISSIM	Hirschmann et al. (2010) - Urban arterial, center of Graz	Tielert et al. (2010) - Traffic light vehicle communication evaluation
PHEMlight	SUMO	COLOMBO - Cooperative Self-Organizing System for low Carbon Mobility at low Penetration Rates	
HBEFA	Mat-SIM	Hülsmann (2014) - Thesis Integrated transport model Munich	
PAP	Local traffic data	Smit (2014) - Development of PAP	
VeTess	Local traffic data	Beckx et al. (2007) - Speed management policies evaluation	Int Panis et al. (2011) - Emission reduction from speed management policies
VT-Micro	Metanet	Zegeye et al. (2010) - Integration of macroscopic traffic with micro emission model	
VSP	VISSIM	Fontes et al. (2015) - Road traffic emission estimation in Aveiro.	Borrego et al. (2016) - Urban scale AQ modelling. VSP with COPERT for HDV
	AIMSUN	Anya et al. (2014) - Emisions study of 2 mile arterial corridor	

3.1.1 Review of studies using different input parameters

Despite some of the inherent limitations of a macroscopic system, recent studies have shown that large improvements can still be achieved by focusing on a better representation of critical components such as the vehicle emission rates, vehicle activity patterns and vehicle fleet distribution. In the Île-de-France André et al. (2018) found as much as 14% and 11% more NO_x and VOC emissions when using the observed vehicle fleet composition compared to the registered one due to a higher presence of diesel vehicles. In Madrid, Pérez et al. (2019) also found a large difference between the fraction of observed (70%) and registered (47%) diesel powered vehicles. Grange et al. (2019) reported a large previously unaccounted temperature effect on emissions, with an estimated 38% average increase in NO_x diesel emissions in Europe. Results from this study are independent from the cold-start effect, which can additionally increase NO_x emissions by up to 39% and 166% for diesel and gasoline vehicles respectively (Faria et al. (2018)). Amato et al. (2014) showed that resuspension alone can contribute as much PM as tailpipe emissions, that with the addition of other non-ehxaust sources (e.g. road, tyre and brake wear) increase the total weight of non-exhaust over PM totals, as reported by Martini and Grigoratos (2014) and Rexeis and Hausberger (2009). However, often the estimated emissions are limited to exhaust (Chen et al. (2017); Fontes et al. (2015)), or non-exhaust wear emissions (Pérez et al., 2019), but few of them include also resuspension.

The coupling of traffic and emission models also allows to estimate the emission impact that different mobility policies could imply, since the traffic flow response to modifications on the network is also simulated. In Barcelona, traffic emissions are currently calculated with regional and local data inventories. The followed methodology is based on static traffic flow data and therefore it is unable to quantify the changes in mobility patterns induced by the application of traffic management strategies.

In this chapter, we present the development of a macroscopic traffic-emission coupled system tailored and tested for Barcelona using multiple sources of local data (e.g. GPS based measurements, traffic loop detectors or a remote sensing device campaign). The coupled system estimates high resolution traffic emissions

for the first crown of the Metropolitan Area of Barcelona, an area with more than two million inhabitants, a vehicle density of approximately 6,000 vehicles·km^{-2} and 26% of the daily trips done by private transport (Ajuntament de Barcelona (2020a)). The developed system is used to: (i) quantify hourly and street-level NO_x and PM_{10} emissions for the year 2017 and (ii) provide an extensive analysis of some key features implemented upon the emission calculation, including spatially-constrained vehicle fleet composition, meteorological influences, non-exhaust PM sources and public bus transport routing.

3.2. Methodology

For this study we use two macroscopic tools suitable for the large domain of the study. (I) The traffic model BCN-VML desccrived in section 2.2.3, and (II) the average speed vehicle emission model HERMESv3 (section 2.3.2).

3.2.1 Calibration of the BCN-VML

The calibration of the BCN-VML model requires adjusting the estimated traffic flow and vehicle speed. The estimated traffic flow for the city of Barcelona and its access roads was calibrated using observed hourly business-as-usual daily traffic flow data from 138 local automatic loop detectors from the Barcelona network (Ajuntament de Barcelona, 2019) (Fig. 3.1a). Some network properties such as road lane capacity and allowed turnings had to be manually adjusted along with the demand to further minimize discrepancies with observations. The comparison between simulated and observed traffic flows shows a R^2 of 0.77 (Fig. 3.1b).

The calibration of the BCN-VML estimated vehicle speed was done based on three different sources of information: (I) TomTom GPS-based historical hourly average speeds (TomTom, 2019), (II) average speed circulation statistics reported by the Barcelona city council (Ajuntament de Barcelona, 2017) and (III) measured hourly speed values reported from permanent detectors located in the suburban ring-roads (Barcelona city council, Mobility and transport department, personal communication, 2017). The comparison between simulated and observed speed values (hourly maximum and daily average) is summarized in Fig. 3.2a. The results are provided separately for the inner city, where the speed limit varies between

30 km/h and 50 km/h, and the ring-roads, where the speed limit varies between 60 km/h and 80 km/h depending on the road section. The BCN-VML vehicle speed overestimated the average speed values at the inner city area by a 65%. Additionally, the hourly speed profiles were neither matching the TomTom speed profiles nor the measured hourly speed values (Fig. 3.2b). The overestimated speed values at the inner city from the BCN-VML output are a consequence of the lack of intersection stopping time. BCN-VML's speeds are at link level, without considering what happens at nodes (i.e. intersections), hence there is no stopping time for each route, leading to unrealistic high speed values, close to the speed limit. On the other hand, the wrong speed profiling from BCN-VML is related to the traffic assignment methodology. STA estimates speeds by the volume delay functions, which depends directly on the traffic flow of the simulated hour, generating an artificial speed profile which does not represent correctly the real speed behavior. In reality, traffic speed is not directly proportional to traffic flow. Instead, it has a steady value near to maximum until congestion is achieved, which happens at a certain point of traffic density, as reported in Thomson and Bull (2002). This behavior is characteristic of STA and will be explained in chapter 4 when compared with a microscopic DTA approach. To overcome this, the substitution of the BCN-VML estimated speeds by the TomTom speed values would only partially solve the issue. As seen by the Fig. 3.2b TomTom speeds underestimate the observed values at the city ring-roads. This bias in TomTom speed values has already been seen in other studies (Gwara, 2017) and a possible reason could reside in that most of the people using these devices in the city are unfamiliar with the route they are following and therefore their speed is lower than the average of other vehicles. The solution applied to correct the estimated vehicle speeds goes through two steps: 1) the BCN-VML speed profile was replaced by the TomTom-based speed profiles, and 2) the estimated speeds by the BCN-VML at the inner city were reduced with a scalability factor obtained from the observed average urban speed. The corrections to the estimated speed profile and maximum speed are shown in Fig. 3.2.

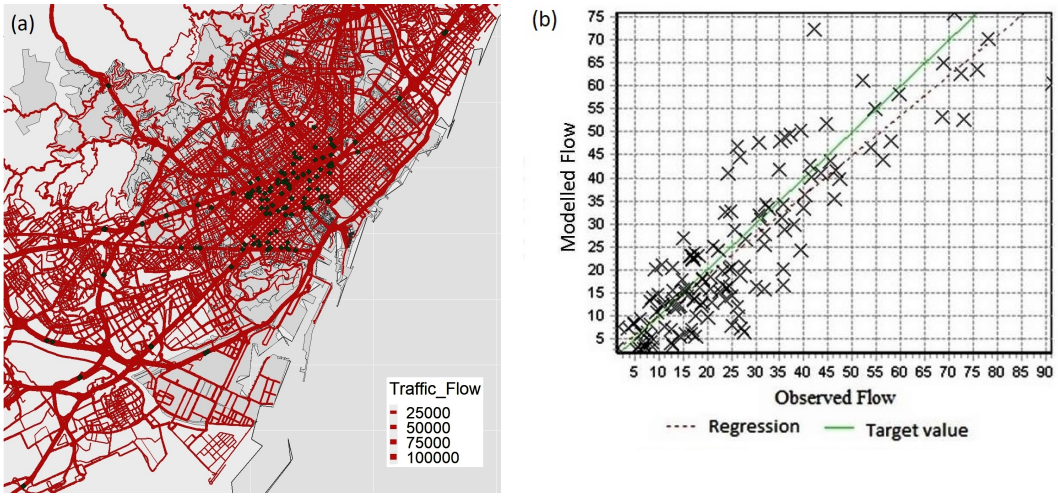

Figure 3.1: (a) Representation of the BCN-VML road network and associated business as usual daily traffic used in the present study, which comprises the city of Barcelona and its surrounding municipalities. Dark green squares indicate the 138 permanent loop detectors used to calibrate the vehicle flow. (b) Regression plot showing observed vs modelled flow (10^3 number of vehicles) from a 24h simulation with BCN-VML. 138 observations, RMSE = 35%, $R^2 = 0.77$, mean relative error = 27%.

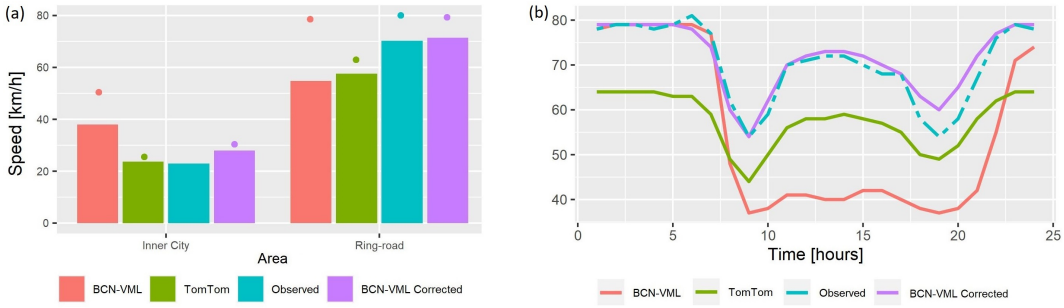

Figure 3.2: (a): 24h average speeds ($km \cdot h^{-1}$) for the inner city and ring-roads for the simulated BCN-VML, TomTom registered, observed values, and the BCN-VML corrected values. Dots represent the maximum speeds for each zone and data source. (b): Hourly speed profile ($km \cdot h^{-1}$) of the simulated BCN-VML, TomTom registered, observed values and the BCN-VML corrected profiles from the suburban ring-roads.

3.2.2 Area-dependent fleet composition

Most of the activity input data needed by HERMESv3 (e.g. mean vehicle speed, annual average daily traffic) is provided in a multiline shapefile, for which each row contains the information of a specific road link. Specific vehicle fleet composition profiles, business-as-usual daily traffic flow and speed temporal profiles are also assigned to each road link. For this study, we generated area-dependent fleet composition profiles derived from a remote-sensing campaign performed in Barcelona in 2017 (AMB and RACC, 2017) and information provided by the Barcelona's Port Authority (Port de Barcelona, 2017). A total of five different fleet composition profiles were assigned to different regions of the city (Fig. 3.3), which were classified as follows: (I) Inner city, with a large presence of motorbikes and mopeds, used in all urban links, (II) eastern ring road, since it is the main in route and out route for the port, heavy duty vehicles have a higher presence than in other areas, (III) port, links on the harbour area are massively dominated by heavy duty vehicles, (IV) western ring road, its composition is dominated by passenger cars, with a low presence of two-wheelers and heavy duty vehicles and (V) highway, motorbikes are practically nonexistent and is dominated by passenger cars and some heavy duty vehicles.

3.3. Coupling BCN-VML and HERMESv3

Figure 3.4 shows the schematic workflow of the BCN-VML and HERMESv3 coupling (further referred as VML-HERMESv3). BCN-VML simulates private vehicle and public bus transport using independent approaches the results of which are then combined into a multiline shapefile read by HERMESv3. The upper part of the figure describes the private transport process and the bottom part the public bus transport one.

Private transport demand is defined by a 24h OD matrix for a business-as-usual day, which is disaggregated into hourly OD matrices by applying hourly traffic flow profiles derived from the local traffic loop detectors. Traffic assignment is done by an iterative user's optimum static equilibrium assignment (STA) for each hour, which results in a shapefile of the whole domain that includes the

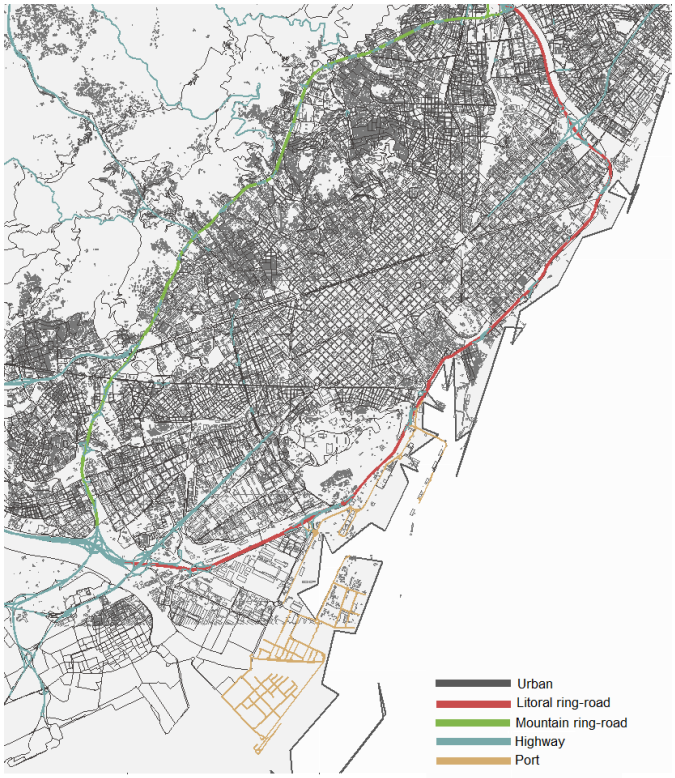

Figure 3.3: BCN-VML domain showing the road types classification used. The black segments represent all urban links, inside and outside Barcelona municipality, red and green links indicate eastern and western ring-road respectively, clear brown links represent the port and clear blue links highways.

simulated hourly traffic speed and volume per link. Emissions from public buses are differentiated from the rest of the fleet as they cannot circulate through all the network and have a different vehicle share composition. To reduce computational time, the public bus transport flow is calculated using the bus frequency and the number of bus lines going through each link while its speed is estimated with a proxy using the private transport speed, as described below.

The following processes are script-based. The code combines the private and public bus transport data and generates the vehicle flow profiles required by HERMESv3. Speed profiles are substituted with the TomTom data, as described in section 3.2.1. Bus speed on each section is estimated with the section's private transport speed and adapted with a factor obtained from the observed average urban bus speed in the city (TMB (2020)). Then, according to different specific network properties, each segment is tagged with its respective zone (e.g. inner city, western ring road, port...). The zone tag will be later read by HERMESv3 to assign the respective fleet composition, prepared aside.

HERMESv3 uses the resulting private and public bus transport multiline shapefile to estimate total hourly emissions per link according to the traffic flow, average link speed and vehicle fleet composition information associated to each section along with the COPERT V emission factors and meteorological information.

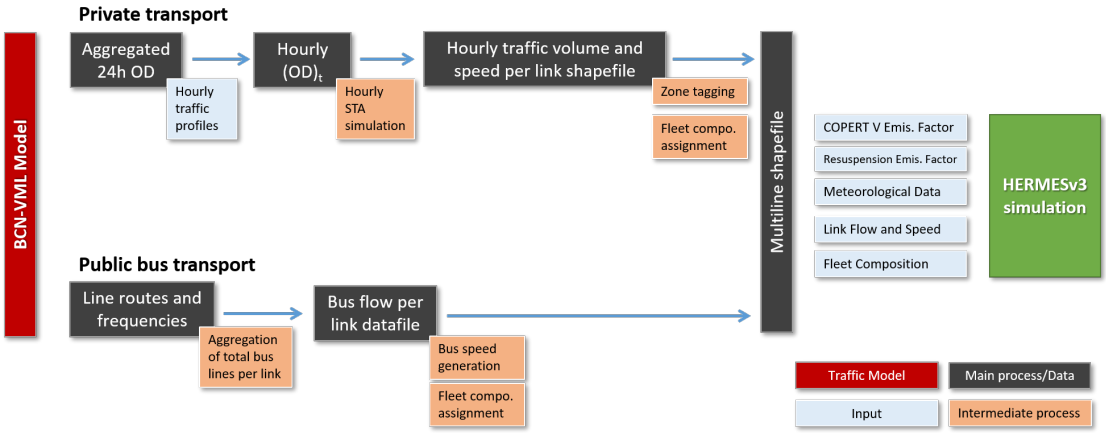

Figure 3.4: Schematic representation of the VML-HERMESv3 coupling, including: Input data, main and intermediate processes and output data. The upper part of the workflow describes the steps associated with private transport while the bottom part describes the public bus transport.

3.4. Results and discussion

In this section the annual emission results from the VML-HERMESv3 system are shown and compared against other available studies along with a discussion of their temporal and spatial distribution. Section 3.4.2 introduces and discusses the impact on emissions of different key features of the macroscopic coupled system.

3.4.1 Annual emission modelling results

The VML-HERMESv3 was used to perform an annual simulation of 2017 for the domain represented in Fig. 3.1.

The NO_x simulation results, at 30m $\times$ 30m resolution are shown in Fig. 3.5a. Major urban corridors are the ones with higher emissions together with the sub-urban ring-roads and main city accesses. This distribution in emissions is in agreement with the business-as-usual daily traffic flow shown in Fig. 3.1a. Due to the high proportion of HDV the port area also presents a relative high emission level despite its low vehicle flow. A representation of the temporal and spatial variation of emissions simulated by the VML-HERMESv3 system at the municipality of Barcelona can be seen in the upper and lower images of Fig. 3.6, respectively. The monthly profile clearly shows a strong emission decrease occurring during the month of August (approximately -26%), which is mainly due to summer holidays. At the weekly level, emissions remain almost constant during the weekday and are followed by a strong weekend decrease (-41%). The hourly time profile shows how emissions reach a maximum level of activity at morning (between 07:00 and 08:00h) and remain at or around this level for the rest of the day-time period (i.e. until 18:00h).

In terms of spatial distribution, it is observed that the district of Eixample is the area of Barcelona with the largest amount of NO_x emissions per square kilometre (291 kg·day^{-1}·km^{-2}). Despite its relative small size (7.47km^2), this district includes some of the main arterial and high-capacity roads connecting multiple areas of the city and therefore concentrates a large amount of traffic activity. On the contrary, two neighboring districts of Eixample (Ciutat Vella and Gràcia) have around half of Eixample's emissions (144 and 150 kg·day^{-1}·km^{-2}, respectively). These two

districts are the ones with the largest fractions of traffic-calming and pedestrian areas. In section 3.4.2 the spatial variations of NO_x emissions in Barcelona are further discussed.

The total annual NO_x and PM_{10} emissions for the municipality of Barcelona were compared against two datasets that also rely on the COPERT emission factors to estimate vehicle emissions: (I) A local emission inventory done by Barcelona Regional (BR) (Barcelona Regional, 2019), which corresponds to the year 2017 and (II) A report from the City Hall of Barcelona corresponding to the year 2013 (Ajuntament de Barcelona, 2015) (Fig. 3.5b). The VML-HERMESv3 model estimates a -5% and a +9% NO_x than the City Hall and the BR reports, respectively. For the first, the difference could be due to the older fleet composition of 2013, associated with higher emission factors. For the second, the difference might be caused by the applied mileage correction used in HERMESv3 for all petrol and diesel vehicles. On the other hand, the discrepancies for PM_{10} are higher. The VML-HERMESv3 model estimates are +18% and +105% larger than the ones provided in the City Hall and BR reports, respectively. These differences may be at least partly due to the inclusion of resuspension in VML-HERMESv3. Exhaust PM emissions have been progressively reduced with the introduction of new vehicle technologies (Guevara (2016)). Therefore, the 2013 City Hall report exhaust PM estimates should be higher than those provided by VML-HERMESv3 and the BR report. However, when adding the non-exhaust (resuspension) PM emissions on top of exhaust PM emissions, we end up with the values shown in Fig. 3.5b. A detailed explanation regarding non-exhaust emissions can be found in section 3.4.2.

3.4.2 Sensitivity to key implemented features

This section provides a thorough emission sensitivity analysis of some of the key input parameters of the VML-HERMESv3 macroscopic coupling system, including: Vehicle fleet composition, public bus transport distribution, meteorology and non-exhaust sources. Unless otherwise stated, for each case the VLM-HERMESv3 coupled system was run using two different versions of the input dataset for a complete working day. The resulting emission results are then compared and discussed.

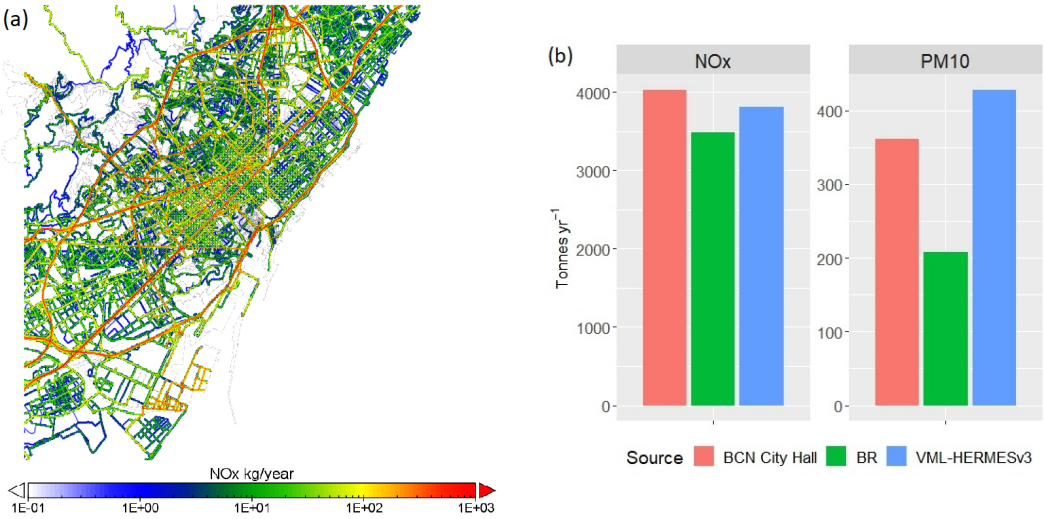

Figure 3.5: (a) Total annual NO_x emissions (kg·year^{-1}) for the study domain at a spatial resolution of 30mx30m. (b) Total annual NO_x and PM_{10} road transport emissions (tonnes yr^{-1}) for the municipality of Barcelona estimated by the VML-HERMESv3 coupled system (blue), reported by the BCN city hall (red), and reported by BR (green).

Vehicle fleet composition

In this section we aim to highlight the importance of a spatially-distributed vehicle fleet composition on large domains. To do so, the estimated emissions using the observed vehicle fleet composition of the VML-HERMESv3 system described in section 3.2.2 (further referred to as COMPO-OBSERVED) are compared against the emissions obtained using the censed vehicle fleet composition for Barcelona (further referred to as COMPO-CENSED). The COMPO-CENSED was derived from the official registration statistics provided by the Spain's national traffic authority (Dirección General de Tráfico (DGT), 2019) and consist of a unique vehicle fleet composition profile that is applied homogeneously to all the road links of the working traffic network. Table 3.2 summarises the shares of the different vehicle categories (i.e. Passenger cars, light duty vehicles, motorcycles, mopeds and heavy duty vehicles) reported by each one of the profiles considered.

The emission results obtained using each one of the vehicle composition profile datasets are summarised in Table 3.3. Overall, total NO_x and PM_{10} emissions are slightly higher when using the COMPO-OBSERVED profiles (+5.8% and +7.4%, respectively). Nevertheless, important discrepancies appear when performing the comparison at the zone level.

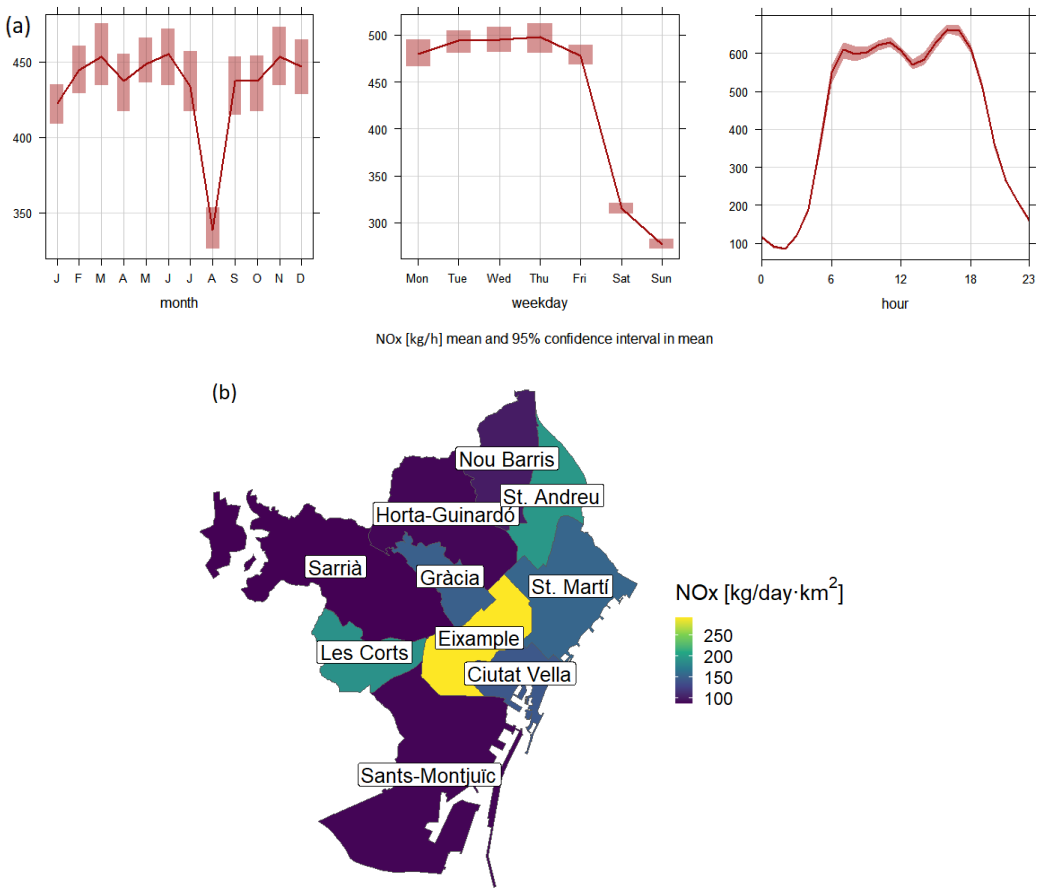

Figure 3.6: (a) Monthly, weekly and diurnal variation of NO_x emissions ($kg \cdot h^{-1}$) in Barcelona. (b) Spatial distribution of daily average NO_x emissions ($kg \cdot day^{-1} \cdot km^{-2}$) at the district level

1. The inner city presents a low discrepancy between emission results (-5.2% NO_x and -7.5% PM_{10} when using COMPO-OBSERVED), which is in line with the fact that both datasets present similar shares of general vehicle categories (table 3.2). Discrepancies are mainly related to the different age and fuel distributions assumed in each case. For instance, in the case of passenger cars, the average age is of 8 years in the COMPO-OBSERVED dataset, whereas in the COMPO-CENSED is of 11 years.

2. At the port the predominance of HDV on the COMPO-OBSERVED (46% of the total vehicle share) enlarges NO_x and PM_{10} emissions by +788% and +279%, respectively.

3. The COMPO-OBSERVED eastern ring road NO_x and PM_{10} emissions are a +33.2% and a +60% higher than the COMPO-CENSED. This difference is

due to the large amount of cargo vehicles (HDV and LDV) on the COMPO-OBSERVED. Note that the high difference in PM_{10} is due to wear emissions, which increase with increasing speed, and resuspension which increase with vehicle weight.

4. For the bus fleet, the COMPO-OBSERVED has a 41.84% of CNG buses in contrast with the 5% from the COMPO-CENSED. This leads to NO_x and PM_{10} emission estimates a -17% and -7.4% lower for the COMPO-OBSERVED dataset in respect to the COMPO-CENSED. Note that the CNG-bus emission factor for NO_x is approximately 60% lower than the diesel bus one.

Although differences in the overall emission estimates are minor, the vehicle share discriminated by zones has shown an important effect on the spatial distribution of the emission estimation.

Table 3.2: Vehicle group share by area (inner city, suburban eastern ring-road (Sub_East), suburban western ring-road (Sub_West), port and highway) and vehicle type (Passenger Car (PC), Light Duty Vehicle (LDV), Motorcycle and Heavy Duty Vehicles (HDV)) from the COMPO-OBSERVED compared with the homogeneous vehicle group share from the COMPO-CENSED.

	COMPO-OBSERVED					COMPO-CENSED
	Inner city	Sub_East	Sub_West	Port	Highway	
PC	60%	66%	77%	39%	74%	62%
LDV	15%	14%	9%	9%	16%	6%
Motorcycles	19%	8%	10%	6%	2%	27%
Mopeds	4%	0%	0%	0%	0%	0%
HDV	3%	12%	5%	46%	9%	5%

Public transport bus service

In this section, the emissions from the specific public bus traffic network that was built using the BCN-VML traffic simulator (see section 3.3) -referred to as BUS_SEP- are compared against an homogeneous distribution of this vehicle category (i.e. 4% of the total traffic flow) across all the road links included in the domain of study -referred to as BUS_AG-. The overall share of 4% is derived from the remote sensing campaign performed in the city. Figure 3.7a shows the resulting public bus network and associated daily flow per link information from the

Table 3.3: NO_x and PM_{10} [kg·day^{-1}] emission results by area (Inner city, suburban eastern ring-road (Sub_East), suburban western ring-road (Sub_West), port and highway) from the COMPO-CENSED (CENSED) and the COMPO-OBSERVED (OBSERVED) and relative emission difference from the COMPO-OBSERVED in respect to the COMPO-CENSED.

	NO_x		PM_{10}		NO_x	PM_{10}
	OBSERVED	CENSED	OBSERVED	CENSED	Difference	Difference
Inner city	9,404	9,915	1167	1262	-5.2%	-7.5%
Sub_East	1,577	1,184	246	153	33.2%	60%
Sub_West	1,120	1,179	166	158	-5%	4.8%
Highway	2,766	2,252	405	287	22.8%	40.9%
Port	1,289	145	57	15	788%	278.7%
Bus	2,312	2,787	161	174	-17.0%	-7.4%
TOTAL	18,469	17,462	2,202	2,050	5.8%	7.4%

BUS_SEP approach. As observed, major urban arterial roads are concentrating most of the bus routes and, subsequently, of the bus flow, while in tertiary and residential streets the number of bus lines is practically null. On the other hand, Fig. 3.7b shows the computed NO_x emission difference (BUS_SEP - BUS_AG) at the road link level during the morning peak hour (i.e. 08:00 AM local time). Yellow and red colors indicate higher emissions from BUS_SEP, while blueish colors indicate higher emissions from BUS_AG. At the city level, total estimated emissions are practically equal. The BUS_SEP approach reports a +2% NO_x and -1% PM_{10} emissions when compared to the BUS_AG. Nevertheless, significant differences are observed when performing a comparison at the street level (Fig. 3.7b). The spatial pattern of the emission differences is in line with the bus flow information reported by BUS_SEP (Fig. 3.7a). Road links with higher bus flow values are the ones presenting larger NO_x difference (up to +300%). On the other hand, heavy trafficked streets without bus lanes are highlighted with blueish colours, as a consequence of the higher emissions that the constant bus weight produces using the BUS_AG approach. This pattern is also observed in the port zone, in which the BUS_AG approach reports a 1.6% of buses. Maximum differences between the two approaches are up to +300% and -20%.

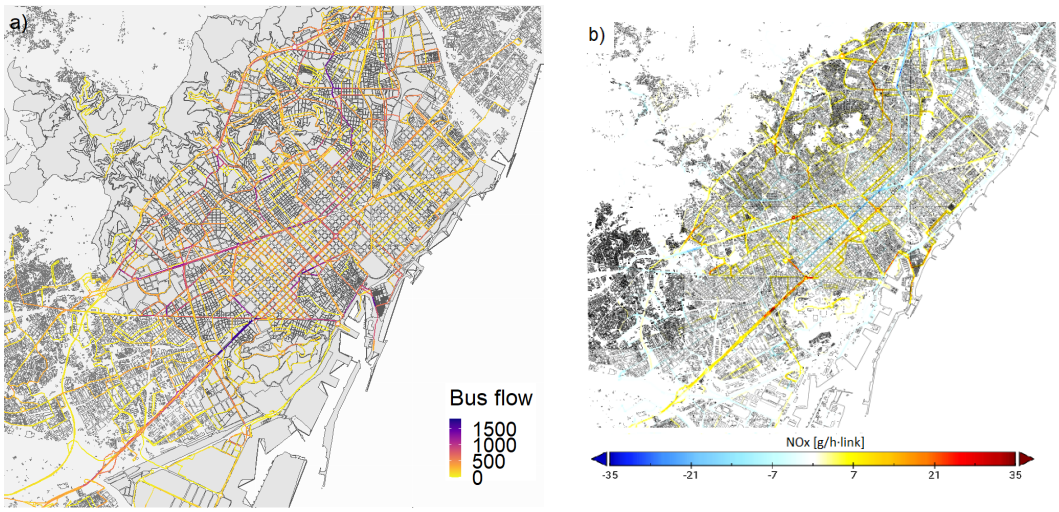

Figure 3.7: Daily flow representation (nº buses day^{-1}·$link^{-1}$) of the BUS_SEP network implemented in the BCN-VML traffic simulator (a) and NO_x (g·h^{-1}·$link^{-1}$) difference between the separated bus approach (BUS_SEP) and the aggregated one (BUS_AG) for the 8 AM local time (b).

Temperature effect

For this sensitivity study, the temperature effect on emissions for the coldest day registered in the city of Barcelona during 2017 is simulated (17^{th} February 2017). The observed average daily temperature at a weather station located in the city center was 8.4ºC (AEMET (2017)). Vehicle emissions increase under cold temperatures due to several mechanical factors, which are represented by two corrections on vehicle hot exhaust emissions. The first, referred to as cold-start emissions, are caused by the extra emissions due to the low performance of engine catalytic systems until they reach their optimum temperature, and affects both NO_x and PM_{10} emissions. Cold-start emissions are already considered in COPERT V and have been included in HERMESv3 following the Tier 3 methodology proposed by the EMEP/EEA guidelines as detailed in Guevara et al. (2020). We consider an average trip length of 6.47km, which is based on the Barcelona mobility report of 2015 (ATM, 2015). The second correction affects NO_x emission from diesel vehicles (Grange et al. (2019); Federal Office for the Environment (2018)) and it is not considered in COPERT V equations. This increase is associated with the Exhaust Gas Recirculation systems and Selective Catalytic Reduction systems operation at low temperatures. For diesel pre-Euro 6 vehicles NO_x increase is due to the dis-

connection of the Exhaust Gas Recirculation system (EGR) at low temperatures to avoid moist condensation issues. Diesel Euro 6 vehicles are also influenced by cold temperatures since the Selective Catalytic Reduction systems (SCR) they are mostly equipped with need NH_3 for NO_x conversion, which comes from the AdBlue. AdBlue is converted into NH_3 in a reaction whose efficiency decreases at low temperatures, increasing NO_x emissions.

To consider the temperature effect, the original COPERT V emission factors included in HERMESv3 were modified according to the temperature and vehicle dependent adjustment factors reported by Matzer et al. (2019). Emissions for the coldest registered day in Barcelona were simulated under three different scenarios: (I) without considering any correction for cold temperature emissions (Temp_Raw), (II) considering cold-start emissions (Temp_CS), and (III) considering cold-start emissions and the diesel NO_x temperature effect (Temp_CS+CF). Table 3.4 summarises the NO_x adjustment factors for diesel vehicles considered in the Temp_CS+CF scenario. Table 3.5 shows the NO_x and PM_{10} emission values simulated for the three scenarios. Estimated NO_x and PM_{10} emission for the Temp_CS scenario are +3% and +4% higher than Temp_Raw, respectively. NO_x difference increases up to +19% when considering the Temp_CS+CF scenario. The resulting increased NO_x emissions are slightly lower than the ones reported by Grange et al. (2019), who estimated an increase between 30% to 45% for the majority of Spain using wintertime air temperatures compared with emissions at 20^{o}C. It is reasonable a lower NO_x increase in Barcelona since the city has mild temperatures due to its coastal situation and the urban build provokes higher temperatures than the suburban and rural locations.

Non-exhaust PM_{10} emissions

In this section, the VML-HERMESv3 model was run with and without the consideration of non-exhaust PM_{10} emission sources (i.e. road, tyre and brake wear and resuspension). Table 3.6 shows the aggregated emission factors (EF) considered in HERMESv3 for non-exhaust and exhaust PM_{10} for the different vehicle groups. These are computed weighting the emission factors of each vehicle technology according to its fractional contribution to the fleet composition in that group and the average urban speed observed in the VLM-HERMESv3 coupled system (28km/h).

Table 3.4: Correction factor for temperatures of 8.4ºC applied to the represented EURO Diesel PC and LDV categories as reported by Matzer et al. (2019).

Euro class	Diesel PC correction factor	Diesel LDV correction factor
Euro 3	1.20	-
Euro 4	1.35	1.35
Euro 5	1.40	1.35
Euro 6a,b	1.45	1.20
Euro 6d-temp	1.00	1.00
Euro 6d	1.00	1.00

Table 3.5: NO_x and PM_{10} emission [kg·day^{-1}] for the coldest day of 2017, without considering temperature effect (Temp_Raw), considering cold-start emissions (Temp_CS) and considering cold-start emissions and diesel NO_x temperature effect (Temp_CS+CF). Difference exposes the relative difference between Temp_Raw and Temp_CS+CF.

	Temp_Raw	Temp_CS	Temp_CS+CF	Relative difference Temp Raw vs Temp_CS+CF
NO_x	15,866	16,375	18,867	19%
PM_{10}	1,899	1,983	1,983	4%

Table 3.6: Comparison between average PM_{10} non-exhaust and exhaust emission factors [g·km^{-1}] as a function of the vehicle category and source type.

	PM_{10} [g·km^{-1}]					
	Road	Tyre	Brake	Resuspension	Total non-exhaust	Exhaust
PC	0.015	0.011	0.008	0.023	0.056	0.014
LDV	0.015	0.017	0.012	0.082	0.126	0.020
HDV	0.076	0.027	0.033	0.460	0.596	0.062
Motorbikes	0.006	0.005	0.005	0.002	0.018	0.014

Table 3.7: Simulated total exhaust and non-exhaust (resuspension, wear) daily PM_{10} [kg] emissions.

Total PM_{10}	Exhaust	Resuspension	Wear
2,145	412	1,127	606

Non-exhaust EF for HDV are the largest, followed by LDV, PC and motorbikes. In all cases except motorbikes, EF for total non-exhaust are much larger than for exhaust (from four times more in case of PC to ten times more in the case of HDV).

A comparison between the two simulations shows an increase of PM_{10} emissions of +410% when considering all the non-exhaust sources. Table 3.7 shows the resulting PM_{10} emissions discriminated by process (exhaust, resuspension and wear). The contribution of non-exhaust sources to total PM_{10} emissions was found to be of 80%, which is in line with the results found by other studies, such as Rexeis and Hausberger (2009) (estimated a contribution between 80 to 90% for 2020 in Europe) and Harrison et al. (2012) (measured a contribution of 77% in London). More specifically, the resuspension process is the one dominating total emissions, with a contribution of 52%. This result is very similar to the one found by de la Paz et al. (2015) for the city of Madrid (contribution of 53%) which is in line with the fact that both cities are influenced by similar dry weather conditions.

The current large contribution of non-exhaust to total PM emissions is expected to keep growing on the following years. This is caused by the technological and legislative improvements in PM exhaust emissions combined with a lack of abatement measures for non-exhaust sources (Guevara, 2016).

3.5. Conclusions

This chapter presents the first coupled macroscopic traffic and emission modeling system tailored for Barcelona. This is done by using multiple sources of local measured data such as GPS based speed circulation statistics, automatic loop detectors or the circulating fleet composition and emission results from a remote sensing device campaign. The system is composed of the traffic simulator Barcelona Virtual Mobility Lab (BCN-VML) and the High-Elective Resolution Modelling Emission System version 3 (HERMESv3), which are based on Visum and COPERT V models, respectively.

An annual simulation showing total NO_x and PM_{10} emissions was performed with the developed coupled system. The computed annual emissions for the year

2017 were 3,800 tonnes for NO_x and 427 tonnes for PM_{10}. The computed annual NO_x and PM_{10} emission values were also compared against two local emission inventories. The VML-HERMESv3 NO_x estimated emissions were in agreement with both inventories showing a discrepancy of -5% and +9%. On the other hand, the PM_{10} differences were higher, up to +105%. This is believed to be caused by the high uncertainty of PM_{10} estimates, and the consideration of all PM non-exhaust sources by the VML-HERMESv3 system.

A sensitivity analysis was performed to quantify the variability of NO_x and PM_{10} estimated emissions to different input parameters, including vehicle fleet composition, public bus transport implementation, temperature and non-exhaust PM sources. The main findings of the sensitivity analysis and intercomparison exercise are summarised below:

- Vehicle fleet composition: High emission differences were found when using the real circulating area-dependent fleet composition versus the homogeneous censed one. These were mostly influenced by the HDV presence from the port area (+788% in NOx and +279% in PM10 for the COMPO-OBSERVED), the fuel (gasoline or diesel) used and the vehicle age.

- Public bus network: The usage of real bus routes showed strong street gradient differences in several sections of more than +300% for NO_x when compared with a constant bus share of 4% for the whole network. In contrast, reductions up to -20% in NO_x emissions were found in sections without bus routes.

- Meteorological influence: An increase of +19% in NO_x and +4% in PM_{10} was found when considering the effect of cold-start and diesel NO_x temperature-dependent processes. Although in Barcelona the temperature effect is reduced due to its mild weather, this can have a significant influence upon the overall emissions in colder regions.

- Non-exhaust PM sources: The inclusion of wear processes (i.e. tyre, brakes and road) and resuspension resulted in an increase of +410% of PM_{10} emissions. Road resuspension, a process which is not considered in COPERT V, was found to be the largest contributor to non-exhaust emissions, representing a 50% of the total.

This research shows how the combination of several input parameters has a key role on the estimated overall and street level gradient emissions. Since the simulation of large urban areas can only be done by a macroscopic or mesoscopic approach, several specific input parameters can still be improved to better assess traffic emissions, as shown in this study. The applicability of the developed system to other areas is conditioned to the available local data and the existence of a VISUM model at the desired location. The availability of local data is especially important for the calibration of the VISUM traffic model and the vehicle fleetshare used. Regarding the emission factors, the COPERT ones can be used as far as the domain is European. Otherwise, there should be a mapping between the COPERT vehicle categories and the local ones.

4. Comparison between macroscopic and microscopic traffic emission estimation

4.1. Introduction

In this chapter we quantify in a limited but representative area of Barcelona the discrepancies between the VML-HERMESv3 macroscopic system developed in this work to estimate the traffic emissions (Chapter 3) and a another developed microscopic approach composed by the microscopic traffic simulator Aimsun Next (Aimsun S.L., 2019) and the PHEMLight instantaneous vehicle emission model (Hausberger et al., 2009a). We use the higher level of detail of the coupled Aimsun-PHEMLight system to observe and discuss the possible emission discrepancies with the VML-HERMESv3 system. More precisely, we want to estimate the influence of the traffic assignment method (i.e., STA or DTA) and the traffic dynamics (i.e., vehicle-to-vehicle interactions) on the emission results computed with the AIMSUN - PHEMLight microscopic system. The expected limitations in estimating traffic emissions by the macroscopic VML-HERMESv3 system in congested situations are caused by the network loading process (STA) and the level of aggregation of vehicle dynamics, which deals with traffic flow as an homogeneous fluid.

Additionally, this chapter analyses the impact of the road gradient in emissions for the three different vehicle groups studied (Passenger Car, HDV, Bus) at the three different types of corridors of the study domain.

4.2. Aimsun - PHEMLight Coupling

The coupling process between Aimsun and PHEMLight is done offline. The individual vehicle drive cycles of Aimsun are passed into PHEMLight to compute

emissions after each simulation. To do that, both modelling softwares had to be adapted. For Aimsun, we developed a Python API which is able to track each vehicle appearing on the network, register its position and time and associate it to a link ID, recording also its speed and the vehicle category (Passenger Car, HDV or BUS). This data is gathered for each vehicle every second and written in a row of a spreadsheet containing the vehicles from the whole simulation time (24h). This ends up in a large data file composed of several thousands of rows, each corresponding to a time-step per vehicle. The PHEMLight model is not developed to work with large traffic flows, but with specific individual vehicles or small fluxes. Since the computational time needed to handle all the vehicle data generated was excessive, the model was re-coded in R to be able to compute the emissions in a viable way. Also, to the R coded version of PHEMLight, we added the vehicle mileage correction factors for petrol and diesel vehicles reported by the Tier 3 methodology of EMEP/EEA (EEA/EMEP, 2017) (chap. 1.A.3.b.i–iv) and Chen and Borken-Kleefeld (2016), respectively.

The vehicle fleet classification system followed by PHEMLight is different than the one followed by HERMESv3, which is based on COPERT. Hence, the 491 vehicle categories of HERMESv3 had to be adapted to the PHEMLight 130 vehicle categorisation in another script-based mapping process. The final emissions are then geolocalised by street segment and aggregated by pollutant.

4.3. Area of study

The domain of study is localised in an area of 0.4 km^2 (Fig. 4.1) and includes three main urban corridors in Barcelona representative of free flow, normal flow and heavy congestion conditions, respectively: (I) Aragó St., a six-lane street with a daily traffic flow of 80,000 veh/day and a green wave traffic light synchronization that allows a fluent flow throughout, (II) Aribau st., a four-lane street with a daily traffic flow of 23,000 vehicles per day and (III) Balmes St., a four-lane street with a daily traffic flow of 35,000 vehicles per day. The Aimsun road network was built based on Open Street Map (OpenStreetMap contributors, 2019), which was manually modified to fulfill all the model requirements. Traffic signalisation and timings, reserved bus lanes and permitted turnings were applied according

to on-site observations. The traffic demand of the Aimsun model was made by the application of traffic generation nodes at the external links of the network. This was followed by a manual calibration process in order to obtain the daily traffic flow values of the BCN-VML VISUM model. This procedure follows the goal of the study: to assess the behaviour of the VML-HERMESv3 system. The traffic simulation was performed by a hourly stochastic DTA approach for which the daily flow assigned to each generator node was split using the same traffic flow profiles applied in the BCN-VML. Regarding the emission computation, the fleet composition used to estimate vehicle emissions with PHEMLight is the same as the "inner city" fleet composition used in the HERMESv3 emission model, described in section 3.2.2.

Figure 4.1: Screenshot of the Aimsun Next microscopic DTA simulation showing the working domain, where the three major streets are pointed: Aribau St on the left (representation of normal flow), Aragó St on the right (representation of free flow) and Balmes St on top (representation of congested flow). Simulated individual vehicles in each street are represented in blue.

4.4. Results

In Fig. 4.2 we show the comparative results of the hourly NO_x and PM_{10} exhaust emissions computed for each of the three analysed streets and modelling system used. Non-exhaust PM_{10} sources were not considered since they are not included in the PHEMLight emission model. Results show that the three streets present higher estimated emission discrepancies during the daytime hours, when the traffic flow and congestion levels are higher. However these modelling differences diverge between the different streets.

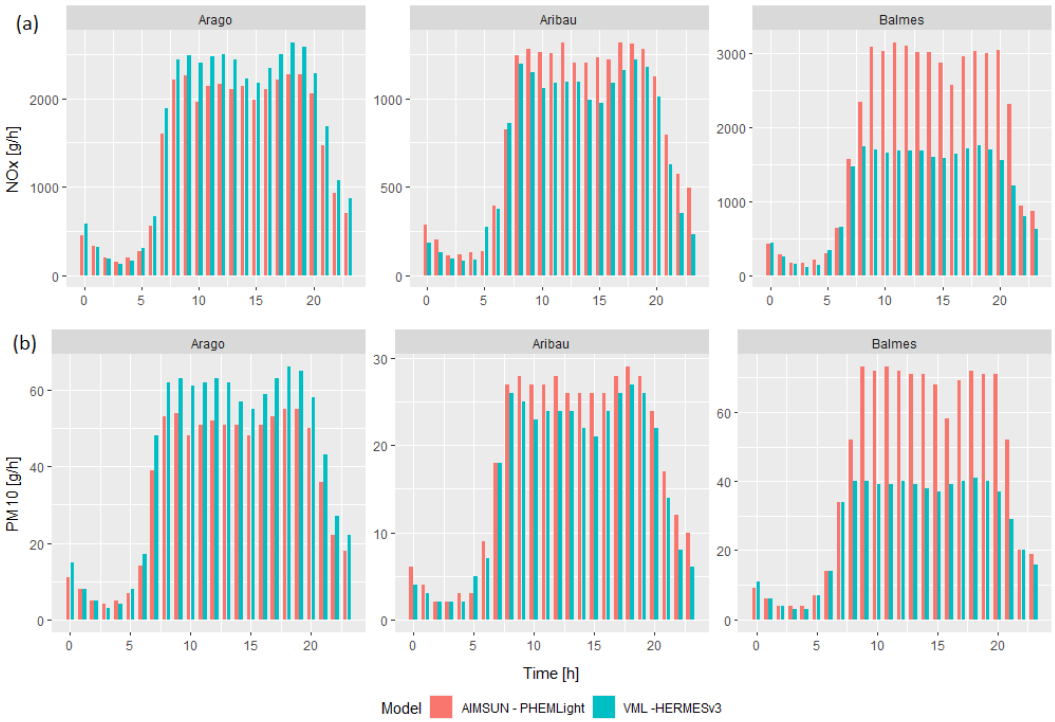

Figure 4.2: Hourly NO_x (a) and PM_{10} (b) estimated emissions ($g \cdot h^{-1}$) for the three streets of study: Aragó, Balmes and Aribau. Red bars indicate emissions computed by the microscopic coupled system (AIMSUN-PHEMLight) and blue bars indicate emissions estimated with the macroscopic approach (VML-HERMESv3).

To better understand the modelling differences, table 4.1 shows for each one of them the volume capacity ratios (V/C) (i.e. vehicle density) at peak hour 9 AM local time, the daily average speed and the total daily NO_x emissions computed with each modelling system. It can be observed that despite the high V/C ratio, in Aragó St. the NO_x emissions computed with the microscopic system are lower than the ones estimated with the macroscopic VML-HERMESv3 system (-11.7%). On the contrary, the microscopic approach estimates a +65% more NO_x in Balmes St. and a +15% in Aribau St.

Two assumptions can probably explain the emission differences observed above. The first lies in the traffic assignment method used: STA for the VML-HERMESv3 system, and DTA for the Aimsun-PHEMLight system. Since the STA cannot propagate queues on the network and model spillback, the links upstream the bottleneck remain unaffected. On the contrary, the congestion occurs downstream the bottleneck. As a consequence link flow may exceed capacity, there is

Table 4.1: Traffic and emission results obtained with the microscopic (AIMSUN-PHEMLight) and macroscopic (VML-HERMESv3) coupled systems for the three streets of study. The volume capacity ratio (V/C), the speed ($km \cdot h^{-1}$) and NO_x emissions ($kg \cdot day^{-1}$) are presented, as well as the NO_x relative difference between microscopic and macroscopic approach for each street.

	VML-HERMESv3			AIMSUN-PHEMLight			NO_x
	V/C	Speed [$km \cdot h^{-1}$]	NO_x [kg/day]	V/C	Speed [$km \cdot h^{-1}$]	NO_x [kg/day]	difference
Aragó	95%	26.4	39	70%	38	35	-11.7%
Balmes	82%	26.4	28	50%	18	46	+65.4%
Aribau	47%	25.3	18	25%	24	20	+15.5%

no queue formation and the demand downstream the bottleneck cannot properly be adjusted. This situation becomes critical in very congested links like Balmes, and therefore can affect the level and location of emissions (Tsanakas et al., 2020). On the other hand, the DTA used by Aimsun can model spillback of the queues as traffic demand exceeds capacity. Traffic flow evolves over time and congestion dynamics are modelled in a more realistic way. Queues occur upstream the bottleneck and queue spillback may occur through the network. Under DTA congestion is better located, which has a significant effect on where peak emissions occur as proved by Wismans et al. (2013) and Tsanakas et al. (2020), among other studies. This can be seen on the average speed simulated by the macroscopic STA and the microscopic DTA. While Aimsun Next estimates the lowest of the average speeds for Balmes, the corrected BCN-VML speed estimates a similar value than in the other two streets. The second assumption is probably bound with the level of aggregation of vehicle dynamics. A macroscopic model does not simulate individual vehicle dynamics, which are of special interest at stop-and-go situations. During these periods engines work consistently at high load provoking strong punctual emission peaks and the idling emissions due to the stopping time as also described by di He et al. (2009). Therefore large emission differences are generated in comparison with an average speed emission model, which tends to sub-estimate emissions in stop-and-go conditions as reported by Khreis and Tate (2017) and Tu et al. (2018) among other studies. This pattern can be observed in Fig. 4.3, which shows the driving cycle (magenta dotted line) and associated NO_x instantaneous emissions (blue line) of a diesel Euro 4 passenger car simulated by the Aimsun-PHEMLight microscopic system for Arago St. (Fig. 4.3a) and Balmes St. (Fig. 4.3b). The associated emissions simulated by the VML-HERMESv3

macroscopic system are also included for comparison purposes. In Aragó St. the AIMSUN-PHEMLight driving cycle has gradual accelerations and a quasi constant speed during the whole cycle. On the contrary, in Balmes St. the simulated cycle is composed by multiple stop-and-go conditions, which generate high emission peaks. The associated constant NO_x emissions for the VML-HERMESv3 system are within the range of the microscopic system. It is also important to mention that the associated driving time to cross the analysed street links differs from both approaches. For the congested street (Balmes), the VML model reports a driving time of 125 seconds, while AIMSUN's microscopic simulated car needs 660 seconds to cross the same link. This difference is a consequence of the stop-and-go driving behaviour and contributes to the absolute emission difference observed in Fig. 4.2. This high discrepancy between simulated driving times is not observed in Aragó St. (82 seconds with AIMSUN versus 86 seconds with VML) due to the free flow condition.

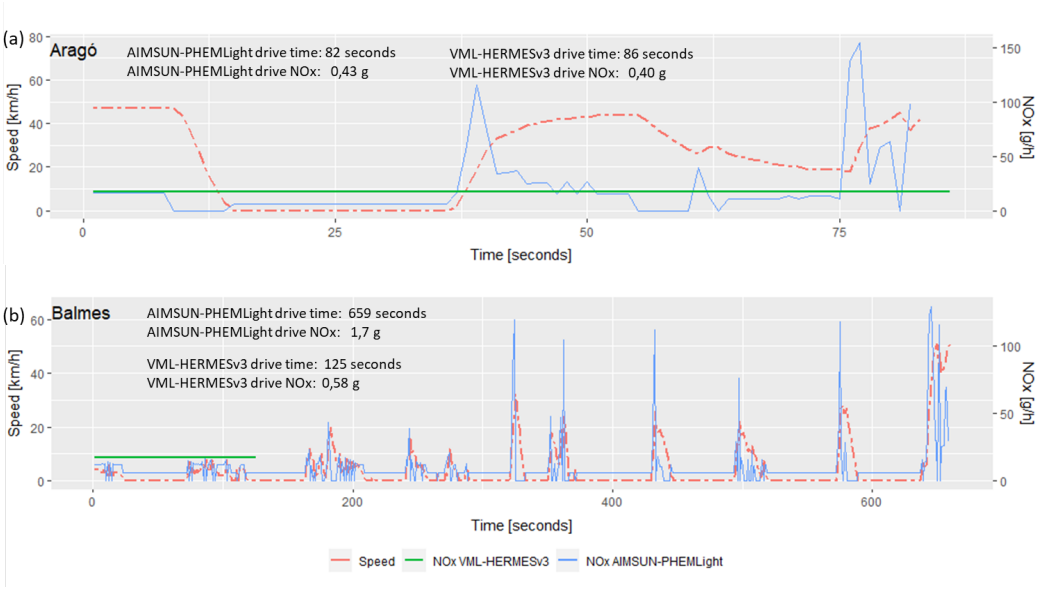

Figure 4.3: Instantaneous speed ($km \cdot h^{-1}$) and associated NO_x emissions ($g \cdot h^{-1}$) for a diesel Euro 4 passenger car simulated by the AIMSUM-PHEMLight microscopic system and VML-HERMESv3 macroscopic system for Aragó St. (a) and Balmes St. (b). The driving time needed to cross each street link (seconds) and total NO_x associated emissions (g) of the sample vehicle are also shown.

4.5. Road gradient effect

Road gradient might have an important effect in emissions since vehicle engines need to overcome the gravity effect, increasing the power needed to sustain speed. Some modelling and empirical examples can be found in Wyatt et al. (2014) and Prakash and Bodisco (2019) respectively. This section expands the microscopic simulation scenario from Section 4.4 by adding the road gradient effect on emissions on the same area. The analysis is done over different vehicle categories (i.e Bus, PC, HDV) and the traffic states of Balmes St and Aribau St, for a positive and a negative gradient of 2% applied to each street.

NO_x Emission results from both simulations are summarised in table 4.2, which also exposes the NO_x relative difference to a flat terrain. The first to notice is that the extra emissions from the positive gradient are balanced with the reduced emissions from the negative one (e.g. NO_x for PC in Aribau: +13.8% and -12.1%). Secondly, heavier vehicles (for the used vehicle fleet PC, HDV, BUS by ascending weight) have a higher increase and decrease for both positive and negative gradient respectively, in respect to flat terrain (e.g. NO_x for HDV in Aribau are of +19.6% and -17.6% vs +13.8% and -12.1% for PC, for positive and negative slope, respectively). And thirdly, road gradient effect is reduced with increased congestion level. Balmes St, which is highly congested (more details in section 4.4), has a lower NO_x difference than Aribau St for both PC and HDV (+10.1% and +19.6% in Balmes and Aribau for HDV). Since buses have a reserved lane for both streets they do not suffer from congestion, and their emission variances between both streets are equal, which confirms the aforementioned statement (+26.4% and +26.0% in Aribau and Balmes for Bus). Although it has been seen that the increase from a uphill street is balanced by the decrease on its equal downhill, this analysis shows that differences are of importance when estimating emissions at street level, which get accentuated by free flow traffic conditions.

Table 4.2: Emission results in NO_x [g] with and without considering road gradient for a 24h microscopic simulation. Results are classified by vehicle type (PC, HDV and BUS) and street (Balmes (congested flow) and Aribau (normal flow)). The relative difference between the positive and negative gradient in respect to no gradient is also shown

	NO_x [g]				
PC	without gradient	+ 2%	-2%	Difference (+)	Difference (-)
Aribau	13,985	15,915	12,286	13.8%	-12.1%
Balmes	33,173	35,659	30,745	7.5%	-7.3%
HDV					
Aribau	3,779	4,520	3,114	19.6%	-17.6%
Balmes	10,309	11,349	9,353	10.1%	-9.3%
Bus					
Aribau	2,566	3,244	2,011	26.4%	-21.6%
Balmes	2,611	3,290	2,058	26.0%	-21.2%

4.6. Conclusions

In this chapter we do a comparison between different modelling approaches for the estimation of traffic emissions. The system used to estimate emissions and analyse the air quality implications of traffic management strategies during this thesis follows a macroscopic approach that has some inner limitations. To quantify the impact of these, we have developed a highly detailed microscopic traffic-emission system able to estimate emissions of each vehicle every second. Both approaches are run in a specific area of the city which contains three urban corridors representative of different traffic states (free-flow, normal flow, congestion). The results of this comparison show that the highest discrepancies between the macroscopic and microscopic approaches occur at congested traffic situations (up to +65% in NOx emissions). In contrast, during free flow, the observed differences were smaller, with +11% more NO_x estimated by the macroscopic system. The DTA versus the STA and the individual vehicle dynamics characterisation of microscopic system versus the macroscopic traffic representation were found to be the reasons for such differences.

In this chapter we additionally performed a test to observe the emission effects of the road gradient over different vehicles (Passenger Cars, HDV, Bus). We used the microscopic simulation of the previous exercise and we added the road gradient to the Aimsun-PHEMLight system. The observed results show how the extra emissions that occur as a consequence of the positive road gradient, are balanced by the decrease in emissions of the parallel street with a negative road gradient (e.g., +13.8% and -12.1% for PC in a free flow street). We also found that the differences observed increase with vehicle weight (Passenger Car, HDV and Bus, by ascending order) and with a lower level of congestion. In this sense, a HDV vehicle will present a higher increase in NOx emissions that a PC vehicle (+19.6% vs +13.58%) and also than the same vehicle circulating through a congested street (+19.6% at free-flow vs a +10.1% in congested situation).

In sum, we have to acknowledge the limitations of the system used, specially in congested situations while also being aware that is the only viable approach for the domain of study of this work. As future research additional improvements on the STA simulation could be considered in order to improve vehicle dynamics on congested situations. Tsanakas et al. (2020) applied the so called "quasidynamic" network loading on a STA simulation, which improved the simulated traffic dynamics during congestion. On another matter, the higher resolution of a microscopic traffic emission model was used by Rakha et al. (2011) using synthetic drive cycles generated with aggregated link traffic data from the mesoscopic traffic model (e.g. average speed, average stop duration or number of vehicle stops per unit distance). In order to improve the vehicle emission estimation at street-level, in future developments the road gradient effect should be taken in account. Although it would not have important implications when computing emissions per area (since the extra and the decrease in emissions are balanced).

5. Quantifying the impacts of traffic restriction policies on air quality in Barcelona (Spain): A multi-scale approach.

This chapter is based on the following publications

D. Rodriguez-Rey, M. Guevara, M^{a}. Paz Linares, J. Casanovas, J. M. Armengol, J. Benavides, A. Soret, O. Jorba, C. Tena, C. Pérez García-Pando, (2022). To what extent the traffic restriction policies applied in Barcelona city can improve its air quality?. Science of The Total Environment, Volume 807, Part 2, 150743, ISSN 0048-9697, https://doi.org/10.1016/j.scitotenv.2021.150743.

D. Rodriguez-Rey, M. Guevara, M. P. Linares, J. Casanovas, J. M. Armengol, J. Benavides, A. Soret, O. Jorba, and C. Pérez García-Pando. A multi-scale approach to evaluate the impact of urban mobility policies in emission and air quality in Barcelona. 20th International Conference on Harmonisation within Atmospheric Dispersion Modelling for Regulatory Purposes. Online, 14-18 June 2021.

5.1. Introduction

As commented in other sections of this Ph.D thesis, Barcelona is not complying with the EU AQD for NO_2. Although over the past years the city has been reducing its NO_2 concentration levels, the traffic air quality monitoring stations still systematically exceed the annual mean NO_2 limit values established by the Air Quality Directive 2008/50/EC (European Parliament, 2008). An exception has been 2020 when no exceedances were recorded due to impact of the COVID-19

lockdown upon mobility (ASPB, 2020). NO_2 limit values are typically exceeded in traffic stations, with traffic accounting for 60% of the NO_2 in the city (Ajuntament de Barcelona, 2015). As mentioned in Chapter 1.1, traffic pollution is of particular concern as it has been associated with increased mortality (Hoek et al., 2001) due to higher cancer risk (Beelen et al., 2008) and worsened respiratory health (Brauer et al., 2002). All in all, Barcelona recently ranked as the 6^{th} city with higher mortality risk from a total of 858 European cities (ISGlobal (2021); Khomenko et al. (2021)).

Partly due to the failed outcomes by the vehicle manufacturers in reducing NO_x from vehicle exhaust gases (i.e., excess diesel NO_x emissions, Benavides et al. (2021a)), Barcelona local authorities are focusing on mobility policies that try to reduce and renew the number of circulating vehicles within the city. These policies include, on the one hand, the implementation of traffic restriction measures aiming at reducing traffic activity in certain areas and corridors of the city and, on the other hand, the application of a Low Emission Zone (LEZ), the objective of which is to accelerate the renewal of the circulating vehicle fleet. To reduce traffic activity in particular urban areas, Barcelona is applying the Superblock system (Fig. 5.1), which consists on the traffic pacification of several streets within an area comprised by several blocks. The traffic pacification measures performed within the superblock comprise a reduced speed limit (10km/h), the usage of urban furniture to hassle traffic -such as urban vegetation, bollards or speed humps- and the introduction of mandatory turnings that throw out the incoming vehicles. The goal of the superblock is to provide a traffic-pacified interior area accessible primarily to active transport (e.g., cycling) and secondarily to residents, diverging through traffic and gaining space for leisure activities (Rueda, 2019). Along with the Superblock system, Barcelona is also applying a set of Tactical Urban Planning Actions to reduce private vehicle space of the city. These actions consist on the implementation of low-cost and scalable elements such as strips of colours, urban furniture or moveable plant beds to transform the urban space. In the case of Barcelona, the introduction of these elements allowed reducing traffic lanes dedicated to private vehicles from major urban corridors in the city, and gaining pedestrian and public transport space.

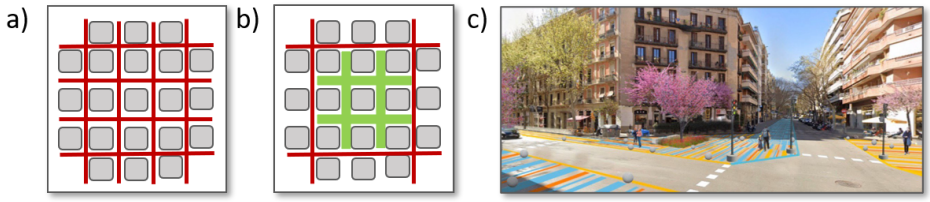

Figure 5.1: a) Area without the application of the superblock model and b) area with the superblock model. The grey squares represent building blocks, the green segments the streets affected by traffic pacification measures and the red segments the non-affected streets c) Image of the aplication of Tactical Urban Planning measures in a crossroad.

To quantify the impact of these measures on emission and air quality levels, the AQD encourages the use of numerical models. This is particularly relevant for Barcelona, where the monitoring network is not dense enough to properly characterise population exposure, and therefore it needs to be combined with modelisation (Duyzer et al., 2015). Air quality models should be used for both assessment and planning; but to do so, the modelling chain has to be fit-for-purpose and properly validated and calibrated.

Mesoscale Eulerian Chemical Transport Models (CTMs), which require as input data estimated emissions and meteorological variables, are currently the most widely used when performing the evaluation of the potential emission reductions (e.g., Pisoni et al. (2019)). As further explained in Chapter 2, these air quality systems are usually combined with traffic and travel demand models (Barceló, 2010) to simulate the effect of restrictions on the traffic activity (e.g., traffic flow, speed) across the city (e.g., San Jose et al. (2018)). The application of such an integrated modelling approach allows estimating the changes induced by the mobility action and their possible rebound effects (e.g., generation of new bottlenecks) not only in the implementation area (e.g., the LEZ), but also, more generally, in the city where it is located and its surroundings.

Despite the satisfactory performance of the CTMs, their limited resolution cannot reproduce the strong urban pollutant concentration gradients usually associated with high load traffic flows (Borge et al., 2014). In order to depict street level concentration gradients, local–scale tools are needed. The most detailed approach is the Computational Fluid Dynamics (CFD), which consists in the direct computation of the pollutant dispersion around the buildings integrating the fun-

damental transport governing equations. In order to deal with the turbulence in the CFD context, there are the Large Eddy Simulation (LES) techniques that explicitly solve the larger turbulent scales while modelling the smaller ones, and the Reynolds Average Navier Stokes (RANS) that compute the time average of each flow characteristic. Due to the high computational load associated with CFD solvers, simpler approaches mainly based on Gaussian dispersion models, have become very popular to assess air quality at the urban scale, specially in large computational domains (e.g., Borge et al. (2014), Jensen et al. (2017), Hood et al. (2018), Benavides et al. (2019)). Gaussian dispersion models use semi–empirical approximations to compute pollution dispersion within the urban canopy. Local-scale tools are usually coupled with regional CTMs to account for the long-range pollutant dispersion (Borge et al. (2018); Benavides et al. (2021a); Jensen et al. (2017); Hood et al. (2018); Denby et al. (2020)). Besides improving the performance of grid-based CTMs, the application of a hybrid air quality modelling approach (i.e. the combination of mesoscale and street-scale dispersion models) can also lead to more detailed results when evaluating urban mobility plans.

The coupling of such hybrid approach with traffic demand models has already been applied to estimate the impact in urban emissions and air quality levels of different structural or short term action plans. Borge et al. (2018) estimated the impact of the Madrid NO_2 protocol using a multi-scale air quality model with a mesoscale approach ($1km^2$) for the citywide, and a street-level approach for one of the main streets in the city. Using different estimated traffic demand scenarios, their results showed that only the most restrictive measure would produce a noticeable air quality improvement (-25% in NO_x emissions). Jensen et al. (2017) estimated the NO_2 concentration values in Denmark using a multi-scale air quality modelling approach. In this case, they combined the Danish Transport Model and GPS vehicle readings to estimate traffic volume and speed, respectively. This data was used by AirGis (Jensen et al., 2001) to estimate NO_2 concentration values at different resolutions with values that ranged between -27% and +12% from observations. In Barcelona, Mueller et al. (2020) studied the health impacts of the complete implementation of the Superblock idea on the city (500 Superblocks). They used the Street 5.2 air quality model (Kunz, 2005) estimating a reduction of 24% in the NO_2 concentration values assuming a 19% reduction in the private

transport. They estimated 291 premature deaths due to NO_2 following a linear exposure-response function (Atkinson et al., 2018). Since the study followed a macroscopic approach obtaining the results at the city level, the most affected areas or streets as well as possible rebound effects were not identified.

In this chapter we quantify the NO_x emissions and NO_2 concentration changes at street level of the different traffic management strategies adopted by the Barcelona City Hall and for the first time their potential undesired rebound effects as a consequence of the new generated vehicle routes. To address this, we perform a multi-scale air quality modelling exercise that couples the CALIOPE-Urban, a modelling framework that combines the CALIOPE mesoscale air quality system (Baldasano et al. (2011); Pay et al. (2014)) with the street-scale dispersion model adapted to street canyons (Benavides et al., 2019) and the traffic-emission model VML – HERMESv3 (Rodriguez-Rey et al., 2021) that allows to estimate the induced traffic emissions as a consequence of road network modifications. Additionally, we compare the mesoscale and street scale computed values to understand and quantify the differences when working at different scales.

5.2. Methodology

In this section we present the domain and period of study, as well as a detailed description of the model workflow. We also describe the traffic restrictions considered in the study along with their implementation in the modelling system.

5.2.1 Domain and period of study

The area of study is the greater area of Barcelona, the same one used for the study in Chapter 3 with a surface of 101km^2 and a traffic density of 6,000 vehicles/km^2 (Ajuntament de Barcelona, 2020a). The study is performed from the 9^{th} to the 25^{th} of November of 2017. This period includes representative days of the observed NO_2 annual mean daily cycle of the city (9^{th} - 16^{th}) and a pollution episode with high NO_2 concentration levels (17^{th} - 25^{th}) to assess the impact of the traffic restriction measures in a critical air quality condition in the city. During this period, there was an exceedance of the NO_2 hourly limit value (200 µg/m^3), and six values above 160 µg/m^3 of NO_2 at the two traffic air quality monitoring stations and in a urban background site.

The NO_2 mean for the representative days of the study period (9^{th} - 16^{th}) and the NO_2 mean for the observed annual values for Eixample are of 63 ($\pm$ 30) $\mu g/m^3$ and of 58 ($\pm$ 26) $\mu g/m^3$, respectively. The representative days NO_2 mean for Gracia is of 60 ($\pm$ 31) $\mu g/m^3$, while the annual observed NO_2 mean is of 51 ($\pm$ 28) $\mu g/m^3$. A detailed description of the representativeness of the selected study period with the annual mean daily cycle can be found in (Benavides et al., 2021b).

5.2.2 Modelling system

The emission and air quality impacts of the different traffic management strategies applied in Barcelona were analyzed using a multi-scale modelling chain based on the coupled traffic-emission model VML-HERMESv3 (Rodriguez-Rey et al., 2021) described in Chapter 3, the mesoscale air quality system CALIOPE (Baldasano et al. (2011); Pay et al. (2014)) and the street scale air quality system CALIOPE-Urban (Benavides et al., 2019) (Fig. 5.2).

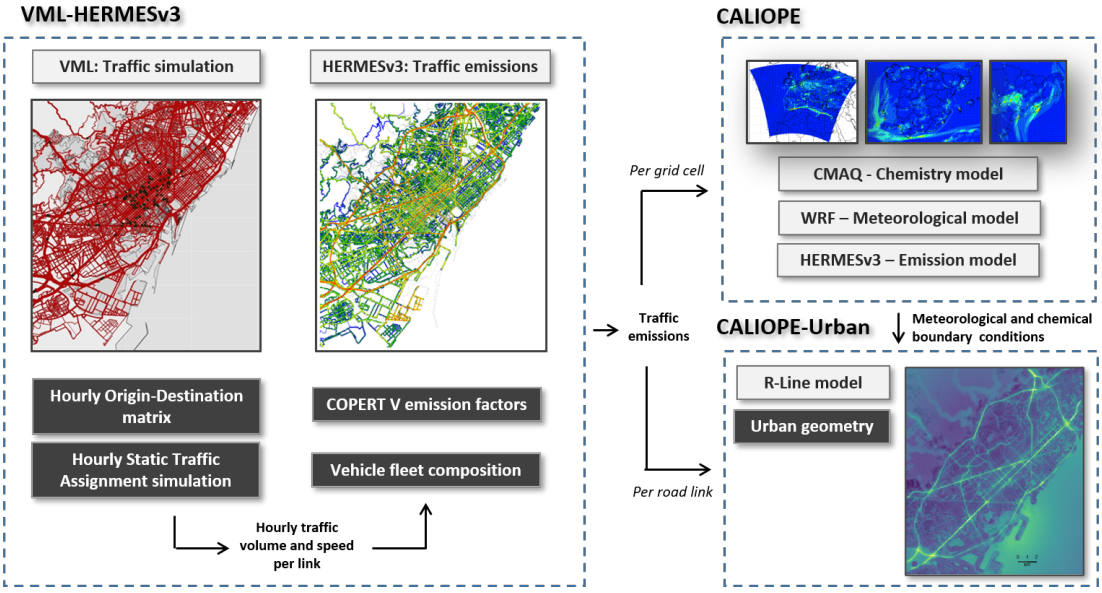

Figure 5.2: Schematic representation of the multi-scale modelling chain used to evaluate the impact of traffic management strategies in Barcelona. Blue dotted lines comprise the modelling systems that compose the tool (VML-HERMESv3: coupled traffic and emission model, CALIOPE: mesoscale air quality system and CALIOPE-Urban: urban scale air quality system), black boxes represent input data, grey boxes stand for the inner models, and black arrows illustrate the transfer of data between models and systems.

Traffic and emission modelling: VML-HERMESv3

The traffic flow and speed are simulated using the coupled traffic-emission system descrived in Chapter 3. To briefly remind the reader, traffic flow and speed are simulated using the Barcelona Virtual Mobility Lab (VML) model (Montero et al., 2018), a model based on PTV VISUM (PTV Group, 2019). Vehicle routing is estimated according to mobility matrices (e.g., Origin-Destination matrices) derived from mobile phone data from March 2017. An Static Traffic Assignment is performed for each hour for a business-as-usual day (for a total of 24 traffic simulations). A calibration process using measured traffic counts and speed values from permanent traffic stations was performed to ensure correct values of traffic flow and speed. Following the traffic simulation, the averaged link-level hourly speed, traffic flow data and the traffic network from the VML are read by the HERMESv3_traffic emission model to compute vehicle emissions at the road link level. HERMESv3_traffic (Guevara et al., 2020) computes hourly exhaust (hot and cold-start) and non-exhaust emissions (tire, road and brake wear and resuspension) based on the Computer Program to calculate Emissions from Road Transport version V (COPERT V, which includes the corrected Diesel emission factors) (EMISIA, 2016), which are included in the tier 3 approach of the European emission inventory guidelines EMEP/EEA (EEA/EMEP, 2017).

Mesoscale air quality modelling: CALIOPE

A detailed description of the CALIOPE system can be found in Section 2.4.1 from Chapter 2. The boundary and initial conditions are obtained by running CALIOPE over three domains: Europe at a 12 km by 12 km horizontal resolution, the Iberian Peninsula at 4 km by 4 km, and the Catalonian region including Barcelona at 1 km by 1 km resolution (Fig. 5.2). A one-way nesting is performed to retrieve the meteorological and chemical conditions from one domain to the inner ones. CALIOPE simulations were initialised with the Global Forecast System (GFS) (NOAA, 2011), boundary conditions for chemistry come from the CAMS reanalysis of atmospheric composition (Inness et al., 2019), and anthropogenic emissions for all domains were processed using HERMESv3. For the European domain, HERMESv3 was run using the TNO-MACCIII (Kuenen et al., 2014) and the HTAPv2.2 (Janssens-Maenhout et al., 2015) inventories for European and non-

European countries, respectively. For the Iberian Peninsula and Catalonia nested domains, emissions were estimated using the bottom-up module of HERMESv3, except for Barcelona domain where the estimated traffic emissions were computed by the VML-HERMESv3 coupled system previously described. Biogenic emissions were computed for all the three domains using the MEGANv2.0.4 model (Guenther et al., 2006).

Street-scale air quality modelling: CALIOPE-Urban

The CALIOPE-Urban street-scale air quality model is applied over the Barcelona domain (Fig. 5.2) at a resolution of 20 meters. This resolution is selected to account for the strong pollutant concentration decay within tens of meters from the road edge (e.g. Black Carbon decay of more than 50% in street canyons within the initial 20 m (Amato et al., 2019)) that occur in compact cities while keeping feasible computational time and memory requirements. The system is composed of the above-mentioned CALIOPE air quality system - from where it takes the meteorology and chemical boundary conditions - and the near road dispersion model R-LINE (Snyder et al., 2013) adapted to street canyons (Benavides et al., 2019). The meteorology and chemical boundary conditions modelled by CALIOPE are downscaled to street level following the parametrisations described in Benavides et al. (2019). The street-scale dispersion model is run using the street-scale and hourly traffic emissions estimated by the VML-HERMESv3 system. These emission values are consistently used for both the street-scale (BCN-20m) and the mesoscale (CATALONIA-1km) modelling domains. Further information regarding CALIOPE-Urban can be found in Benavides et al. (2019).

Generation of urban geometry

As described in Benavides et al. (2019) R-Line was adapted to incorporate the orientation of roadways (and thus the buildings) where the wind direction follows the street direction. To do so, wind speed and direction were adapted to simulate the "channeling" around buildings, similarly to Fisher et al. (2006). To compute this, R-Line needs the urban geometry of the study domain (Fig. 5.3). The urban geometry data consist on the ground plan and height of all the buildings in the study domain, which for this study was developed from two sources: The

buildings ground plan was obtained from the Catalan Cartography Institute (ICC by its Catalan initials, (ICC, 2020)), while the building height came from LIDAR data, from the Spanish Ministry of Transport and Mobility (PNOA, 2020). The process to combine both data-sets is script based. First, the buildings ground plan is loaded to be then intersected with the LIDAR dots over each building. Building height is obtained from the average of the 90% percentile of all intersected dots. By this way we exclude outlayers like turrets or chimneys which would artificially increase the calculated height. The final building height above the ground is obtained from subtracting the ground level, deducted from the closest LIDAR dot outside the building ground plan.

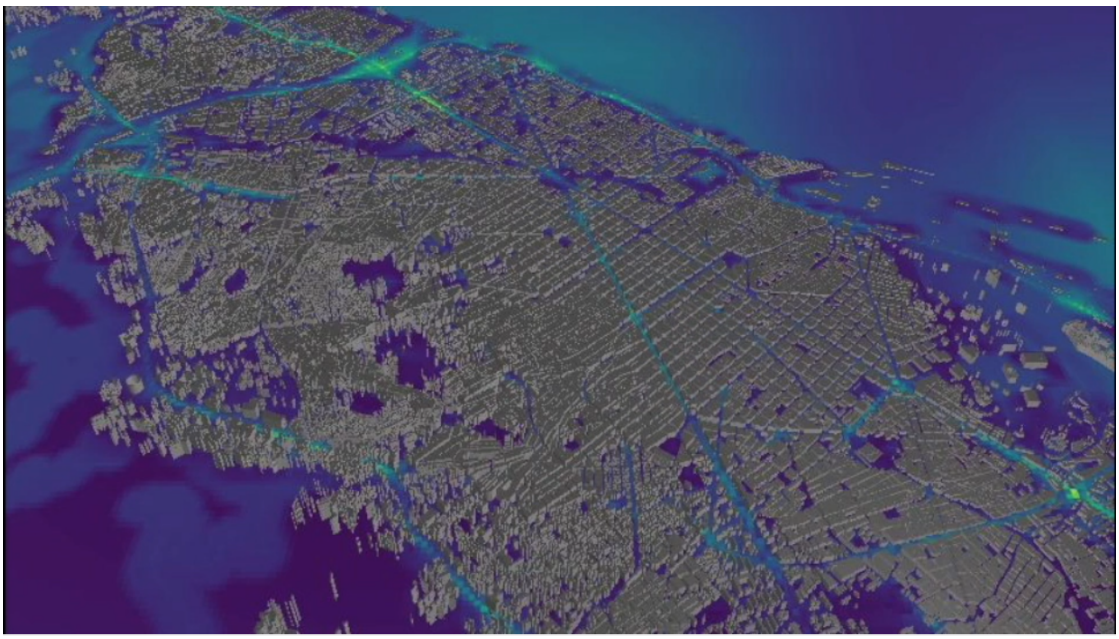

Figure 5.3: 3D image of the generated building height above the ground.

5.2.3 Traffic restriction measures

We consider 3 different traffic restriction measures that are currently being applied or planned to be applied in the near future in Barcelona: (I) Tactical Urban Planning -TUP-, (II) Superblocks -SPB- and (III) the Low Emission Zone -LEZ-. The LEZ is applied in almost all the simulated domain, with some excluded areas and ways (Fig. 5.4a). It forbids the entrance of gasoline vehicles below Euro 3, diesel vehicles below Euro 4 and motorbikes/mopeds below Euro 2. Detailed descriptions

of these measures can be found in Area Metropolitana de Barcelona (2020) and Ajuntament de Barcelona (2020d). Based on the set of measures presented by the Barcelona City Hall, we consider TUP actions that aim to remove vehicle lanes in major urban corridors of the city. In total we have reduced a total of 31.67 km from vehicle lanes, represented by the dotted blue lines in Fig. 5.4b. Additionally, we have implemented a total of eight superblock areas represented by the orange polygons in Fig. 5.4b. The considered Superblocks are the ones with specific information of the planned actions made within. The specific streets modified and Superblocks applied can be found in the supplementary material.

In order to quantify the impact of each of these measures and differentiate their specific potential undesired rebound effects, we have simulated them individually and collectively, as specified in Table 5.1. On top of these scenarios, we have also modelled a Base Case (business-as-usual) scenario, which is taken as the reference for the comparison. The criteria to select the simulated scenarios was based on the ability of the traffic-emission-air quality system to estimate the new vehicle route equilibrium and the traffic associated emissions. Hence, the unique application of measures affecting vehicle emission factors (i.e., LEZ) were not considered for air quality simulations since similar studies have already been published elsewhere (Soret et al., 2014).

One of the major difficulties in simulating the effects of traffic restrictions on vehicle fluxes is to estimate how the demand (e.g., total number of trips) will be affected due to their implementation. In this study, we assumed both the most pessimistic and optimistic scenarios, which are: (i) the number of total circulating vehicles will not change despite the measures implemented; and (ii) the traffic demand will suffer a -25% reduction once all the three different strategies are fully implemented, which is the expected reduction estimated by the Barcelona city council (Ajuntament de Barcelona, 2020d). In total, we simulated seven NO_x emission scenarios (one for each combination of traffic management strategies) and modelled the impact on NO_2 air quality levels in four of them due to the large computational load that it requires (Table 5.1). NO + NO_x (NO_x) and VOCs were simulated for all emission scenarios although only NO_x is represented since VOCs are used for the GRS chemical processes of CALIOPE-Urban. Even though Particular Matter (PM) is a pollutant with severe health issues, it will not be

simulated in this study since the GRS module used by R-Line can only compute the dispersion of primary species (e.g., black carbon).

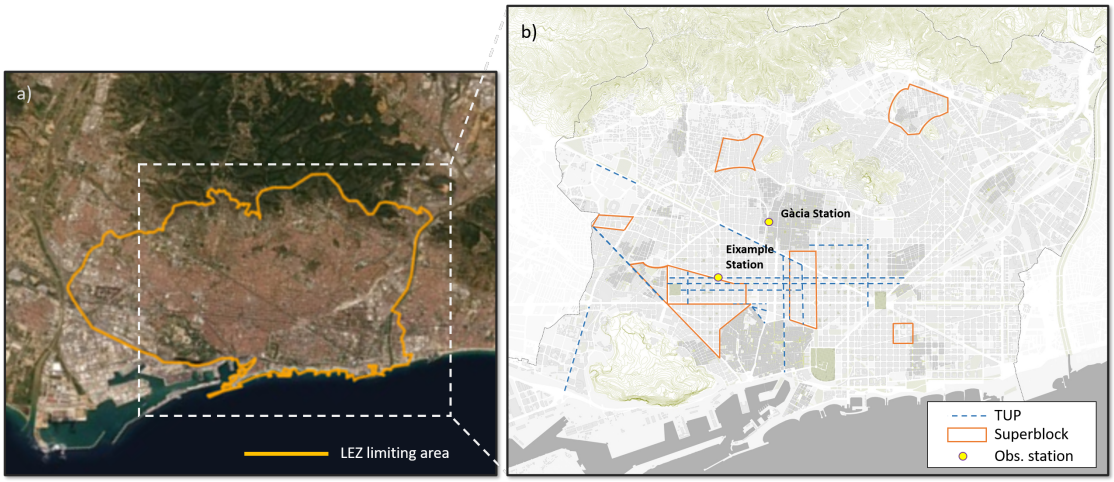

Figure 5.4: Barcelona study domain showing a) the area where the Low Emission Zone is applied (orange) and b) the Superblocks (orange squares), the streets where tactical urban planning (TUP) actions were implemented (dashed blue lines), and the Barcelona urban traffic air quality monitoring stations (yellow dots). Adapted from Ajuntament de Barcelona (2020e). The ortogonal image from a) was obtained from Leaflet — Tiles © Esri — Source: Esri, i-cubed, USDA, USGS, AEX, GeoEye, Getmapping, Aerogrid, IGN, IGP, UPR-EGP, and the GIS User Community.

Tactical Urban Planing and Superblocks scenario

Changes on the traffic flow and speed induced by the TUP and SPB strategies were modelled following the description of measures reported in Ajuntament de Barcelona (2020b) and Ajuntament de Barcelona (2020c). To do so, we have modified target features of the original VML road network. The modifications include the removal of traffic lanes, changes in the street capacities and allowed maximum speed, and the addition of new turns to characterize SPB measures. The reduction of vehicle lanes of the TUP measures was directly applied to the VML network. The VML road capacity is calculated by the multiplication of the user-defined number of lanes and capacity of each lane, which depends on the specific road type (e.g., highway, urban corridor, etc). The number of lanes of the street links affected by the TUP measures were manually modified. Specific information of the modified links can be found in the supplementary material. For the SPB areas, in addition to the above-mentioned modifications, the construction

Table 5.1: List of scenarios and combination of traffic management measures considered in the study (TUP, Tactical Urban Planing; SPB, Superblocks; and LEZ, Low Emission Zone). Emissions have been modelled for all the scenarios, while we specify the scenarios where the air quality impact (AQ) has been modelled.

nº	Scenario	AQ
1	Base Case: Original 2017 network	Yes
2	Base Case + TUP	No
3	Base Case + SPB	No
4	Base Case + TUP + SPB	Yes
5	Base Case + LEZ	No
6	Base Case + TUP + SPB + LEZ	Yes
7	Base Case + TUP + SPB + LEZ + demand reduction (-25%)	Yes

of traffic-pacified street segments was modelled using a new segment type with a specific reduced capacity and speed (Table 2.2). All modifications are made to prevent the circulation of modelled traffic flow as shown in Fig. 5.5.

Low Emission Zone scenario

The LEZ scenario, which forbids the entrance of the most polluting vehicles in the city, was simulated by adapting the description of the vehicle fleet composition profiles used in HERMESv3 to the restrictions associated to this measure. We assumed an optimistic scenario in which all banned vehicles are replaced by new Euro 6 vehicles. We wanted to reflect the tendency of drivers to switch from diesel to gasoline cars that can already be detected from the sales of gasoline-powered cars (European Automobile Manufacturers Association, 2021). To do so, we used the new registered vehicle data in Barcelona for 2019 (DGT, 2020), and applied the observed gasoline/diesel sales distribution to the new Euro 6 vehicles that appeared as a consequence of the LEZ. We did not substitute the banned vehicles by zero or low emission vehicles based on the Barcelona city hall expected vehicle fleet composition renewal for the next years, which accounts for less than 3% of zero or low emission vehicles by 2022 (Institut Cerdà, 2019).

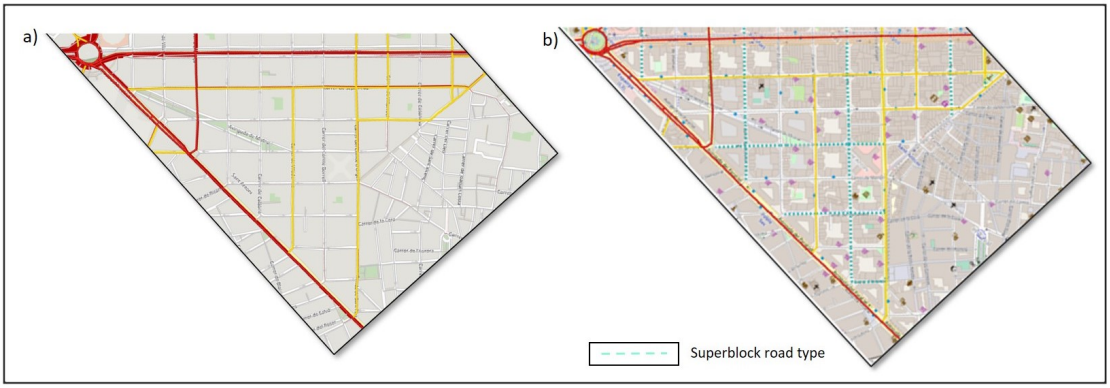

Figure 5.5: Screenshot of the VML traffic simulator network for (a) the Base Case scenario, and for (b) scenario SPB where a specific road type has been generated (blue dotted line) to represent the superblock restrictions. The colored segments indicate other street types with different parameters restricting vehicle movement (e.g., as a consequence of a traffic light green wave). From higher movement to lower: Red, yellow, grey, dottet blue. Detailed information about the traffic simulation can be found in Rodriguez-Rey et al. (2021).

Figure 5.6 compares the observed vehicle fleet composition in 2017 (AMB and RACC, 2017) and the estimated one after applying the LEZ. The share of Euro 6 diesel vehicles increases from 14% to 20%, while the share of Euro 6 gasoline vehicles increases from 6% to 19%. The obtained LEZ fleet composition was applied to the road links within the LEZ domain represented by the orange area in Fig. 5.4a. Due to the difficulties in assessing the LEZ impact on traffic flow (Holman et al., 2015), this scenario does not imply reductions in the simulated traffic demand.

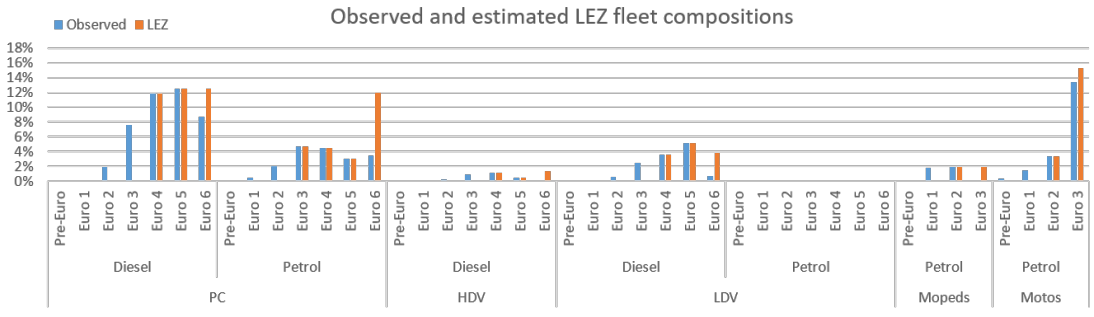

Figure 5.6: Observed vehicle fleet composition in 2017 (blue) and estimated Low Emission Zone (LEZ) vehicle fleet composition (orange) per vehicle type and Euro category. PC refers to Passenger Car, HDV to Heavy Duty Vehicle, and LDV to Light Duty Vehicle.

5.3. Results and discussion

Section 5.3.1 presents the NO_x emission results computed for the Base Case scenario and a comparison of the CALIOPE and CALIOPE-Urban NO_2 modelled concentrations against observations registered at the two urban traffic monitoring stations shown in (Fig. 5.4b). The model performance at the other urban background monitoring stations can be found in the supplementary material. The emissions and air quality results for each of the traffic management scenarios are presented and discussed in Section 5.3.2 and 5.3.3 respectively.

5.3.1 Base Case scenario

Figures 5.7a and 5.7b show the road traffic emissions for the Base Case scenario used as input in the CALIOPE (1 km $\times$ 1 km) and CALIOPE-Urban (20 m $\times$ 20 m) systems, respectively. The VML-HERMESv3 estimated link-level vehicle emissions which are used by CALIOPE-Urban, are mapped onto the 1 $\times$ 1 km^2 gridded domain for CALIOPE in order to ensure consistency between modelling scales. Note that in Fig. 5.7b emission results are presented at a 50 m $\times$ 50 m resolution only for representation purposes. Both figures show that the highest NO_x values are found in the ring roads and the city center, where the main urban corridors are found. However, the street-level results allow representing the strong emission gradients that cannot be reproduced at 1 km $\times$ 1 km. Similarly, a large heterogeneity of the NO_2 distribution is observed with CALIOPE-Urban (BCN-20m), while the mesoscale CALIOPE (BCN-1km) modelling results show a rather uniform distribution of NO_2 levels across the city, the largest values being found near the port area (Fig. 5.7c and Fig. 5.7d).

Figure 5.8 shows the NO_2 average diurnal cycle observed at the Eixample and Gràcia stations (black dotted lines) and modelled by the CALIOPE and CALIOPE-Urban systems for the Base Case scenario (brown and pink lines, respectively). Standard statistics computed using the modelled and simulated concentrations are summarised in Table 5.2. CALIOPE-Urban is capable of capturing the morning and afternoon NO_2 peaks at the Eixample station, while it slightly overestimates the afternoon peak hour at Gràcia by 3% and estimates it earlier. Yet, the system is not able to properly capture the concentrations observed dur-

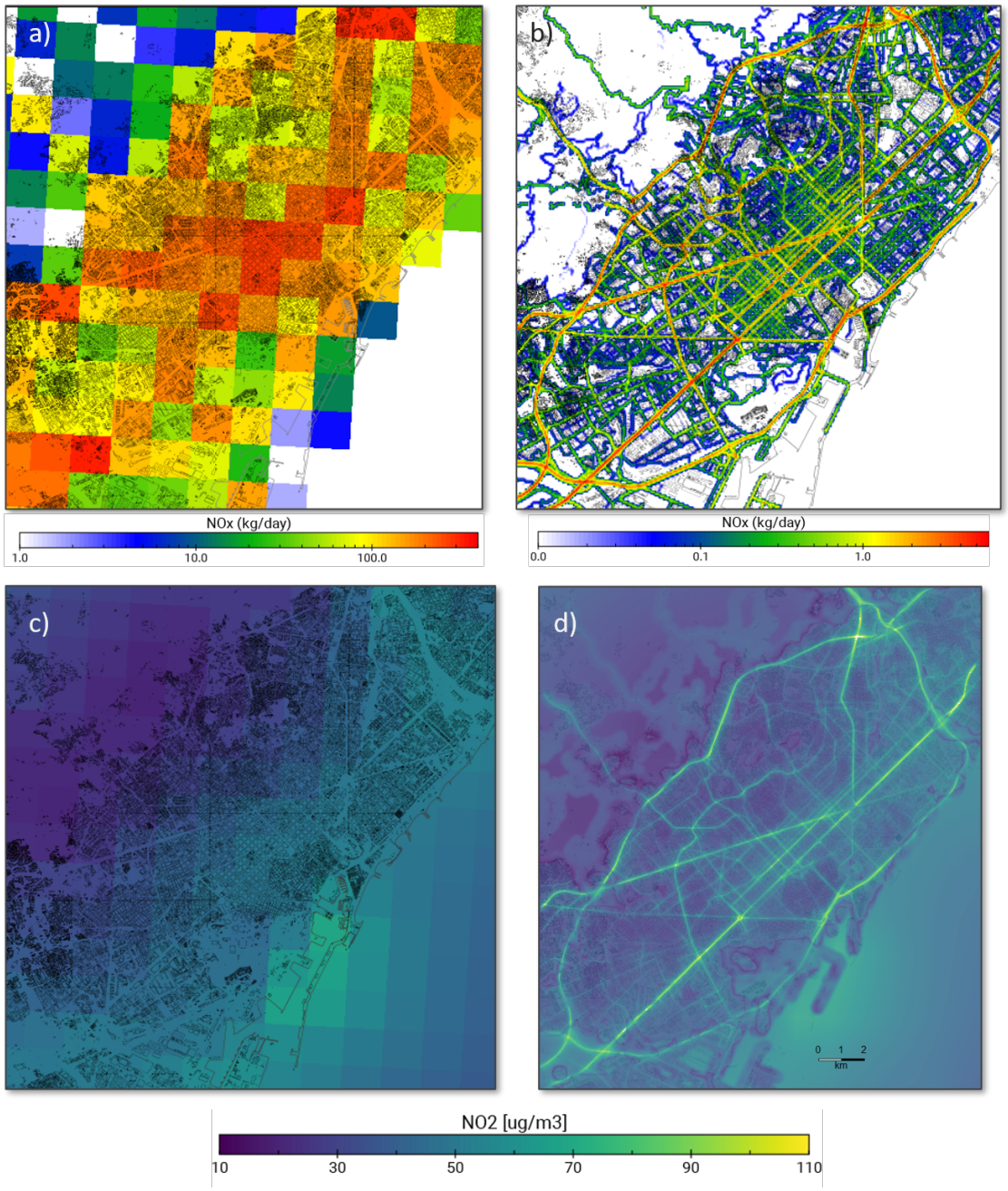

Figure 5.7: Average daily NO_x traffic emissions (kg/day) modelled by VML-HERMESv3 at a resolution of 1 km × 1km (a) and 50 m × 50 m (b), and average daily NO_2 concentrations ($\mu g/m^3$) modelled by CALIOPE and CALIOPE-Urban at a spatial resolution of 1 km × 1 km (c) and 20 m × 20 m (d).

ing the valley hours (11-16h), and it presents an underestimation of 30 µg/m^3 (-38%) in both stations. This behaviour in CALIOPE-Urban is inherited from the CALIOPE regional model, which cannot properly reproduce the vertical mixing of pollutants during daytime. Results clearly indicate that CALIOPE-Urban improves the modelling performance in capturing the NO_2 peaks with respect to the mesoscale approach (CALIOPE) while providing a more detailed information at the street-level. In both stations CALIOPE-urban reduces the mean bias observed with CALIOPE by half (-12 and -16 µg/m^3 vs -24 and -33 µg/m^3, respectively) and increases the FAC2 (fraction of predictions within a factor of two observations) by 0.21 and 0.11 in Gràcia and Eixample respectively, while maintaining a similar correlation (0.54 vs 0.58 and 0.52 vs 0.55 for Gràcia and Eixample).

Table 5.2: NO_2 model evaluation statistics calculated for the urban (CALIOPE-Urban) and mesoscale (CALIOPE) system at Eixample and Gràcia stations for the period of study (7 to 25 November 2017). *FAC2* refers to the fraction of modelled results within a factor of 2 of observations, *MB* refers to the mean bias, *RMSE* refers to root-mean-square Error, and r to the correlation coefficient.

Site	Model	FAC2	MB	RMSE	r
Eixample	CALIOPE	0.67	-23.99	38.01	0.52
	CALIOPE-Urban	0.77	-12.00	32.65	0.55
Gràcia	CALIOPE	0.54	-33.34	46.36	0.54
	CALIOPE-Urban	0.75	-15.88	36.00	0.58

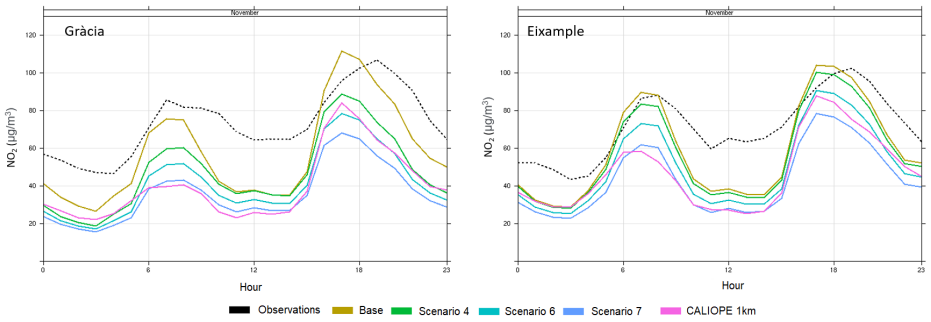

Figure 5.8: NO_2 average diurnal cycle observed (dotted back) and modelled with CALIOPE-Urban for the Base Case scenario (brown), scenario 4 (green), scenario 6 (sky blue) and scenario 7 (blue), and with CALIOPE for the Base Case scenario (pink) at Gràcia and Eixample urban traffic stations during the period of study (7 to 25 November 2017).

5.3.2 Impact of traffic strategies on NO_x emissions

Figure 5.9 shows the aggregated NO_x daily mean emissions for the base case scenario over the complete modelling domain, and the relative difference with the scenarios 2 to 7 for the period of study. According to these results, emissions are only reduced on those scenarios where the LEZ or the traffic demand reduction of -25% are implemented (scenarios 5 to 7). For all the other scenarios, when only TUP or SPB strategies are considered, the impact on the total NO_x emissions is negligible (+0.1%, due to the new generated congested areas). Maximum reductions (-30%) are achieved when all the traffic management strategies are combined and a -25% reduction of the number of vehicles is assumed. The combination of all strategies without changes on the number of circulating vehicles shows overall NO_x reductions of -13.1%.

Despite not having any impact on the overall emissions, a significant redistribution of emissions at the street level can be observed when only implementing the TUP and SPB measures (scenarios 2 - TUP -, 3 - SPB -, and 4 - TUP+SPB -), which is caused by the re-routing of traffic assignment. To illustrate that, Fig. 5.10a shows the daily mean NO_x difference in an aggregated grid of 100 m $\times$ 100 m between the scenarios 2 to 7 with the Base Case scenario. Note that emissions at Fig. 5.10a are shown in a grid of 100m for representation purposes, but the original emission outputs are obtained and passed to VML at the road link level. Since scenario 4 is the one combining TUP and SPB measures, in Fig. 5.10b we take a closer look into how the traffic flow (in annual average daily traffic, AADT) and associated NO_x emissions change in five representative street cells. The mentioned streets over the analysed emission cells are illustrative, since the 100 m $\times$ 100 m emission grid cell could also contain parts of other street segments. In this sense, the cell in one of the urban corridors with higher traffic load and emissions, Aragó (1) (Fig. 5.10b), shows an average reduction of -17% (-1.3 kg $NO_x/100m^2$) in the simulated NO_x emission levels along the cell with a traffic flow reduction of -24% (-21,000 vehicles/day) (Fig. 5.10b). On the other hand, NO_x emission increases up to +17% (+0.5 kg $NO_x/100m^2$) are observed in other adjacent cells (e.g., Tarragona (4) or Viladomat (5)) as a consequence of a traffic flow increase of +30% (from 20,203 to 26,280 vehicles/day) and 125% (from 4,380 to 9.870 vehicles/day) respectively Fig. 5.10b). Viladomat (5) is of particular interest since the street is

within a Superblock area but it is still absorbing the traffic through it. This street also contains a traffic count station which allow us to compare the simulated traffic flow values with the observations from 2019, before the COVID-19 pandemic but after the implementation of the Superblock. The observed traffic flow in this street between 2017 and 2019 has increased a 118% (from 4,866 to 10,643 vehicles/day) which is in agreement with the simulated BCN-VML estimated values. We cannot perform this scenario validation for all the network since the other applied TUP and SPB measures were finished after the COVID-19 pandemic, when traffic activity had a drastic decrease.

In other terms, we have not found evidence of linearity between the absolute or relative traffic flow increment/decrement with the absolute or relative increase or decrease in NO_x emissions. This might be caused by the emission dependency in both traffic flow and speed, by the presence of other segments within the grid adding extra emissions and the difficulties of the macroscopic system in recreating vehicle emissions under congested situations. As described in Chapter 3, the macroscopic system cannot properly estimate the location of bottlenecks and the start-stop vehicle behaviour, which implies an underestimation of vehicle emissions in these situations.

Our results reveal that large Superblocks cannot avoid the through pass of vehicles within the designated area if traffic pacification measures are not applied in all streets within the superblock (Fig. 5.5). Smaller Superblocks like the Poble Nou and Sarrià show NO_x emission decreases in all their streets that can reach up to -15%. This is due to the already low traffic load of such areas, that now discourage the through traffic, becoming areas used only by residents and services.

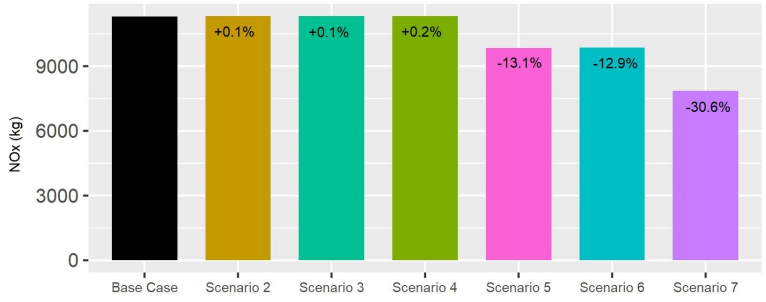

Figure 5.9: NO_x daily mean emissions (kg) for all scenarios and the relative differences (%) between the Base Case and the other simulated scenarios.

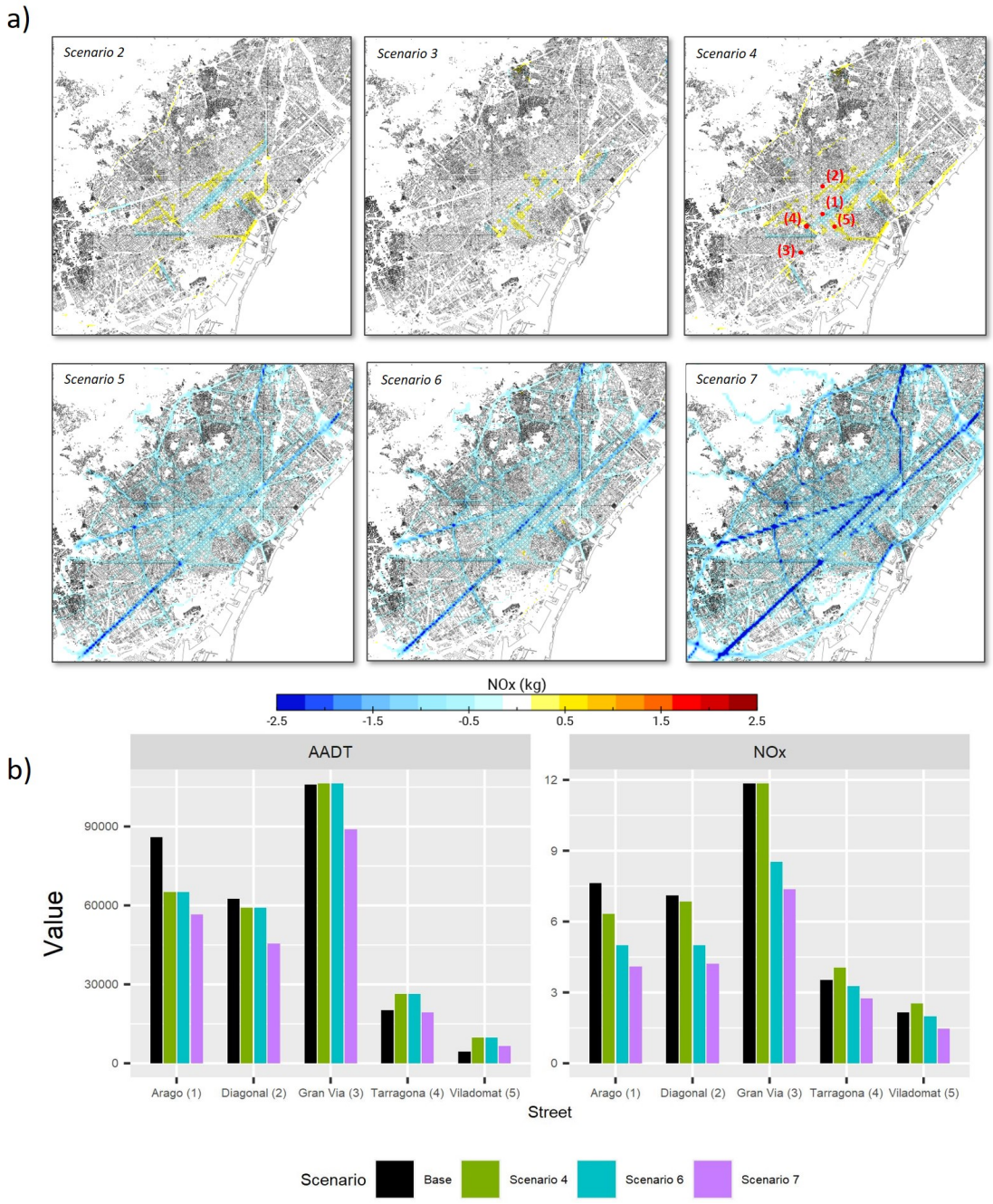

Figure 5.10: a) Daily mean NO_x emission differences (kg/100m^2) from the Base Case scenario with the scenarios 2 to 7 for the period of study. Scenario 4 also shows the location of the streets commented in b): Aragó (1), Diagonal (2), Gran Via (3), Tarragona (4) and Viladomat (5). Part b) shows the annual average daily traffic (AADT) and daily mean NO_x emissons (kg) of the above-mentioned streets for the Scenarios Base Case, 4, 6 and 7.

5.3.3 Impact of traffic strategies on NO_2 air quality levels

Figure 5.11 illustrates the differences between modelled NO_2 concentrations averaged over the period of study in scenarios 4, 6 and 7 and the Base Case scenarios using CALIOPE (left column) and CALIOPE-Urban (right column) systems. In line with the emission results, the impact of traffic measures on NO_2 concentrations is mainly observed when LEZ and/or the traffic demand reduction of -25% are implemented (scenarios 6 and 7). Under these two scenarios (6 and 7), NO_2 daily mean reductions of -5 to -10 µg/m^3 (-10% to -20%) and of -10 to -25 µg/m^3 (-20% to -30%) are observed in the main urban corridors, respectively, during the period of study. In both scenarios, the largest NO_2 decreases occur in the most trafficked streets due to the presence of less polluting vehicles (LEZ) and the implementation of TUP and SPB measures in such streets. When only TUP and SPB measures are considered (scenario 4), NO_2 impacts are very limited. NO_2 reductions and increases of similar intensity (±5 µg/m^3) are observed as a function of the street due to the traffic re-routing, as explained in section 5.3.2. The strong street gradients and associated NO_2 concentration changes modelled with CALIOPE-Urban cannot be reproduced with the CALIOPE mesoscale system, which captures NO_2 reductions of only -6 to -10 µg/m^3 and between -3 to -6 µg/m^3 for the scenarios 7 and 6, respectively.

As shown in Table 5.3, with CALIOPE-Urban and under the most restrictive scenario with a demand reduction of -25% (scenario 7) the NO_2 averaged daily maximums would be reduced by a -36% and -22.5% in Gràcia and Eixample monitoring stations. This would represent a reduction of the observed daily maximum from 111 to 71 µg/m^3 (-39 µg/m^3) and from 105 to 81 µg/m^3 (-23 µg/m^3) of NO_2 for Gràcia and Eixample monitoring stations. If we perform the same exercise for the average daily mean, the observed NO_2 daily mean for Gràcia would be of 45.5 µg/m^3 (-38%) and of 52.4 µg/m^3 (-26.6%) for Eixample. On the other hand, the NO_2 reductions captured by the mesoscale CALIOPE system are around half (-18% and -17% for the daily average mean and daily maximum, respectively).

Table 5.3: Period-averaged daily mean and period-averaged daily maximum modelled NO_2 values ($\mu g/m^3$) for the Base Case scenario and the relative difference with the scenarios 4, 6 and 7 at the Gràcia and Eixample air quality station.

		CALIOPE-Urban		CALIOPE	
Scenario	Station	Daily mean average	Daily maximum	Daily mean average	Daily maximum
NO_2 base case	Gràcia	57.4	111.0	39.3	82.0
($\mu g/m^3$)	Eixample	59.2	105.0	46.5	87.0
Scenario 4	Gràcia	-18.6%	-18.7%	0.0%	0.0%
(Diff. %)	Eixample	-4.4%	-2.0%	0.0%	0.0%
Scenario 6	Gràcia	-28.6%	-26.2%	-10.4%	-6.1%
(Diff. %)	Eixample	-15.0%	-11.8%	-10.8%	-8.0%
Scenario 7	Gràcia	-38.0%	-36.4%	-18.1%	-17.1%
(Diff. %)	Eixample	-26.6%	-22.5%	-18.3%	-17.2%

Our work provides an estimate of the expected emissions and concentration levels after the application of the traffic restrictions in Barcelona. Based on the relative reductions obtained, we estimate that all the simulated scenarios would fail in reducing the annual average value below the AQD limit of ≤ 40 µg/m^3 of NO_2 in the two traffic stations for the considered study period. Yet, under scenarios 6 and 7, the NO_2 hourly exceedance of 216 µg/m^3 that occurred in November 2017 would very likely have been avoided.

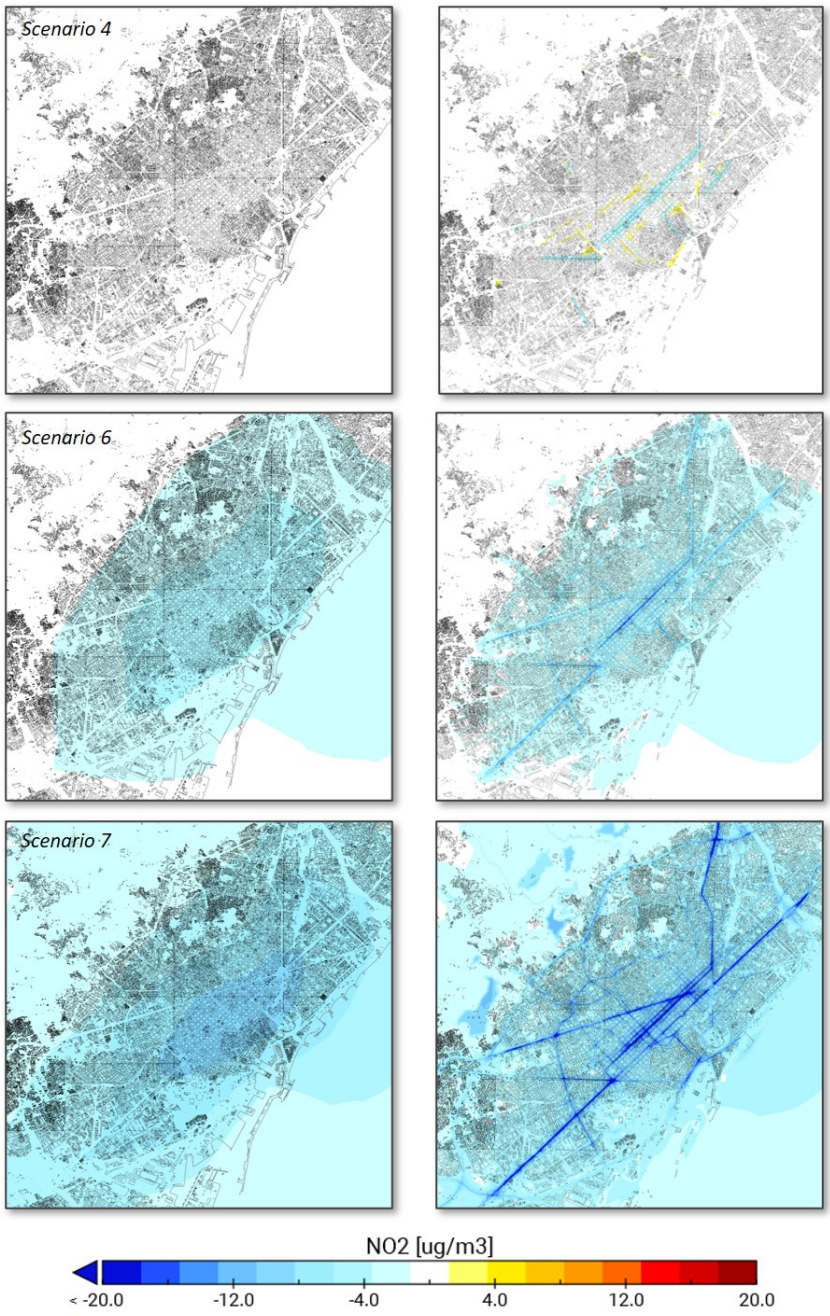

Figure 5.11: Daily mean NO_2 concentration difference ($\mu g/m^3$) between the base case and the scenarios 4, 6 and 7 for the November period. Left column shows the mesoscale values from CALIOPE model (1km resolution) while right column shows the CALIOPE-Urban street scale model results (20m resolution). Bluewish and yellowish colors indicate a decrease and increase in emissions, respectively.

5.4. Conclusions

We quantified the impact of different traffic management strategies on the NO_x emissions and NO_2 concentration levels in the city of Barcelona. To do so, we performed a multi-scale air quality modelling exercise that combines mesoscale (1×1 km) and street-scale (20×20 meters) air quality modelling tools, fed by a coupled macroscopic traffic and vehicle emission model. A total of 7 NO_x emission scenarios and 4 NO_2 air quality scenarios were simulated during a bi-weekly time period, which coincides with an air pollution episode that took place in November 2017. The scenarios comprise simulations of individual and varying combinations of the mobility measures currently being applied in Barcelona: a Low Emission Zone (LEZ), which aims to forbid the entrance of most polluting vehicles, Tactical Urban Planing (TUP) measures, which reduce the space that private transport has on specific streets of the city, and the Superblocks (SPB), which prevent the entrance of vehicles in a certain urban area delimited by several blocks. We additionally added a scenario where all these measures were combined with a traffic demand reduction of -25% based on the City Hall's expectations over the next years. The main findings and conclusions of this work are as follows:

- The largest road transport NO_x emission reductions in Barcelona (-30%) are obtained when combining all traffic management strategies (LEZ, TUP and SPB) together with the -25% traffic demand reduction. The computed reductions are only of -13% when traffic demand is kept constant.

- When only implementing measures related to the reduction of private transport space (TUP and SPB), overall NO_x changes are negligible (+0.1%). Nevertheless, these measures generate a traffic redistribution along the network, which shows a noticeable impact on the street-level emission distribution, with NO_x variations up to $\pm$17% in specific streets as a consequence of the new vehicle routing and the variation in traffic flow and speed. We have not found evidence of linearity between the traffic flow and speed variation and the increment or decrement in NO_x emissions.

- The impact on NO_2 air quality levels follows the same pattern as for emissions. Scenarios comprising all the traffic strategies with and without the

-25% demand reduction show the largest NO_2 reductions at the main urban corridors (with daily mean reductions of -10 to -25 µg/m^3 and -5 to -10 µg/m^3, respectively and daily max reductions up to -70 µg/m^3 and -50 µg/m^3, respectively). When only implementing the TUP and SPB measures, limited increases and decreases of NO_2 are observed ($\pm$5 µg/m^3) due to traffic re-routing.

– The expected differences at the two traffic air quality monitoring stations of the city (Gràcia and Eixample) when implementing all traffic strategies and the demand reduction are of -38% and -27% for the daily mean average, and of -36% and -23% when considering the averaged daily max values for Gràcia and Eixample, respectively. These values decrease by approximately a 10% without considering the demand reduction.

– The NO_2 daily mean and peak concentration reductions modelled with the mesoscale system are almost two times lower than the ones obtained with the urban scale system. Despite presenting consistent results, the mesoscale system is not capable of modelling the strong street gradients and associated NO_2 concentration changes induced by the mobility restrictions. Considering these results, we recommend that the evaluation of urban traffic management strategies is performed applying a multi-scale modelling approach with street scale resolution for an optimal result.

– Although traffic management strategies lead to significant emissions and air quality improvements, the reductions achieved are insufficient to ensure proper air quality levels. These strategies must be accompanied by a large decrease in the total number of vehicles circulating throughout the city.

The methodology followed in this study can provide highly-detailed data for health assessment studies, like the one performed by Mueller et al. (2020). On the same direction, it could be used for an ex-ante evaluation of further mobility policies applied by policy-makers, providing some insights before its application. In Barcelona, since the current measures appear to be insufficient to reduce the NO_2 levels below the EU AQD, the authors suggest the study of other proven-effective measures in reducing traffic demand like the congestion charging scheme, with successful results in Milan, London or Stockholm (Croci, 2016) combined

with a more restrictive LEZ (Bigazzi and Rouleau, 2017).

This research shows that the application of a multi-scale air quality tool, combining traffic, emission and street dispersion models is essential to properly capture the induced NO_x and NO_2 variations generated by the application of different traffic management strategies. We acknowledge the limitations of the macroscopic traffic model to properly recreate the start-stop vehicle behaviour under congested situations, which implies an underestimation in vehicle emissions, as shown in Chapter 3. The macroscopic tool is however appropriate to estimate the impact of the analysed strategies at urban scale. The usage of a microscopic tool able to properly estimate traffic flow and vehicle emissions at the studied domain it is currently not a viable option due to the data and computational load needed. We also acknowledge the limitations of the study related to traffic demand modelling. It was assumed constant over the different scenarios studied, with the exception of scenario 7 which had a demand reduction of -25%. In reality, a modal transfer could occur between the private and public transport, or to other active ways of mobility (e.g., cycling) due to the private transport restrictions. In future works we plan to keep with the analysis of possible new TMS such as the application of green corridors (Ajuntament de Barcelona, 2021) or to study the impact of additional measures that are currently not being considered by the city council such as the implementation of a congestion charge.

6. Conclusions

In this Ph.D thesis we quantified and evaluated the impact of multiple traffic management strategies on the NO_2 emissions and air quality levels for the city of Barcelona, Spain. To this end, we developed and validated a multi-scale and coupled traffic-emission-air quality modelling system tailored for the area of study. The developed system is based on a macroscopic traffic simulator and an average-speed vehicle emission model combined with an Eulerian mesoscale and a Gaussian street-scale air quality modelling tools. The system allows to estimate the induced emission and air quality impacts of the applied mobility policies at very high spatial (from 1km $\times$ 1km to 20m $\times$ 20m) and temporal (1 hour) resolutions. The main results derived from this Ph.D thesis are summarised in section 6.1, while a series of recommendations and future works are exposed in section 6.2. Finally, section 6.3 exposes the concluding remarks and thoughts of the manuscript.

6.1. General conclusions

Chapter 2 presents the fundamentals in traffic, emission and air quality modelling and gives a description of the traffic, vehicle emission and air quality tools used in this work. The traffic simulator used is the BCN-VML, based on the macroscopic traffic model PTV-Visum. The model comprises a region of around 6.000km^2 and a population of two million inhabitants generating and attracting 4 million vehicle trips every day. The simulation process goes through 24-hourly simulations by a static traffic assignment approach, which generate hourly private and public bus traffic flow and speed for every link of the network for a business as usual day. This data is then read by the average-speed vehicle emission model HERMESv3, which computes NO_x, CO, NMVOC, PM, SO_x and NH_3 traffic emissions based on the emission factors of COPERT V following the Tier 3 methodology of EMEP/EEA. The coupling is script-based and assures a correct mapping of the links with their generated speed and traffic flow profiles together with their specific zone-dependent vehicle fleet composition. The link-level estimated NO_x and NMVOC hourly traffic

emission are then passed to the mesoscale CALIOPE air quality system (1km^2 horizontal resolution) and to the street-scale CALIOPE-Urban air quality system (20m horizontal resolution) to compute NO_2 concentration values.

Chapter 3 describes the calibration of the BCN-VML and the coupling with the HERMESv3 vehicle emission model, followed by a sensitivity analysis of the developed system to some of the key input emission parameters. Our aim was to give a methodological guidance in traffic emission estimates for large urban areas, while showing the potential discrepancies in the emission estimates depending on the quality of the data used. The traffic flow and speed calibration of the BCN-VML was based on multiple street-level observational datasets, including traffic counts and TomTom GPS-based speed profiles. The vehicle fleet composition of the system was upgraded to include a total of five different zone-dependent fleet compositions corresponding to specific areas of the city, based on the results of a remote sensing device campaign performed in Barcelona in 2017. Additionally, the public bus transport routes and frequencies were included to compute their specific emissions with the correspondent circulating bus fleet composition.

This chapter also presents a comparison of the annual NO_x and PM_{10} emissions computed with the coupled system for the year 2017 against the results reported by two local emission inventories in Barcelona followed by an spatial and temporal evaluation, whose main highlights are:

- The VML-HERMESv3 estimated NO_x results are in agreement with the other two inventories (range of -5% to +9%). Larger discrepancies of +18% and +105% were observed when results are compared to the annual PM estimated values. These are believed to be caused by the inclusion of resuspension in the HERMESv3 system, not considered by the other two inventories.

- The spatial distribution of traffic emissions across the city is quite heterogeneous. Eixample district is the area with higher emissions (291 kg·day^{-1}·km^{-2}). These results contrast when compared to its neighbouring districts -Ciutat Vella and Gràcia- where total estimated NO_x emissions are halved (144 and 150 kg·day^{-1}·km^{-2} respectively). It is noteworthy that these two districts contain a large fraction of traffic-calming and pedestrian areas that already existed in 2017.

– Regarding the temporal profile, Barcelona shows a steady activity level during daylight hours (7:00h to 18:00h) and during weekdays for most of the year. Traffic emissions only decrease during nighttime, weekends (-41%) and summer holidays (e.g., August, -26%).

The sensitivity analysis previously mentioned is focused on different approaches in regard of vehicle fleet composition, public bus transport implementation, temperature impact or the application of non-exhaust PM emissions. Results show that:

– There is an important zonal impact of an area-dependent vehicle fleet composition against an homogeneous one (up to +788% in NO_x in the port area). This is also observed when considering the current public bus transport routes instead of assigning a fixed bus contribution to every link on the network (+300% NO_x in specific links).

– Homogeneous differences up to +19% in NO_x are observed when considering temperature influence in vehicle emissions (e.g., cold-start extra emissions) or the consideration of non-exhaust PM sources (+410% in PM_{10} emissions).

During this sensitivity analysis, it is noteworthy that the observed differences are notable and independent of the level of detail used (i.e., macroscopic, mesoscopic or microscopic), which does not entail higher computational load or complexity to the modelling system, but more specific data of the area of study. Finally, it is worth to remark that the VML-HERMESv3 system developed in this chapter is also transferable to other locations. For that matter, the new location of study should only need a built VISUM network and some basic traffic data -such as the vehicle fleet composition and local street traffic counters- in order to implement the methodology in here presented. If the location would be outside Europe, probably a mapping between the COPERT vehicle categories and the local ones should also be needed.

Chapter 4 presents a comparison of the emission results estimated by the developed macroscopic system with a microscopic approach. This chapter exposes the discrepancies between both modelling approaches and the limitations of the macroscopic system in estimating vehicle emissions, which mostly occur during congested situations. In an area of 0.4 km^2 in Barcelona, three different streets with

different congestion levels (free flow, normal flow and congested) are analysed. This chapter also uses the higher level of detail of the microscopic system to perform an analysis of the road gradient impact on emissions. Main results show that:

- The microscopic system estimated +65% more NO_x emissions for the congested street. Streets at free flow and normal flow showed similar NO_x emission results (-11% and +15% respectively).
- These differences are believed to be caused by the traffic assignment process (Static or Dynamic traffic assignment) and the vehicle to vehicle start-stop behaviour during congestion, which highly increases emission factors and the time needed by each vehicle to cross the link.
- The extra emissions caused by a positive road gradient are balanced by these of the negative one (e.g., +13.8% and -12.1% for PC in a free flow street).
- Vehicle weight was found to be directly related with the extra emissions of the road gradient (+13.8%, +19.6% and +26.4% for PC, HDV and BUS respectively).
- The congestion level also affected the extra emissions carried by the road gradient. These were diminished under congested conditions, and increased during free-flow (+10.1% in congested situation vs +19.6% at free-flow for a HDV).

Finally, chapter 5 quantifies the impact of multiple traffic management strategies on Barcelona's NO_x emissions and NO_2 air quality levels by means of high-resolution modelling. The novelty of this study lied mainly in two aspects, namely: 1) the ability of the VML-HERMES coupled system to generate the new vehicle routes that vehicles will perform after the implementation of the different traffic restrictions, and observe the induced impacts in emissions and air quality from the new vehicle route equilibrium and 2) the multi-scale nature of the study, which allows quantifying the impact of the measures at the grid-level (1km $\times$ 1km) and street-level (20m $\times$ 20m) by combining the same modelled emissions with the CALIOPE and CALIOPE-urban systems, respectively. The measures included, on the one hand, the implementation of traffic restriction measures aiming at reducing traffic activity in certain areas and corridors of the city and, on the other

hand, the application of a Low Emission Zone (LEZ). Traffic activity is reduced by the application of the Superblocks model and by the Tactical Urban Planning measures. These measures were simulated during a by-weekly period in November of 2017 in an individual and combined basis for a total of six different NO_x emission scenarios. Additionally, a seventh scenario combining all the measures with a traffic demand reduction of the -25% was also simulated since this is the expected demand reduction over the next years by the Barcelona City Hall. Due to the highest computational load required to compute air quality simulations, the NO_2 concentration levels were simulated for four different scenarios at both 1km $\times$ 1km and a 20 $\times$ 20 meters resolution. The main findings show:

- The largests NO_x emission reductions over the city are obtained by the LEZ (-13%) and the addition of the demand reduction over all the other measures (-30%).

- Measures affecting specific areas or streets do not present overall emission reductions, although they have important street-level impacts ($\pm$17%) in specific areas as a consequence of the new traffic routing.

- The results in NO_2 concentration values follow the same pattern as the simulated NO_x emissions. Daily mean reductions up to -25 µg/m^3 in NO_2 are observed when combining all measures and the demand reduction, with a slighter decrease of -10 µg/m^3 when traffic demand is kept constant.

- Results showed that even with the application of all the measures and the demand reduction, NO_2 concentration values at the two traffic air quality stations would still not comply with the EU AQD during the analysed study period.

- The modelled NO_2 daily mean and peak concentration reductions by the mesoscale system are almost two times lower than the ones obtained by the street-scale system (-38% and -18% estimated NO_2 reductions in Gràcia station by the street-scale and mesoscale systems, respectively). This shows that despite presenting consistent results, the mesoscale system is not capable of modelling the strong street gradients and associated NO_2 concentration changes induced by the mobility restrictions.

Considering all the above, the most relevant conclusions from this Ph.D thesis are as follows:

- It is essential to perform a proper evaluation of your modelling domain, time coverage and availability of data to select the correct tools and the approach to follow during the simulation process. The modeller has to be aware of the limitations and advantages of the selected approach to try to overcome the firsts and benefit the most from the second. For the case of this work, the modelisation of the whole city forced us to use a macroscopic approach, for which we did a specific study to quantify its limitations in traffic modelling and emission estimation and try to overcome them. It is obvious that a microscopic approach would result in a better performance of traffic dynamics simulation and emission estimation, but the simulation of a particular area of the city would not achieve the initial objectives of the thesis.

- The availability and usage of local observed data is crucial during the model building process. The high emission discrepancies between the different fleet compositions used or the validation of the simulated vehicle speed confirms this statement. We also had to estimate an optimistic vehicle fleet composition after the application of the LEZ due the lack of recent observed vehicle fleet data, which might over-estimate the benefits of the LEZ.

- The usage of traffic simulators is highly recommended for vehicle emission estimations. Regardless of their particular workflow and level of detail, they allow the emission modeller to move from static to dynamic traffic data. This is useful not only for scenario modelling, but also to keep an updated traffic network to feed to the emission model without a manual adjustment of traffic flows and speeds over time. This is a new paradigm in emission modelling that will soon ensure that traffic and emission models are always found together.

- Despite the higher computational cost and data needed, the application of street-scale systems is essential for the evaluation of any kind of urban policy. It is important to put efforts in this part of the simulation process since a mesoscale evaluation would dilute air quality effects and miss the street-

gradient variances.

– Modelled results are not future projections but they are a first approximation of the values to come. And in this sense, the applied measures in Barcelona aimed at reducing its pollution levels below the EU air quality limits or the more stringent WHO air quality guidelines appear to be insufficient.

6.2. Future research

Despite the advances in scenario modelling for Barcelona presented in this Ph.D thesis, further assessments and improvements to solve some of the shortcomings of the system can still be done, in this sense:

Extension of time coverage and pollutants considered
The modelled results of the system have been used to estimate if the applied restrictions would comply with the annual EU daily mean limit values. Although this exercise was giving some indices of the expected reduction level from the applied measures, a more robust comparison could be done with an annual air quality assessment, instead of the two-weeks covered. Additionally, often air quality simulations are closely bound with health impact assessments and population exposure. In this sense, it would be necessary to consider also PM_{10} and $PM_{2.5}$ species due to their important health implications. On the same direction, the consideration of O_3 would give some insights about how the NO_2 reductions in Barcelona affect the ozone generation at the downwind areas of the city, and observe the mesoscale implications of local measures.

Generation of demand data
Travel demand data can be obtained by two different methods. The first -used in this Ph.D work- is based on static Origin-Destination matrices. These are build by observed population activity from GPS based data or by personal surveys. Although this approach has the advantage of considering all connection trips by adding them on the boundary areas of the domain, it is static on time. The OD matrices are built based on a specific time period, and if not updated their might not be longer representative. Often these matrices have to be manually adjusted to fit the current observed traffic flow data, as it was the case of this work. This

handicap is solved by the activity based demand approach. This method generates the travel demand based on population activity data (e.g., home density, work offices, social or commercial facilities, ...). By this approach any changes on the study domain that can carry a travel demand modification (e.g., a new job center, a shopping mall or a residential area) can be applied on the activity based model and considered when generating the demand for each specific simulation. On the other hand, this methodology requires detailed activity data and the generated demand is limited to the study domain, so this has to be large enough to account for connection trips.

Intermodality

Modal choice is a critical parameter when estimating traffic emissions in a urban environment. The application of different mobility policies often discourages or encourages the use of private transport leading to an associated shift in the modal share. In this sense, the application of multinominal logit models has been used elsewhere for the modal share estimation (Bueno et al. (2017); Romero et al. (2019)). The application of these models is however data-intensive, and they are often fed with individual or household travel surveys done by local authorities. The generated demand data has to be extended to cover not only private transport activity but all trips from the domain, and the traffic simulator software has to allow public transport infrastructure (e.g., metro and tram lanes). For this study, the traffic simulator in which the BCN-VML model is based already covers this last requirement, and hence further efforts to obtain the needed data to allow a multi-modal model could be done in a near future. By this exercise, current hypothesis applied in the thesis (such a reduction of -25% in traffic demand) could be also simulated and contrasted with the expected traffic demand reduction values reported by the Barcelona City Hall. Additionally, other measures involving travel economic cost and time, such as the congestion charge, could also be evaluated to observe the variation of the private transport demand as a function of the charged value.

Mesoscopic approaches

During the literature review of this thesis and in the conclusion section of Chapter 4, some works adapting macroscopic methodologies with some parameters of microscopic or mesoscopic approaches have already been commented. These methods increase the level of detail of the macroscopic approach by adding some characteristics of a mesoscopic or microscopic approach without all the specific data and computational resources required by these methods. Particularly, both the traffic assignment method and the vehicle dynamics can be improved with few more data. The static traffic assignment can be improved to the so called "quasi-dynamic" traffic assignment, which considers queuing and spillback. This is done by a post-process of the traditional STA, where links are loaded to their maximum capacity, up from this point, a second assignment is done distributing the exceeding link flow to the segments upstream. By these method, the level of congestion and its location is better represented. Although studies applying this method do not report substantial changes on the estimated emission totals, improvements in the spatial distribution of emissions which may lead to differences in dispersion, air quality and exposure for specific areas are observed. Different approaches have also been applied for the improvement of vehicle dynamics estimation at link-level. Rakha et al. (2011) used synthetic drive cycles to estimate the time that a vehicle spends in cruising, idling, decelerating and accelerating, to then estimate the emissions of these modes by microscopic emission models and associate them to the total distance of the link. This method cannot be directly applied into a macroscopic system since it requires mesoscopic dynamic variables such as the number of stops, stop delay and average speed per link to generate the synthetic drive cycles. But the association of synthetic drive cycles to link segments is worth to study. Another approach used by Negrenti (1999) applied congestion correction factors representing the speed variability along a link. Although the author does not exactly describe the magnitude and application of the congestion factor, we know that these are based on macroscopic dynamic variables such as traffic density and average link speed. Other works using simplified DTA and microscopic traffic emission models can be found in Gori et al. (2015), Zhou et al. (2015) or Nesamani et al. (2007). All of them combine characteristics of macroscopic and microscopic traffic and vehicle emission models to improve the estimation of vehicle emissions by adding few more additional data and computational cost to the system.

6.3. Defining urban mobility: Final remarks

The current urban mobility is rapidly changing in many urban conurbations around the word. Not only Barcelona, the focus of this Ph.D thesis, but also cities like Paris, Milan, London or New York are modifying its urban built to adapt to the legislated air quality values. If the XX century became the growth and expansion of the private transport and the space it had on cities, the XXIst century is being characterised by the re-gain of the urban space by pedestrians, active ways of transport and public transport. A clear example of that can be found in trams: from one of the most common ways of transportation at the beginning of the XX century, to almost disappear by the end of the century, to gain again prominence at the beginning of the XXIst. Something similar to what can be observed to cycle as a way of transportation, instead of being considered only a sport activity. These changes in urban habits are backed and encouraged by the application of new urban concepts that are arising among different leading conurbations. The Superblocks model that Barcelona is applying and we have studied in this thesis is just one more in a series of different new urban concepts, such as the 15-Minute city currently applied in Paris, the low traffic neighbourhood (London) or the car free city or neighbourhood (Vauban neighbourhood in Freiburg, Germany) (Nieuwenhuijsen, 2021). Generally, all these models tent to discourage private car and increase the usage of public and active transport.

However, although these ideas might look promising, the modification of mobility habits and urban structures is not something that policy makers usually want to do. During the realisation of this Ph.D, we have realised that the application of traffic restrictions and traffic emission reductions is lead by an every time more stringent regulation rather than a will to change the urban environment and transport culture. The recently updated WHO air quality guidelines which have drastically decreased the NO_2 annual mean (from 40 to 10 $\mu g/m^3$) are expected to lead the EU and national limit values to further encourage urban changes. The application of numerical tools then becomes a necessary element to guide the urban transformation process and assess policy makers on the magnitude and the level of restriction of the applied measures in order to comply with the legislated values.

Barcelona is an example of a city changing its mobility paradigm. Although the applied traffic restrictions go in the good direction, this thesis has shown that their expected outcomes are still not enough. A large part of the Barcelona inner traffic comes from areas outside of the city and hence further efforts should be done to offer sustainable alternatives for such commuters (e.g. increase the metropolitan train lines and frequencies) combined with measures that discourage the comfort of using private transportation; such as the application of a congestion charge to enter the city. Only by these means we will continue in shifting the social concept of one person - one car, to move to a shared and multi-modal way of transport (e.g. train - bike - metro). New technological appliances already offer the technical instruments to apply that, such as the Mobility as a Service (MaaS) concept which combines different transport modes to offer a user-tailored mobility package. Only with the will of people first and the governmental authorities second and with the support of modelling tools we will be able to change mobility and bring it to the XXIst century with more sustainable, greener and healthier cities for all.

7. Bibliography

H. Abou-Senna, E. Radwan, K. Westerlund, and C. D. Cooper. Using a traffic simulation model (vissim) with an emissions model (moves) to predict emissions from vehicles on a limited-access highway. *Journal of the Air & Waste Management Association*, 63(7):819–831, 2013. doi: 10.1080/10962247.2013.795918.

AEMET. Open Data, 2017. URL https://opendata.aemet.es/centrodedescargas/inicio. Last access: February 2020.

Aimsun S.L. *Aimsun Next 8.4 Users Manual*. 2019. URL https://www.aimsun.com/latest/final-release-aimsun-next-8-4/. Last Access: October 2017.

Ajuntament de Barcelona. Pla de mobilitat urbana pmu 2013-2018, 2014. URL https://ajuntament.barcelona.cat/ecologiaurbana/sites/default/files/PMU_Sintesi_Catala.pdf. Last access: July 2020.

Ajuntament de Barcelona. Pla de millora de la qualitat de l'aire de Barcelona 2015-2018, 2015. URL https://ajuntament.barcelona.cat/ecologiaurbana/ca/que-fem-i-per-que/ciutat-productiva-i-resilient/pla-de-qualitat-de-l-aire-de-bcn. Last access: July 2020.

Ajuntament de Barcelona. Dades bàsiques de mobilitat Informe 2017. Technical report, 2017. URL https://www.barcelona.cat/mobilitat/sites/default/files/documentacio/dadesbasiquesmobilitat-2017.pdf. Last access: October 2019.

Ajuntament de Barcelona. Mobility gauging detail of the city of Barcelona, 2019. URL https://opendata-ajuntament.barcelona.cat/data/en/dataset?q={&}name=aforaments-detall. Last access: May 2019.

Ajuntament de Barcelona. Sabies que Barcelona es la ciutat d'Europa amb més densitat de vehicles?, 2020a. URL https://ajuntament.barcelona.cat/qualitataire/ca/noticia/

\sabies-que-barcelona-es-la-ciutat-deuropa-amb-mes-densitat-de-vehicles_403904. Last access: August 2020.

Ajuntament de Barcelona. Una Mobilitat sostenible en un nou Espai Pùblic. Technical report, 2020b. URL https://www.barcelona.cat/mobilitat/ca/nova-mobilitat/una-nova-mobilitat-sostenible-en-un-nou-espai-public. Last access: July 2020.

Ajuntament de Barcelona. Una Mobilitat sostenible en un nou Espai Pùblic - Fase 2. Technical report, 2020c. URL https://www.barcelona.cat/mobilitat/ca/nova-mobilitat/una-nova-mobilitat-sostenible-en-un-nou-espai-public. Last access: July 2020.

Ajuntament de Barcelona. Pla de mobilitat urbana 2024, 2020d. URL https://www.barcelona.cat/mobilitat/sites/default/files/documentacio/pmu_bcn_2024_per_ceuim_20201214_compressed.pdf. Last access: May 2021.

Ajuntament de Barcelona. Superilla Barcelona, 2020e. URL https://ajuntament.barcelona.cat/superilles/sites/default/files/\Presentacio_SUPERILLA_BARCELONA.pdf. Last access: August 2021.

Ajuntament de Barcelona. Superilla Barcelona: Guanyadors dels concursos eixos verds i places, 2021. URL https://ajuntament.barcelona.cat/superilles/sites/default/files/Guanyadors_concurs_SuperillaBarcelona.pdf. Last access: September 2021.

F. Amato, A. Karanasiou, T. Moreno, A. Alastuey, J. A. Orza, J. Lumbreras, R. Borge, E. Boldo, C. Linares, and X. Querol. Emission factors from road dust resuspension in a Mediterranean freeway. *Atmospheric Environment*, 61: 580–587, 2012. ISSN 13522310. doi: 10.1016/j.atmosenv.2012.07.065. URL http://dx.doi.org/10.1016/j.atmosenv.2012.07.065.

F. Amato, F. R. Cassee, H. A. C. Denier van der Gon, R. Gehrig, M. Gustafsson, W. Hafner, R. M. Harrison, M. Jozwicka, F. J. Kelly, T. Moreno, A. S. H. Prevot,

M. Schaap, J. Sunyer, and X. Querol. Urban air quality: The challenge of traffic non-exhaust emissions. *Journal of Hazardous Materials*, 275:31–36, 2014. ISSN 18733336. doi: 10.1016/j.jhazmat.2014.04.053. URL http://dx.doi.org/10.1016/j.jhazmat.2014.04.053.

F. Amato, N. Pérez, M. López, A. Ripoll, A. Alastuey, M. Pandolfi, A. Karanasiou, A. Salmatonidis, E. Padoan, D. Frasca, M. Marcoccia, M. Viana, T. Moreno, C. Reche, V. Martins, M. Brines, M. Minguillón, M. Ealo, I. Rivas, B. van Drooge, J. Benavides, J. Craviotto, and X. Querol. Vertical and horizontal fall-off of black carbon and no2 within urban blocks. *Science of The Total Environment*, 686:236–245, 2019. ISSN 0048-9697. doi: https://doi.org/10.1016/j.scitotenv.2019.05.434.

AMB. Quaderns PDU metropolità: Urban innovation, mobility and metropolitan metabolism. Technical report, Àrea Metropolitana de Barcelona, 2014. URL https://issuu.com/ambcomunicacio/docs/quaderns_pdu_metropolit___08. Last access: September 2020.

AMB and RACC. Caracterització dels vehicles i les seves emissions a l'àrea metropolitana de Barcelona. Technical report, Àrea Metropolitana de Barcelona, Barcelona, 2017. URL http://saladepremsa.racc.cat/wp-content/uploads/2017/09/Dossier{_}estudi{_}Vehicles-i-Emissions-Area-Metropolitana.pdf. Last access: November 2019.

G. Amirjamshidi, T. S. Mostafa, A. Misra, and M. J. Roorda. Integrated model for microsimulating vehicle emissions, pollutant dispersion and population exposure. *Transportation Research Part D: Transport and Environment*, 18:16–24, 2013. ISSN 1361-9209. doi: https://doi.org/10.1016/j.trd.2012.08.003.

F. An, M. Barth, J. Norbeck, and M. Ross. Development of comprehensive modal emissions model: Operating under hot-stabilized conditions. *Transportation Research Record*, 1587(1):52–62, 1997a. doi: 10.3141/1587-07. URL https://doi.org/10.3141/1587-07.

F. An, M. Barth, J. Norbeck, and M. Ross. Development of Comprehensive Modal Emissions Model: Operating Under Hot-Stabilized Conditions. *Transportation Research Record*, 1587(1):52–62, 1997b. ISSN 0361-1981. doi: 10.3141/1587-07.

URL http://trb.metapress.com/openurl.asp?genre=article{&}id=doi:10.3141/1587-07.

M. André, A. Pasquier, and M. Carteret. Experimental determination of the geographical variations in vehicle fleet composition and consequences for assessing low-emission zones. *Transportation Research Part D: Transport and Environment*, 65:750–760, 2018. ISSN 13619209. doi: 10.1016/j.trd.2018.10.005. URL https://doi.org/10.1016/j.trd.2018.10.005.

S. Anenberg, J. Miller, R. Minjares, L. Du, D. Henze, F. Lacey, C. Malley, L. Emberson, V. Franco, Z. Klimont, and C. Heyes. Impacts and mitigation of excess diesel-related nox emissions in 11 major vehicle markets. *Nature*, 545:467–471, 05 2017. doi: 10.1038/nature22086.

S. Anenberg, G. Miller, D. Henze, and R. Minjares. A global snapshot of the air pollution-related health impacts of transportation sector emissions in 2010 and 2015. Technical report, International Council on Clean Transportation, 2019. URL https://theicct.org/sites/default/files/publications/Global_health_impacts_transport_emissions_2010-2015_20190226.pdf. Last Access: Feburary 2021.

A. Anya, N. Rouphail, H. Frey, and B. Schroeder. Application of aimsun microsimulation model to estimate emissions on signalized arterial corridors. *Transportation Research Record: Journal of the Transportation Research Board*, 2428:75–86, 12 2014. doi: 10.3141/2428-09.

Area Metropolitana de Barcelona. Zona de Baixes Emissions, 2020. URL https://www.zbe.barcelona/en/index.html. Last access: November 2020.

ASPB. Agència de Salut Pública de Barcelona: Informe de qualitat de l'aire de Barcelona. Technical report, 2020. URL https://www.aspb.cat/documents/qualitat-aire-2020/. Last access: March 2021.

R. Atkinson, B. Barratt, B. Armstrong, H. Anderson, S. Beevers, I. Mudway, D. Green, R. Derwent, P. Wilkinson, C. Tonne, and F. Kelly. The impact of the congestion charging scheme on ambient air pollution concentrations in london. *Atmospheric Environment*, 43(34):5493–5500, 2009. ISSN 1352-2310. doi: https://doi.org/10.1016/j.atmosenv.2009.07.023.

R. Atkinson, B. Butland, H. Anderson, and R. Maynard. Long-term concentrations of nitrogen dioxide and mortality: A meta-analysis of cohort studies. *Epidemiology*, 29:1, 05 2018. doi: 10.1097/EDE.0000000000000847.

ATM. Mobilitat: Dades i evolució 2015. Technical report, 2015. URL https://observatori.atm.cat/mobilitat-dades-i-evolucio/Mobilitat_dades_i_evolucio_2015.pdf. Last access: February 2021.

ATM. ENQUESTA DE MOBILITAT EN DIA FEINER 2020 (EMEF. Technical report, 2020. Last access: February 2021.

ATM, AMB, A. Barcelona, AMTU, and IDESCAT. EMEF 2015: Daily Mobility Data in Metropolitan Area of Barcelona (Enquesta de Mobilitat En Dia Feiner-EMEF). Technical report, 2015. Last access: December 2021.

A. Badia, O. Jorba, A. Voulgarakis, D. Dabdub, C. Pérez García-Pando, A. Hilboll, M. Gonçalves, and Z. Janjic. Description and evaluation of the multiscale online nonhydrostatic atmosphere chemistry model (nmmb-monarch) version 1.0: gas-phase chemistry at global scale. *Geoscientific Model Development*, 10(2):609–638, 2017. doi: 10.5194/gmd-10-609-2017. URL https://gmd.copernicus.org/articles/10/609/2017/.

J. Baldasano, M. Pay, O. Jorba, S. Gassó, and P. Jiménez-Guerrero. An annual assessment of air quality with the caliope modeling system over spain. *Science of The Total Environment*, 409(11):2163–2178, 2011. ISSN 0048-9697. doi: https://doi.org/10.1016/j.scitotenv.2011.01.041.

J. Baldasano, A. Soret, M. Guevara, F. Martínez, and S. Gassó. Integrated assessment of air pollution using observations and modelling in santa cruz de tenerife (canary islands). *The Science of the total environment*, 473-474C:576–588, 01 2014. doi: 10.1016/j.scitotenv.2013.12.062.

J. M. Baldasano, L. P. Güereca, E. López, S. Gassó, and P. Jimenez-Guerrero. Development of a high-resolution (1km×1km, 1h) emission model for spain: The high-elective resolution modelling emission system (hermes). *Atmospheric Environment*, 42(31):7215–7233, 2008a. ISSN 1352-2310. doi: https://doi.org/10.1016/j.atmosenv.2008.07.026.

J. M. Baldasano, P. Jiménez-Guerrero, O. Jorba, C. Pérez, E. López, P. Güereca, F. Martín, M. G. Vivanco, I. Palomino, X. Querol, M. Pandolfi, M. J. Sanz, and J. J. Diéguez. Caliope: an operational air quality forecasting system for the iberian peninsula, balearic islands and canary islands; first annual evaluation and ongoing developments. *Advances in Science and Research*, 2(1):89–98, 2008b. doi: 10.5194/asr-2-89-2008. URL https://asr.copernicus.org/articles/2/89/2008/.

J. Barceló. *Models, Traffic Models, Simulation, and Traffic Simulation*, pages 1–62. Springer New York, New York, NY, 2010. ISBN 978-1-4419-6142-6. doi: 10.1007/978-1-4419-6142-6_1. URL https://doi.org/10.1007/978-1-4419-6142-6_1.

Barcelona city council, Mobility and transport department, personal communication, 2017. URL https://www.barcelona.cat/mobilitat/ca. Last access: March 2020.

Barcelona Regional. Informe dels Resultats del Balanç d'Emissions i la Modelització de la Qualitat de l'Aire de la ZBE (Zona de Baixes Emissions) de Barcelona i Municipis Propers. Technical report, 2019. URL https://ajuntament.barcelona.cat/qualitataire/sites/default/files/br_impacteestimat_zbe_bcn.pdf. Last access: October 2019.

B. Bartin, S. Mudigonda, and K. Ozbay. Impact of electronic toll collection on air pollution levels: Estimation using microscopic simulation model of large-scale transportation network. *Transportation Research Record*, 2011(1):68–77, 2007. doi: 10.3141/2011-08. URL https://doi.org/10.3141/2011-08.

S. Basart, C. Pérez García-Pando, S. Nickovic, E. Cuevas, and J. Baldasano. Development and evaluation of the bsc-dream8b dust regional model over northern africa, the mediterranean and the middle east. *Tellus B*, 64:18569, 06 2012. doi: 10.3402/tellusb.v64io.18569.

C. Beckx, L. Int Panis, R. Torfs, D. Janssens, and S. Broekx. The application of the simulation software vetess to evaluate the environmental impact of traffic measures. *Proceedings of 10th International Conference on Computers in Urban Planning and Urban Management, CUPUM*

2007, 07 2007. URL https://www.researchgate.net/publication/268266766_The_application_of_the_simulation_software_VeTESS_to_evaluate_the_environmental_impact_of_traffic_measures. Last access: February 2021.

R. Beelen, G. Hoek, P. A. van den Brandt, R. A. Goldbohm, P. Fischer, L. J. Schouten, B. Armstrong, and B. Brunekreef. Long-term exposure to traffic-related air pollution and lung cancer risk. *Epidemiology*, 19(5):702–710, 2008. ISSN 1044-3983. doi: 10.1097/EDE.0b013e318181b3ca.

G. Bel and J. Rosell. Effects of the 80km/h and variable speed limits on air pollution in the metropolitan area of barcelona. *Transportation Research Part D: Transport and Environment*, 23:90–97, 2013. ISSN 1361-9209. doi: https://doi.org/10.1016/j.trd.2013.04.005.

J. Benavides, M. Snyder, M. Guevara, A. Soret, C. Pérez García-Pando, F. Amato, X. Querol, and O. Jorba. Caliope-urban v1.0: coupling r-line with a mesoscale air quality modelling system for urban air quality forecasts over barcelona city (spain). *Geoscientific Model Development*, 12(7):2811–2835, 2019. doi: 10.5194/gmd-12-2811-2019. URL https://gmd.copernicus.org/articles/12/2811/2019/.

J. Benavides, M. Guevara, M. G. Snyder, D. Rodríguez-Rey, A. Soret, C. P. García-Pando, and O. Jorba. On the impact of excess diesel NOX emissions upon NO2 pollution in a compact city. *Environmental Research Letters*, 16(2), 2021a. ISSN 17489326. doi: 10.1088/1748-9326/abd5dd.

J. Benavides, M. Guevara, M. G. Snyder, D. Rodríguez-Rey, A. Soret, C. P. García-Pando, and O. Jorba. Response 1, Reviewer 1. 2021b. doi: 10.1088/1748-9326/ABD5DD/V2/RESPONSE1.

Y. Bernard, J. German, A. Kentroti, and R. Muncrief. Catching defeat devices: How systematic vehicle testing can determine the presence of suspicious emission control strategies. Technical report, International Council on Clean Transportation, 2019. URL https://theicct.org/publications/detecting-defeat-devices-201906. Last accesss: September 2021.

A. Y. Bigazzi and M. Rouleau. Can traffic management strategies improve urban air quality? a review of the evidence. *Journal of Transport & Health*, 7:111–124, 2017. ISSN 2214-1405. doi: https://doi.org/10.1016/j.jth.2017.08.001.

H. Boogaard, N. A. Janssen, P. H. Fischer, G. P. Kos, E. P. Weijers, F. R. Cassee, S. C. van der Zee, J. J. de Hartog, K. Meliefste, M. Wang, B. Brunekreef, and G. Hoek. Impact of low emission zones and local traffic policies on ambient air pollution concentrations. *Science of The Total Environment*, 435-436:132–140, 2012. ISSN 0048-9697. doi: https://doi.org/10.1016/j.scitotenv.2012.06.089.

R. Borge, J. Lumbreras, J. Pérez, D. de la Paz, M. Vedrenne, J. M. de Andrés, and M. E. Rodríguez. Emission inventories and modeling requirements for the development of air quality plans. application to madrid (spain). *Science of The Total Environment*, 466-467:809–819, 2014. ISSN 0048-9697. doi: https://doi.org/10.1016/j.scitotenv.2013.07.093.

R. Borge, J. L. Santiago, D. de la Paz, F. Martín, J. Domingo, C. Valdés, B. Sánchez, E. Rivas, M. T. Rozas, S. Lázaro, J. Pérez, and Álvaro Fernández. Application of a short term air quality action plan in madrid (spain) under a high-pollution episode - part ii: Assessment from multi-scale modelling. *Science of The Total Environment*, 635:1574 – 1584, 2018. ISSN 0048-9697. doi: https://doi.org/10.1016/j.scitotenv.2018.04.323.

C. Borrego, J. Amorim, O. Tchepel, D. Dias, S. Rafael, E. Sá, C. Pimentel, T. Fontes, P. Fernandes, S. Pereira, J. Bandeira, and M. Coelho. Urban scale air quality modelling using detailed traffic emissions estimates. *Atmospheric Environment*, 131:341–351, 2016. ISSN 1352-2310. doi: https://doi.org/10.1016/j.atmosenv.2016.02.017.

P. Boulter, I. Mccrae, and T. Barlow. A review of instantaneous emission models for road vehicles. *Transport Research Laboratory*, 2007. ISSN 0968-4093. URL `http://worldcat.org/isbn/1846086701`.

M. Brauer, G. Hoek, P. Van Vliet, K. Meliefste, P. H. Fischer, A. Wijga, L. P. Koopman, H. J. Neijens, J. Gerritsen, M. Kerkhof, J. Heinrich, T. Bellander, and B. Brunekreef. Air pollution from traffic and the development of respiratory infections and asthmatic and allergic symptoms in children. *American journal*

of respiratory and critical care medicine, 166(8):1092–1098, 2002. doi: 10.1164/rccm.200108-007OC.

L. M. Braun, D. A. Rodriguez, T. Cole-Hunter, A. Ambros, D. Donaire-Gonzalez, M. Jerrett, M. A. Mendez, M. J. Nieuwenhuijsen, and A. de Nazelle. Short-term planning and policy interventions to promote cycling in urban centers: Findings from a commute mode choice analysis in barcelona, spain. *Transportation Research Part A: Policy and Practice*, 89:164–183, 2016. ISSN 0965-8564. doi: https://doi.org/10.1016/j.tra.2016.05.007.

P. C. Bueno, J. Gomez, J. R. Peters, and J. M. Vassallo. Understanding the effects of transit benefits on employees' travel behavior: Evidence from the new york-new jersey region. *Transportation Research Part A: Policy and Practice*, 99: 1–13, 2017. ISSN 0965-8564. doi: https://doi.org/10.1016/j.tra.2017.02.009.

D. Byun and K. Schere. Review of the governing equations, computational algorithms and other components of the models-3 community multiscale air quality (cmaq) modeling system. *Applied Mechanics Review*, 59:51–78, 11 2005. doi: https://doi.org/10.1115/1.2128636.

C3S. Copernicus Climate Change Service (C3S): ERA5: Fifth generation of ECMWF atmospheric reanalyses of the global climate, Copernicus Climate Change Service Climate Data Store (CDS), 2017. URL `https://cds.climate.copernicus.eu/cdsapp{#}!/home`. Last access: July 2019.

California Air Resources Board. Emfac, 2021. URL `https://arb.ca.gov/emfac/`. Last access: July 2021.

V. Cantillo and J. d. D. Ortuzar. Restricting the use of cars by license plate numbers: A misguided urban transport policy. *DYNA*, 81: 75 – 82, 12 2014. ISSN 0012-7353. doi: 10.15446/dyna.v81n188.40081. URL `http://www.scielo.org.co/scielo.php?script=sci_arttext&pid=S0012-73532014000600009&nrm=iso`.

CARNET. CARNET Barcelona - Future Mobility Research Hub, 2017. URL `http://www.carnetbarcelona.com/`. Last access: January 2020.

D. C. Carslaw, S. D. Beevers, J. E. Tate, E. J. Westmoreland, and M. L. Williams. Recent evidence concerning higher nox emissions from passenger cars and light duty vehicles. *Atmospheric Environment*, 45(39):7053–7063, 2011. ISSN 1352-2310. doi: https://doi.org/10.1016/j.atmosenv.2011.09.063.

R. Chamberlin, B. Swanson, E. Talbot, J. Dumont, and S. Pesci. Analysis of moves and cmem for evaluating the emissions impact of an intersection control change. In *Transportation Research Board 90th Annual Meeting*, 2010. URL `https://rsginc.com/files/staff/117.Analysis%20of%20MOVES%20and%20CMEM%20for%20Evaluating%20the%20Emissions%20Impacts%20of%20an%20Intersection%20Control%20Change.pdf`. Last access: May 2021.

K. CHEN and L. YU. Microscopic traffic-emission simulation and case study for evaluation of traffic control strategies. *Journal of Transportation Systems Engineering and Information Technology*, 7(1):93–99, 2007. ISSN 1570-6672. doi: https://doi.org/10.1016/S1570-6672(07)60011-7.

R. Chen, V. Aguilera, V. Mallet, F. Cohn, D. Poulet, and F. Brocheton. A sensitivity study of road transportation emissions at metropolitan scale. *Journal of Earth Sciences and Geotechnical Engineering*, 7(1), 2017. URL `https://hal.inria.fr/hal-01676006`.

Y. Chen and J. Borken-Kleefeld. Nox emissions from diesel passenger cars worsen with age. *Environmental Science and Technology*, 50:3327–3332, 04 2016. doi: 10.1021/acs.est.b04704.

M. Costa and J. M. Baldasano. Development of a source emission model for atmospheric pollutants in the barcelona area. *Atmospheric Environment*, 30(2): 309–318, 1996. ISSN 1352-2310. doi: https://doi.org/10.1016/1352-2310(95)00221-J.

E. Croci. Urban road pricing: A comparative study on the experiences of london, stockholm and milan. *Transportation Research Procedia*, 14:253–262, 2016. ISSN 2352-1465. doi: https://doi.org/10.1016/j.trpro.2016.05.062. Transport Research Arena TRA2016.

A. Csikós and I. Varga. Real-time modeling and control objective analysis of motorway emissions. *Procedia - Social and Behavioral Sciences*, 54:1027–1036, 2012.

ISSN 1877-0428. doi: https://doi.org/10.1016/j.sbspro.2012.09.818. Proceedings of EWGT2012 - 15th Meeting of the EURO Working Group on Transportation, September 2012, Paris.

A. Daly and P. Zannetti. Chapter 2: Air pollution modeling – an overview, 2007. URL http://home.iitk.ac.in/~anubha/Modeling.pdf. Last Access: May 2021.

L. Davis. The effect of driving restrictions on air quality in mexico city. *Journal of Political Economy*, 116:38–81, 02 2008. doi: 10.1086/529398.

L. Davis. Saturday driving restrictions fail to improve air quality in mexico city. *Scientific Reports*, 7:41652, 02 2017. doi: 10.1038/srep41652.

D. de la Paz, R. Borge, M. Vedrenne, J. Lumbreras, F. Amato, A. Karanasiou, E. Boldo, and T. Moreno. Implementation of road dust resuspension in air quality simulations of particulate matter in Madrid (Spain). *Frontiers in Environmental Science*, 3(NOV), 2015. ISSN 2296665X. doi: 10.3389/fenvs.2015.00072.

R. Delgado, I. Toll, C. Soriano, and J. Baldasano. Vehicle emission model of air pollutants from road traffic. application to catalonia (spain) for 1994. *Advances in Air Pollution*, 8, 01 2000. URL https://www.witpress.com/elibrary/wit-transactions-on-ecology-and-the-environment/42/3908.

B. R. Denby, M. Gauss, P. Wind, Q. Mu, E. Grøtting Wærsted, H. Fagerli, A. Valdebenito, and H. Klein. Description of the uemep_v5 downscaling approach for the emep msc-w chemistry transport model. *Geoscientific Model Development*, 13(12):6303–6323, 2020. doi: 10.5194/gmd-13-6303-2020. URL https://gmd.copernicus.org/articles/13/6303/2020/.

S. Dey, B. Caulfield, and B. Ghosh. Modelling uncertainty of vehicular emissions inventory: A case study of ireland. *Journal of Cleaner Production*, 213:1115–1126, 2019. ISSN 0959-6526. doi: https://doi.org/10.1016/j.jclepro.2018.12.125.

DGT. DGT Tablas estadisticas, 2020. URL https://www.dgt.es/es/seguridad-vial/\estadisticas-e-indicadores/matriculaciones-definitivas/tablas-estadisticas/. Last access: November 2020.

H. di He, W.-Z. Lu, and Y. Xue. Prediction of pm10 concentrations at urban traffic intersections using semi-empirical box modelling with instantaneous velocity and acceleration. *Atmospheric Environment*, 43(40):6336 – 6342, 2009. ISSN 1352-2310. doi: https://doi.org/10.1016/j.atmosenv.2009.09.027.

D. Dias, J. H. Amorim, E. Sá, C. Borrego, T. Fontes, P. Fernandes, S. R. Pereira, J. Bandeira, M. C. Coelho, and O. Tchepel. Assessing the importance of transportation activity data for urban emission inventories. *Transportation Research Part D: Transport and Environment*, 62:27–35, 2018. ISSN 1361-9209. doi: https://doi.org/10.1016/j.trd.2018.01.027.

Dirección General de Tráfico (DGT). Estadísticas e indicadores. Parque de vehículos: tablas estadísticas., 2019. URL http://www.dgt.es/es/seguridad-vial/estadisticas-e-indicadores/. Last access: October 2020.

J. Duyzer, D. van den Hout, P. Zandveld, and S. van Ratingen. Representativeness of air quality monitoring networks. *Atmospheric Environment*, 104:88–101, 2015. ISSN 1352-2310. doi: https://doi.org/10.1016/j.atmosenv.2014.12.067.

EEA. Suspended particulates (TSP/SPM). Technical report, 2008. URL https://www.eea.europa.eu/publications/2-9167-057-X/page021.html. Last Access: May 2021.

EEA. National emission reduction commitments directive, 2016. URL https://www.eea.europa.eu/themes/air/air-pollution-sources-1/national-emission-ceilings. Last Acess: June 2021.

EEA. Healthy environment, healthy lives: how the environment influences health and well-being in Europe. Technical report, European Environment Agency, 2019. URL https://www.eea.europa.eu/publications/healthy-environment-healthy-lives. Last Access: June 2021.

EEA. Air quality in europe - 2020 report, 2020. URL https://www.eea.europa.eu/publications/air-quality-in-europe-2020-report. Last Access: May 2021.

EEA/EMEP. Air pollutant emission inventory guidebook 2016. Technical report, European Environment Agency, 2017. URL hhttps://www.eea.europa.eu/publications/emep-eea-guidebook-2016. Last Access: September 2020.

S. Eggleston, N. Gorißen, R. Joumard, R. Rijkeboer, Z. Samaras, and K. Zierock. Corinair Working Group on Emissions Factors for Calculating 1985 Emissions from Road Traffic. Volume 1: Methodology and Emission Factors. Final report. contract No 88/6611/0067, EUR 12260 EN. Technical report, 1989. URL https://hal.archives-ouvertes.fr/hal-01254189/document. Last Access: May 2021.

R. B. Ellison, S. P. Greaves, and D. A. Hensher. Five years of london's low emission zone: Effects on vehicle fleet composition and air quality. *Transportation Research Part D: Transport and Environment*, 23:25–33, 2013. ISSN 1361-9209. doi: https://doi.org/10.1016/j.trd.2013.03.010.

EMEP. Emep (european monitoring and evaluation programme), 2021. URL Y78QHUTRNG. Last access: June 2021.

EMISIA. COPERT V, 2016. URL https://copert.emisia.com/. Last access: September 2018.

European Automobile Manufacturers Association. Fuel types of new passenger cars, 2021. URL https://www.acea.be/statistics/tag/category/share-of-diesel-in-new-passenger-cars. Last access: March 2021.

European Comission. Urban acess regulations in europe, 2021. URL https://urbanaccessregulations.eu/userhome/map. Last access: May 2021.

European Commission. Directive 2001/81/ec of the european parliament and of the council on national emission ceilings for certain atmospheric pollutants., 2001. URL https://eur-lex.europa.eu/legal-content/EN/TXT/?uri=celex%3A32001L0081. Last access: August 2021.

European Commission. New and improved car emissions tests become mandatory on 1st September, 2017. URL https://ec.europa.eu/growth/content/new-and-improved-car-emissions-tests-become-mandatory-1-september_en. Last access: June 2021.

European Economic Community. Council directive 70/220/eec of 20 march 1970 on the approximation of the laws of the member states relating to measures to be taken against air pollution by gases from positive-ignition engines of motor vehicles., 1970. URL https://eur-lex.europa.eu/legal-content/EN/ALL/?uri=CELEX%3A31970L0220. Last access: August 2021.

European Parliament. Directive 2008/50/ec of the european parliament and of the council of 21 may 2008 on ambient air quality and cleaner air for europe, 2008. Last access: June 2021.

M. Fallah Shorshani, M. André, C. Bonhomme, and C. Seigneur. Modelling chain for the effect of road traffic on air and water quality: Techniques, current status and future prospects. *Environmental Modelling and Software*, 64:102–123, 2015a. ISSN 13648152. doi: 10.1016/j.envsoft.2014.11.020.

M. Fallah Shorshani, M. André, C. Bonhomme, and C. Seigneur. Modelling chain for the effect of road traffic on air and water quality: Techniques, current status and future prospects. *Environmental Modelling and Software*, 64:102–123, 2015b. ISSN 1364-8152. doi: https://doi.org/10.1016/j.envsoft.2014.11.020.

M. V. Faria, R. A. Varella, G. O. Duarte, T. L. Farias, and P. C. Baptista. Engine cold start analysis using naturalistic driving data : City level impacts on local pollutants emissions and energy consumption. *Science of the Total Environment*, 630:544–559, 2018. ISSN 0048-9697. doi: 10.1016/j.scitotenv.2018.02.232. URL https://doi.org/10.1016/j.scitotenv.2018.02.232.

Federal Office for the Environment. *Real-driving emissions from diesel passenger cars measured by remote sensing and as compared with PEMS - CONOX Task 2 report.* Number C. Switzerland, 2018. ISBN 9789188319708. URL https://www.bafu.admin.ch/bafu/en/home/topics/air/publications-studies/studies.html.

B. Fisher, J. Kukkonen, M. Piringer, M. W. Rotach, and M. Schatzmann. Meteorology applied to urban air pollution problems: concepts from cost 715. *Atmospheric Chemistry and Physics*, 6(2):555–564, 2006. doi: 10.5194/acp-6-555-2006. URL https://acp.copernicus.org/articles/6/555/2006/.

T. Fontes, S. R. Pereira, P. Fernandes, J. M. Bandeira, and M. C. Coelho. How to combine different microsimulation tools to assess the environmental impacts of road traffic? Lessons and directions. *Transportation Research Part D: Transport and Environment*, 34:293–306, 2015. ISSN 13619209. doi: 10.1016/j.trd.2014.11.012. URL http://dx.doi.org/10.1016/j.trd.2014.11.012.

M. Friedrich. A multi-modal transport model for integrated planning. *World Transport Research: Selected Proceedings of the 8th World Conference on Transport Research*, 1999. URL http://worldcat.org/isbn/0080435904.

R.-Z. Gilda, C. Rusu-Zagar, I. Iorga, and A. Iorga. Air pollution particles pm10, pm2,5 and the tropospheric ozone effects on human health. *Procedia - Social and Behavioral Sciences*, 92, 10 2013. doi: 10.1016/j.sbspro.2013.08.761.

P. Gipps. A behavioural car-following model for computer simulation. *Transportation Research Part B: Methodological*, 15(2):105–111, 1981. ISSN 0191-2615. doi: https://doi.org/10.1016/0191-2615(81)90037-0.

O. Gomez and J. Baldasano. Biogenic voc emission inventory for catalonia, spain. *WIT Transactions on Ecology and the Environment*, 36:7, 05 1999. doi: 10.2495/EURO990222.

S. Gori, S. La Spada, L. Mannini, and M. Nigro. Emission dynamic mesosimulation model to evaluate traffic strategies in congested urban networks. *IET Intelligent Transport Systems*, 9(3):333–342, 2015. doi: https://doi.org/10.1049/iet-its.2013.0026. URL https://ietresearch.onlinelibrary.wiley.com/doi/abs/10.1049/iet-its.2013.0026.

S. K. Grange, N. J. Farren, A. R. Vaughan, R. A. Rose, and D. C. Carslaw. Strong Temperature Dependence for Light-Duty Diesel Vehicle NOx Emissions. *Environmental Science and Technology*, 53(11):6587–6596, 2019. ISSN 15205851. doi: 10.1021/acs.est.9b01024.

A. Guenther, T. Karl, P. Harley, C. Wiedinmyer, P. I. Palmer, and C. Geron. Estimates of global terrestrial isoprene emissions using megan (model of emissions of gases and aerosols from nature). *Atmospheric Chemistry and Physics*, 6(11):3181–3210, 2006. doi: 10.5194/acp-6-3181-2006. URL https://acp.copernicus.org/articles/6/3181/2006/.

M. Guevara. Emissions of primary particulate matter. In *Airborne Particulate Matter: Sources, Atmospheric Processes and Health*, pages 1–34. The Royal Society of Chemistry, 2016. ISBN 978-1-78262-491-2. doi: 10.1039/9781782626589-00001. URL http://dx.doi.org/10.1039/9781782626589-00001.

M. Guevara, F. Martínez, G. Arévalo, S. Gassó, and J. M. Baldasano. An improved system for modelling spanish emissions: Hermesv2.0. *Atmospheric Environment*, 81:209–221, 2013. ISSN 1352-2310. doi: https://doi.org/10.1016/j.atmosenv.2013.08.053.

M. Guevara, C. Tena, M. Porquet, O. Jorba, and C. Pérez García-Pando. HERMESv3, a stand-alone multi-scale atmospheric emission modelling framework – Part 1: global and regional module. *Geoscientific Model Development*, 12 (5):1885–1907, 2019. doi: 10.5194/gmd-12-1885-2019. URL https://gmd.copernicus.org/articles/12/1885/2019/.

M. Guevara, C. Tena, M. Porquet, O. Jorba, and C. Pérez García-Pando. HERMESv3, a stand-alone multi-scale atmospheric emission modelling framework – Part 2: The bottom–up module. *Geoscientific Model Development*, 13:873–903, 2020. ISSN 1991-962X. doi: https://doi.org/10.5194/gmd-13-873-2020.

B. Gwara. Validation of tomtom historical average speeds on freeway segments in gauteng, south africa, 2017. URL http://hdl.handle.net/10019.1/101307. Last Access: September 2018.

R. M. Harrison, A. M. Jones, J. Gietl, J. Yin, and D. C. Green. Estimation of the contributions of brake dust, tire wear, and resuspension to nonexhaust traffic particles derived from atmospheric measurements. *Environmental Science and Technology*, 46(12):6523–6529, 2012. ISSN 0013936X. doi: 10.1021/es300894r.

S. Hausberger and D. Krajzewicz. Deliverable 4.2 - Extended Simulation Tool PHEM coupled to SUMO with User Guide. Technical report, 2009. URL https://elib.dlr.de/98047/1/COLOMBO_D4.2_ExtendedPHEMSUMO_v1.7.pdf. Last Access: February 2018.

S. Hausberger, R. Luz, M. Rexeis, and S. Zallinger. PHEM User Manual, 2009a. URL https://graz.pure.elsevier.com/en/publications/user-guide-for-the-model-phem. Last Access: February 2018.

S. Hausberger, M. Reixis, M. Zallinger, and R. Luz. Emission Factors from the Model PHEM for the HBEFA Version 3. Technical report, 2009b. URL https://www.hbefa.net/e/documents/HBEFA_31_Docu_hot_emissionfactors_PC_LCV_HDV.pdf. Last Access: February 2018.

Here. HERE, 2020. URL www.here.com. Last Access: July 2018.

O. Hertel, J. Salmond, W. Bloss, I. Salma, S. Vardoulakis, R. Maynard, M. Williams, and M. E. Goodsite. *Air Quality in Urban Environments*. Issues in Environmental Science and Technology. The Royal Society of Chemistry, 2009. ISBN 978-1-84755-907-4. doi: 10.1039/9781847559654. URL http://dx.doi.org/10.1039/9781847559654.

K. Hirschmann, M. Zallinger, M. Fellendorf, and S. Hausberger. A new method to calculate emissions with simulated traffic conditions. In *13th International IEEE Conference on Intelligent Transportation Systems*, pages 33–38, 2010. doi: 10.1109/ITSC.2010.5625030.

G. Hoek, P. Fischer, P. Van Den Brandit, S. Goldbohm, and B. Brunekreef. Estimation of long-term average exposure to outdoor air pollution for a cohort study on mortality. *Journal of Exposure Science & Environmental Epidemiology*, 11 (6):459–469, 2001. ISSN 1559-064X. doi: 10.1038/sj.jea.7500189.

C. Holman, R. Harrison, and X. Querol. Review of the efficacy of low emission zones to improve urban air quality in european cities. *Atmospheric Environment*, 111:161–169, 2015. ISSN 1352-2310. doi: https://doi.org/10.1016/j.atmosenv.2015.04.009.

N. Holmes and L. Morawska. A review of dispersion modelling and its application to the dispersion of particles: An overview of different dispersion models available. *Atmospheric Environment*, 40(30):5902–5928, 2006. ISSN 1352-2310. doi: https://doi.org/10.1016/j.atmosenv.2006.06.003.

C. Hood, I. MacKenzie, J. Stocker, K. Johnson, D. Carruthers, M. Vieno, and R. Doherty. Air quality simulations for london using a coupled regional-to-local modelling system. *Atmospheric Chemistry and Physics*, 18(15):11221–11245, 2018. doi: 10.5194/acp-18-11221-2018. URL https://acp.copernicus.org/articles/18/11221/2018/.

A. Horni, K. Nagel, and K. Axhausen. *The Multi-Agent Transport Simulation MATSim*. 04 2016. doi: 10.5334/baw.

H. Huang, D. Fu, and W. Qi. Effect of driving restrictions on air quality in lanzhou, china: Analysis integrated with internet data source. *Journal of Cleaner Production*, 142, 09 2016. doi: 10.1016/j.jclepro.2016.09.082.

Y. Huang, C. Lei, C.-H. Liu, P. Perez, H. Forehead, S. Kong, and J. L. Zhou. A review of strategies for mitigating roadside air pollution in urban street canyons. *Environmental Pollution*, 280:116971, 2021. ISSN 0269-7491. doi: https://doi.org/10.1016/j.envpol.2021.116971.

F. Hülsmann. Integrated agent-based transport simulation and air pollution modelling in urban areas - the example of munich, 2014. URL https://d-nb.info/1059856999/34. Last Access: May 2020.

ICC, 2020. URL http://www.icc.cat/appdownloads/?c=dlftopo5m. Last Access: August 2020.

A. Inness, M. Ades, A. Agusti-Panareda, J. Barre, A. Benedictow, A.-M. Blechschmidt, J. J. Dominguez, R. Engelen, H. Eskes, J. Flemming, V. Huijnen, L. Jones, Z. Kipling, S. Massart, M. Parrington, V. Peuch, M. Razinger, S. Remy, M. Schulz, and M. Suttie. The cams reanalysis of atmospheric composition. *Atmospheric Chemistry and Physics*, 19(6):3515–3556, 2019. doi: 10.5194/acp-19-3515-2019. URL https://acp.copernicus.org/articles/19/3515/2019/.

Institut Cerdà. Assistència tècnica per al desplegament del Pla director de mobilitat: Anàlisis del parc de vehicles, objectius i pla estratègic per al foment de l'adquisició de vehicles de baixes emissions. Technical report, 2019. URL https://doc.atm.cat/ca/_dir_pdm_estudis/Informe_ParcVehiclesBaixesEmissions_31102019.pdf. Last access: February 2021.

Institut d'Estadística de Catalunya. Estimacions de població per sexe, 2019. URL https://www.idescat.cat/. Last access: March 2020.

L. Int Panis, C. Beckx, S. Broekx, I. De Vlieger, L. Schrooten, B. Degraeuwe, and L. Pelkmans. Pm, nox and co2 emission reductions from speed management policies in europe. *Transport Policy*, 18(1):32–37, 2011. ISSN 0967-070X. doi: https://doi.org/10.1016/j.tranpol.2010.05.005.

ISGlobal. ISGLobal Ranking of cities, 2021. URL https://isglobalranking.org/. Last access: February 2021.

G. Janssens-Maenhout, M. Crippa, D. Guizzardi, F. Dentener, M. Muntean, G. Pouliot, T. Keating, Q. Zhang, J. Kurokawa, R. Wankmuller, H. Denier van der Gon, J. J. P. Kuenen, Z. Klimont, G. Frost, S. Darras, B. Koffi, and M. Li. Htap_v2.2: a mosaic of regional and global emission grid maps for 2008 and 2010 to study hemispheric transport of air pollution. *Atmospheric Chemistry and Physics*, 15(19):11411–11432, 2015. doi: 10.5194/acp-15-11411-2015. URL https://acp.copernicus.org/articles/15/11411/2015/.

S. S. Jensen, R. Berkowicz, H. Sten Hansen, and O. Hertel. A danish decision-support gis tool for management of urban air quality and human exposures. *Transportation Research Part D: Transport and Environment*, 6(4):229–241, 2001. ISSN 1361-9209. doi: https://doi.org/10.1016/S1361-9209(00)00026-2.

S. S. Jensen, M. Ketzel, T. Becker, J. Christensen, J. Brandt, M. Plejdrup, M. Winther, O.-K. Nielsen, O. Hertel, and T. Ellermann. High resolution multi-scale air quality modelling for all streets in denmark. *Transportation Research Part D: Transport and Environment*, 52:322 – 339, 2017. ISSN 1361-9209. doi: https://doi.org/10.1016/j.trd.2017.02.019.

P. Jiménez, R. Parra, S. Gassó, and J. M. Baldasano. Modeling the ozone weekend effect in very complex terrains: a case study in the northeastern iberian peninsula. *Atmospheric Environment*, 39(3):429–444, 2005. ISSN 1352-2310. doi: https://doi.org/10.1016/j.atmosenv.2004.09.065.

C. Johansson, L. Burman, and B. Forsberg. The effects of congestions tax on air quality and health. *Atmospheric Environment*, 43(31):4843–4854, 2009. ISSN

1352-2310. doi: https://doi.org/10.1016/j.atmosenv.2008.09.015. Urban Air Quality.

S. Khomenko, M. Cirach, E. Pereira-Barboza, N. Mueller, J. Barrera-Gómez, D. Rojas-Rueda, K. de Hoogh, G. Hoek, and M. Nieuwenhuijsen. Premature mortality due to air pollution in European cities: a health impact assessment. *The Lancet Planetary Health*, 3(5):e121 – e134, 2021. ISSN 2542-5196. doi: 10.1016/S2542-5196(20)30272-2.

H. Khreis and J. Tate. Alternative Methods for Vehicle Emission Modelling and Its Impact on Local Road Transport Emission Inventories in Bradford, UK. *Journal of Transport & Health*, 5:S50, 2017. ISSN 22141405. doi: 10.1016/j.jth.2017.05.341. URL http://dx.doi.org/10.1016/j.jth.2017.05.341.

Kineo. Kineo, Ingeniería de Tráfico, 2017. URL https://www.kineo.es/en/. Last Access: March 2019.

C. Krogscheepers and K. Kacir. Latest trends in micro simulation : an application of the paramics model, 2001. URL http://hdl.handle.net/2263/8186. Last Access: March 2018.

M. Kryza, M. Jóźwicka, A. Dore, and M. Werner. The uncertainty in modelled air concentrations of nox due to choice of emission inventory. *International Journal of Environment and Pollution*, 57:123, 01 2015. doi: 10.1504/IJEP.2015.074495.

J. J. P. Kuenen, A. J. H. Visschedijk, M. Jozwicka, and H. A. C. Denier van der Gon. TNO-MACC_II emission inventory; a multi-year (2003-2009) consistent high-resolution European emission inventory for air quality modelling. *Atmospheric Chemistry and Physics*, 14(20):10963–10976, 2014. doi: 10.5194/acp-14-10963-2014. URL https://acp.copernicus.org/articles/14/10963/2014/.

Kunz. KTT Umweltberatung und Software Street 5.2., 2005. URL https://www.firmenwissen.de/az/firmeneintrag/66424/7290247684/KTT_UMWELTBERATUNG_UND_SOFTWARE_DR_KUNZ_GMBH.html. Last Access: April 2021.

D. Lejri, A. Can, N. Schiper, and L. Leclercq. Accounting for traffic speed dynamics when calculating COPERT and PHEM pollutant emissions at the urban scale. *Transportation Research Part D*, 63:588–603, 2018. ISSN 1361-9209. doi: 10.1016/j.trd.2018.06.023. URL https://doi.org/10.1016/j.trd.2018.06.023.

N. E. Ligterink. Refined vehicle and driving-behaviour dependencies in the versit+ emission model, 01 2009. URL http://resolver.tudelft.nl/uuid:b79baf31-d368-4759-b98b-425fa6beb0fc. Last Access: February 2018.

M. P. Linares. A mesoscopic traffic simulation based dynamic traffic assignment, 2014. URL http://hdl.handle.net/10803/144939. Last Access: March 2019.

LRTAP. Convention on long-range transboundary air pollution, 1979. URL https://unece.org/sites/default/files/2021-05/1979%20CLRTAP.e.pdf. Last access: June 2021.

V. Lurkin, J. Hambuckers, and T. van Woensel. Urban low emissions zones: A behavioral operations management perspective. *Transportation Research Part A: Policy and Practice*, 144:222–240, 2021. ISSN 0965-8564. doi: https://doi.org/10.1016/j.tra.2020.11.015.

W. Lyons and L. Olsson. Detailed mesometeorological studies of air pollution dispersion in the chicago lake breeze1. *Monthly Weather Review - MON WEATHER REV*, 101, 05 1973. doi: 10.1175/1520-0493(1973)101⟨0387:DMSOAP⟩2.3.CO;2.

M. Y. Madi. Investigating and Calibrating the Dynamics of Vehicles in Traffic Micro-simulations Models. *Transportation Research Procedia*, 14:1782–1791, 2016. ISSN 23521465. doi: 10.1016/j.trpro.2016.05.144. URL http://dx.doi.org/10.1016/j.trpro.2016.05.144.

M. Madireddy, B. De Coensel, A. Can, B. Degraeuwe, B. Beusen, I. De Vlieger, and D. Botteldooren. Assessment of the impact of speed limit reduction and traffic signal coordination on vehicle emissions using an integrated approach. *Transportation Research Part D: Transport and Environment*, 16(7):504–508, 2011. ISSN 1361-9209. doi: https://doi.org/10.1016/j.trd.2011.06.001.

S. Maerivoet and B. De Moor. Transportation planning and traffic flow models, 07 2005. URL arXiv:physics/0507127. Last Access: May 2020.

G. Martini and T. Grigoratos. Non-exhaust traffic related emissions. Brake and tyre wear PM, 2014. ISSN 1018-5593. URL https://ec.europa.eu/jrc. Last Access: February 2018.

MATSim. The MATSim user guide, 2021. URL https://www.matsim.org/docs/userguide/. Last Access: May 2021.

C. Matzer, K. Weller, M. Dippold, S. Lipp, M. Rock, M. Rexels, and S. Hausberger. Update of Emission Factors for HBEFA Version 4.1; Final Report, I-05/19/CM EM-I-16/26/679, 2019. URL https://www.hbefa.net/e/documents/HBEFA41_Report_TUG_09092019.pdf. Last Access: March 2020.

Millán, M.-J. Sanz-Sanchez, R. Salvador, and E. Mantilla. Atmospheric dynamics and ozone cycles related to nitrogen deposition in the western mediterranean. *Environmental pollution (Barking, Essex : 1987)*, 118:167–86, 02 2002. doi: 10.1016/S0269-7491(01)00311-6.

M. M. Millán, E. Mantilla, R. Salvador, A. Carratalá, M. J. Sanz, L. Alonso, G. Gangoiti, and M. Navazo. Ozone cycles in the western mediterranean basin: Interpretation of monitoring data in complex coastal terrain. *Journal of Applied Meteorology*, 39(4):487 – 508, 2000. doi: 10.1175/1520-0450(2000)039⟨0487:OCITWM⟩2.0.CO;2. URL https://journals.ametsoc.org/view/journals/apme/39/4/1520-0450_2000_039_0487_ocitwm_2.0.co_2.xml.

A. Misra, M. J. Roorda, and H. L. MacLean. An integrated modelling approach to estimate urban traffic emissions. *Atmospheric Environment*, 73:81–91, 2013. ISSN 1352-2310. doi: https://doi.org/10.1016/j.atmosenv.2013.03.013.

MITECO. Evaluación de la calidad del aire en España. Technical report, 2019. URL https://www.miteco.gob.es/es/calidad-y-evaluacion-ambiental/temas/atmosfera-y-calidad-del-aire/informeevaluacioncalidadaireespana2018_tcm30-498764.pdf. Last Access: May 2021.

L. Montero, P. Linares, J. Salmerón, G. Recio, E. Lorente, and J. José Vázquez. Barcelona Virtual Mobility Lab The multimodal transport simulation testbed for emerging mobility concepts evaluation. *International Academy, Research, and Industry Association (IARIA)*, pages 2–5, 2018. URL http://hdl.handle.net/2117/123910.

L. Montero, X. Ros-Roca, R. Herranz, and J. Barceló. Fusing mobile phone data with other data sources to generate input od matrices for transport models. *Transportation Research Procedia*, 37:417–424, 2019. ISSN 2352-1465. doi: https://doi.org/10.1016/j.trpro.2018.12.211. URL https://www.sciencedirect.com/science/article/pii/S2352146518306276. 21st EURO Working Group on Transportation Meeting, EWGT 2018, 17th – 19th September 2018, Braunschweig, Germany.

J. W. Moore and E. A. Moore. Environmental chemistry. In *Environmental Chemistry*. Academic Press, 1976. ISBN 978-0-12-505050-0. doi: https://doi.org/10.1016/B978-0-12-505050-0.50001-X.

N. Mueller, D. Rojas-Rueda, H. Khreis, M. Cirach, D. Andrés, J. Ballester, X. Bartoll, C. Daher, A. Deluca, C. Echave, C. Milà, S. Márquez, J. Palou, K. Pérez, C. Tonne, M. Stevenson, S. Rueda, and M. Nieuwenhuijsen. Changing the urban design of cities for health: The superblock model. *Environment International*, 134:105132, 2020. ISSN 0160-4120. doi: https://doi.org/10.1016/j.envint.2019.105132.

E. Negrenti. The 'corrected average speed' approach in enea's tee model: an innovative solution for the evaluation of the energetic and environmental impacts of urban transport policies. *Science of The Total Environment*, 235(1):411–413, 1999. ISSN 0048-9697. doi: https://doi.org/10.1016/S0048-9697(99)00249-1.

K. Nesamani, L. Chu, M. G. McNally, and R. Jayakrishnan. Estimation of vehicular emissions by capturing traffic variations. *Atmospheric Environment*, 41(14):2996–3008, 2007. ISSN 1352-2310. doi: https://doi.org/10.1016/j.atmosenv.2006.12.027.

M. J. Nieuwenhuijsen. New urban models for more sustainable, liveable and healthier cities post covid19; reducing air pollution, noise and heat island effects

and increasing green space and physical activity. *Environment International*, 157:106850, 2021. ISSN 0160-4120. doi: https://doi.org/10.1016/j.envint.2021.106850.

NOAA. Global Forecast System (GFS) Atmospheric Model, 2011. URL https://www.ncdc.noaa.gov/data-access/model-data/model-datasets/global-forcast-system-gfs. Last Access: August 2020.

U. of Florida. TRANSYT-7F (T7F), 2021. URL https://mctrans.ce.ufl.edu/hcs/t7f/. Last Access: May 2020.

OpenStreetMap contributors. Planet dump retrieved from https://planet.osm.org , 2019. URL https://www.openstreetmap.org. Last Access: September 2021.

Paramics. 3D traffic simulation, 2021. URL https://mctrans.ce.ufl.edu/hcs/t7f/. Last Access: March 2019.

R. Parra, P. Jiménez, and J. Baldasano. Development of the high spatial resolution emicat2000 emission model for air pollutants from the north-eastern iberian peninsula (catalonia, spain). *Environmental Pollution*, 140(2):200–219, 2006. ISSN 0269-7491. doi: https://doi.org/10.1016/j.envpol.2005.07.021.

M. Pay, M. Piot, O. Jorba, S. Gassó, M. Gonçalves, S. Basart, D. Dabdub, P. Jiménez-Guerrero, and J. Baldasano. A full year evaluation of the caliope-eu air quality modeling system over europe for 2004. *Atmospheric Environment*, 44(27):3322–3342, 2010. ISSN 1352-2310. doi: https://doi.org/10.1016/j.atmosenv.2010.05.040.

M. T. Pay, F. Martínez, M. Guevara, and J. M. Baldasano. Air quality forecasts on a kilometer-scale grid over complex spanish terrains. *Geoscientific Model Development*, 7(5):1979–1999, 2014. doi: 10.5194/gmd-7-1979-2014. URL https://gmd.copernicus.org/articles/7/1979/2014/.

M. T. Pay, G. Gangoiti, M. Guevara, S. Napelenok, X. Querol, O. Jorba, and C. Pérez García-Pando. Ozone source apportionment during peak summer events over southwestern europe. *Atmospheric Chemistry and Physics*, 19 (8):5467–5494, 2019. doi: 10.5194/acp-19-5467-2019. URL https://acp.copernicus.org/articles/19/5467/2019/.

J. Pérez, J. M. de Andrés, R. Borge, D. de la Paz, J. Lumbreras, and E. Rodríguez. Vehicle fleet characterization study in the city of Madrid and its application as a support tool in urban transport and air quality policy development. *Transport Policy*, 74(December 2017):114–126, 2019. ISSN 1879310X. doi: 10.1016/j.tranpol.2018.12.002. URL https://doi.org/10.1016/j.tranpol.2018.12.002.

E. Pisoni, P. Christidis, P. Thunis, and M. Trombetti. Evaluating the impact of "sustainable urban mobility plans" on urban background air quality. *Journal of Environmental Management*, 231:249–255, 2019. ISSN 0301-4797. doi: https://doi.org/10.1016/j.jenvman.2018.10.039.

PNOA. Ministerio de transportes, movilidad y agenda urbana: Lidar, 2020. URL https://pnoa.ign.es/productos_lidar. Last Access: August 2020.

Port de Barcelona. RePort, 2017. URL http://www.portdebarcelona.cat/en/web/el-port/report. Last access: March 2017.

S. Prakash and T. A. Bodisco. An investigation into the effect of road gradient and driving style on NOX emissions from a diesel vehicle driven on urban roads. *Transportation Research Part D: Transport and Environment*, 72:220–231, 2019. ISSN 13619209. doi: 10.1016/j.trd.2019.05.002. URL https://doi.org/10.1016/j.trd.2019.05.002.

PTV Group. PTV VISUM 18 Manual, 2019. URL http://vision-traffic.ptvgroup.com/en-uk/\products/ptv-vissim/use-cases/emissions-modelling/. Last Access: November 2021.

C. Pérez, M. Sicard, O. Jorba, A. Comerón, and J. M. Baldasano. Summertime re-circulations of air pollutants over the north-eastern iberian coast observed from systematic earlinet lidar measurements in barcelona. *Atmospheric Environment*, 38(24):3983–4000, 2004. ISSN 1352-2310. doi: https://doi.org/10.1016/j.atmosenv.2004.04.010. Includes Special Issue Section on Results from the Austrian Project on Health Effects of Particulates (AUPHEP).

Z. Qiu and X. Li. At-grade intersection configuration influences on pedestrian exposure to pm2.5. *Clean Technologies and Environmental Policy*, 17, 05 2015. doi: 10.1007/s10098-015-0975-0.

C. Quaassdorff, R. Borge, J. Pérez, J. Lumbreras, D. de la Paz, and J. M. de Andrés. Microscale traffic simulation and emission estimation in a heavily trafficked roundabout in Madrid (Spain). *Science of the Total Environment*, 566-567:416–427, 2016. ISSN 18791026. doi: 10.1016/j.scitotenv.2016.05.051.

H. Rakha, K. Ahn, and A. Trani. Development of vt-micro model for estimating hot stabilized light duty vehicle and truck emissions. *Transportation Research Part D: Transport and Environment*, 9(1):49–74, 2004. ISSN 1361-9209. doi: https://doi.org/10.1016/S1361-9209(03)00054-3.

H. Rakha, H. Yue, and F. Dion. Vt-meso model framework for estimating hot-stabilized light-duty vehicle fuel consumption and emission rates. *Canadian Journal of Civil Engineering*, 38, 11 2011. doi: 10.1139/l11-086.

R. Ramos, V. Cantillo, J. Arellana, and I. Sarmiento. From restricting the use of cars by license plate numbers to congestion charging: Analysis for medellin, colombia. *Transport Policy*, 60:119–130, 2017. ISSN 0967-070X. doi: https://doi.org/10.1016/j.tranpol.2017.09.012.

N. Ratrout, S. M. Rahman, and K. Box. A comparative analysis of currently used microscopic and macroscopic traffic simulation software. *The Arabian Journal for Science and Engineering*, 34, 05 2009. ISSN 1319-8025. URL https://inis.iaea.org/search/searchsinglerecord.aspx?recordsFor=SingleRecord&RN=40088987.

M. Rexeis and S. Hausberger. Trend of vehicle emission levels until 2020 - Prognosis based on current vehicle measurements and future emission legislation. *Atmospheric Environment*, 43(31):4689–4698, 2009. ISSN 13522310. doi: 10.1016/j.atmosenv.2008.09.034. URL http://dx.doi.org/10.1016/j.atmosenv.2008.09.034.

D. Rodriguez-Rey, M. Guevara, M. P. Linares, J. Casanovas, J. Salmerón, A. Soret, O. Jorba, C. Tena, and C. Pérez García-Pando. A coupled macroscopic traffic and pollutant emission modelling system for barcelona. *Transportation Research Part D: Transport and Environment*, 92:102725, 2021. ISSN 1361-9209. doi: https://doi.org/10.1016/j.trd.2021.102725.

D. Rojas-Rueda, A. de Nazelle, O. Teixidó, and M. Nieuwenhuijsen. Replacing car trips by increasing bike and public transport in the greater barcelona metropolitan area: A health impact assessment study. *Environment International*, 49:100–109, 2012. ISSN 0160-4120. doi: https://doi.org/10.1016/j.envint.2012.08.009.

F. Romero, J. Gomez, T. Rangel, and J. M. Vassallo. Impact of restrictions to tackle high pollution episodes in madrid: Modal share change in commuting corridors. *Transportation Research Part D: Transport and Environment*, 77: 77–91, 2019. ISSN 1361-9209. doi: https://doi.org/10.1016/j.trd.2019.10.021.

S. Rueda. *Superblocks for the Design of New Cities and Renovation of Existing Ones: Barcelona's Case*, pages 135–153. Springer International Publishing, Cham, 2019. ISBN 978-3-319-74983-9. doi: 10.1007/978-3-319-74983-9_8. URL https://doi.org/10.1007/978-3-319-74983-9_8.

R. San Jose, J. Camaño, L. Pérez, and R. Barras. A health impact assessment of traffic restrictions during madrid no2 episode. *IOP Conference Series: Earth and Environmental Science*, 182:012003, 09 2018. doi: 10.1088/1755-1315/182/1/012003.

Seinfeld and Pandis. *Atmospheric Chemistry and Physics: From Air Pollution to Climate Change*. Willey, 3rd edition edition, 2016. ISBN 978-1-118-94740-1. URL https://www.wiley.com/en-us/Atmospheric+Chemistry+and+Physics%3A+From+Air+Pollution+to+Climate+Change%2C+3rd+Edition-p-9781118947401. Last Access: April 2017.

A. Selmoune, Y. Du, Q. Cheng, and Z. Liu. Influencing factors in congestion pricing acceptability: A literature review. *Journal of Advanced Transportation*, 60:119–130, 2020. ISSN 0197-6729. doi: 10.1155/2020/4242964. URL https://doi.org/10.1155/2020/4242964.

D. T. Silverman, C. M. Samanic, J. H. Lubin, A. E. Blair, P. A. Stewart, R. Vermeulen, J. B. Coble, N. Rothman, P. L. Schleiff, W. D. Travis, R. G. Ziegler, S. Wacholder, and M. D. Attfield. The Diesel Exhaust in Miners Study: A Nested Case–Control Study of Lung Cancer and Diesel Exhaust. *JNCI: Journal of the National Cancer Institute*, 104(11):855–868, 06 2012. ISSN 0027-8874. doi: 10.1093/jnci/djs034. URL https://doi.org/10.1093/jnci/djs034.

A. Sjodin, J. Borken-Kleefeld, D. Carslaw, J. Tate, G.-M. Alt, J. Fuente, Y. Bernard, U. Tietge, P. Mcclintock, R. Gentala, N. Vescio, and S. Hausberger. Real-driving emissions from diesel passenger cars - remote sensing meaurements compared with pems and chassis dynamometer. Technical report, 05 2018. Last Access: September 2019.

W. C. Skamarock and J. B. Klemp. A time-split nonhydrostatic atmospheric model for weather research and forecasting applications. *Journal of Computational Physics*, 227(7):3465 – 3485, 2008. ISSN 0021-9991. doi: https://doi.org/10.1016/j.jcp.2007.01.037. Predicting weather, climate and extreme events.

R. Smit. Pap: A simulation tool for vehicle emissions and fuel consumption software with a high resolution in time and space. *Vehicle Technology Engineer, SAE Australasia*, pages 17–21, 01 2014. URL https://51431d88-662c-4884-b7bc-b5b93a225b7d.filesusr.com/ugd/d0bd25_f6100cc1abcf4c07b336a9bd289c095a.pdf.

R. Smit, R. Smokers, and E. Rabé. A new modelling approach for road traffic emissions: Versit+. *Transportation Research Part D: Transport and Environment*, 12(6):414–422, 2007. ISSN 1361-9209. doi: https://doi.org/10.1016/j.trd.2007.05.001.

M. G. Snyder, A. Venkatram, D. K. Heist, S. G. Perry, W. B. Petersen, and V. Isakov. Rline: A line source dispersion model for near-surface releases. *Atmospheric Environment*, 77:748 – 756, 2013. ISSN 1352-2310. doi: https://doi.org/10.1016/j.atmosenv.2013.05.074.

G. Song, L. Yu, and Y. Zhang. Applicability of Traffic Microsimulation Models in Vehicle Emissions Estimates. *Transportation Research Record: Journal of the Transportation Research Board*, 2270(January 2012):132–141, 2012. ISSN 0361-1981. doi: 10.3141/2270-16. URL http://trrjournalonline.trb.org/doi/10.3141/2270-16.

A. Soret, P. Jimenez–Guerrero, and J. M. Baldasano. Comprehensive air quality planning for the barcelona metropolitan area through traffic management. *Atmospheric Pollution Research*, 2(3):255–266, 2011. ISSN 1309-1042. doi: https://doi.org/10.5094/APR.2011.032.

A. Soret, M. Guevara, and J. Baldasano. The potential impacts of electric vehicles on air quality in the urban areas of barcelona and madrid (spain). *Atmospheric Environment*, 99:51–63, 2014. ISSN 1352-2310. doi: https://doi.org/10.1016/j.atmosenv.2014.09.048.

C. Soriano, J. Baldasano, W. Buttler, and K. Moore. Circulatory patterns of air pollutants within the barcelona air basin in a summertime situation: Lidar and numerical approaches. *Boundary-Layer Meteorology*, 98:33–55, 01 2001. doi: 10.1023/A:1018726923826.

A. Stevanovic, J. Stevanovic, K. Zhang, and S. Batterman. Optimizing traffic control to reduce fuel consumption and vehicular emissions: Integrated approach with vissim, cmem, and visgaost. *Transportation Research Record*, 2128(1):105–113, 2009. doi: 10.3141/2128-11. URL `https://doi.org/10.3141/2128-11`.

A. Stevanovic, J. Stevanovic, J. So, and M. Ostojic. Multi-criteria optimization of traffic signals: Mobility, safety, and environment. *Transportation Research Part C: Emerging Technologies*, 55:46–68, 2015. ISSN 0968-090X. doi: https://doi.org/10.1016/j.trc.2015.03.013. Engineering and Applied Sciences Optimization (OPT-i) - Professor Matthew G. Karlaftis Memorial Issue.

D. Tartakovsky, L. Kordova – Biezuner, E. Berlin, and D. M. Broday. Air quality impacts of the low emission zone policy in haifa. *Atmospheric Environment*, 232: 117472, 2020. ISSN 1352-2310. doi: https://doi.org/10.1016/j.atmosenv.2020.117472.

I. Thomson and A. Bull. La congestión del tránsito: Causas y consecuencias económicas y sociales. *Revista de la CEPAL*, 76: 109–121, 2002. URL `https://www.cepal.org/es/publicaciones/6381-la-congestion-transito-urbano-causas-consecuencias\-economicas-sociales`. Last Access: September 2020.

T. Tielert, M. Killat, H. Hartenstein, R. Luz, S. Hausberger, and T. Benz. The impact of traffic-light-to-vehicle communication on fuel consumption and emissions. In *2010 Internet of Things (IOT)*, pages 1–8, 2010. doi: 10.1109/IOT.2010.5678454.

A. Tiwary and J. Colls. *Air pollution: measurement, modelling & mitigation. Third edition*. 08 2009. ISBN 9781315272481. doi: 10.1201/9781315272481.

TMB. Transport Metropolità de Barcelona, 2019. URL https://www.tmb.cat/es/barcelona/autobuses/lineas. Last access: October 2019.

TMB. Basic data 2020, 2020. URL https://www.tmb.cat/documents/20182/94438/Dades+viatgers+bus+metro+2020{_}CA{_}EN/41aa4b84-420e-4fb0-adc9-3f3e3f87eb65. Last access: February 2020.

TomTom. TomTom, 2019. URL https://www.tomtom.com. Last access: November 2019.

N. Tsanakas, J. Ekström, and J. Olstam. Estimating Emissions from Static Traffic Models: Problems and Solutions. *Journal of Advanced Transportation*, 2020:1–17, 2020. ISSN 0197-6729. doi: 10.1155/2020/5401792.

R. Tu, I. Kamel, A. Wang, B. Abdulhai, and M. Hatzopoulou. Development of a hybrid modelling approach for the generation of an urban on-road transportation emission inventory. *Transportation Research Part D: Transport and Environment*, 62:604–618, 2018. ISSN 13619209. doi: 10.1016/j.trd.2018.04.011. URL https://doi.org/10.1016/j.trd.2018.04.011.

UNECE. Protocol to abate acidification, eutrophication and ground-level ozone, 1999. URL https://unece.org/environment-policyair/protocol-abate-acidification-eutrophication-and-ground-level-ozone. Last Access: June 2021.

United Nations. 2018 Revision of World Urbanization Prospects, 2018. URL https://www.un.org/development/desa/publications/2018-revision-of-world-urbanization-prospects.html. Last access: 2021-05.

U.S. EPA. User's guide to MOBILE 6.1 and MOBILE 6.2. Technical report, 2003. URL https://www.epa.gov/transportation-air-pollution-and-climate-change. Last Access: February 2019.

U.S. EPA. Motor vehicle emission simulator (moves): User guide for moves, 2014. URL https://www.epa.gov/moves. Last Access: February 2019.

UT Graz. Handbook of Emission Factors for Road Transport (HBEFA), 2019. URL https://www.hbefa.net/e/index.html. Last Access: March 2020.

A. Valencia, A. Venkatram, D. Heist, D. Carruthers, and S. Arunachalam. Development and evaluation of the r-line model algorithms to account for chemical transformation in the near-road environment. *Transportation Research Part D: Transport and Environment*, 59:464 – 477, 2018. ISSN 1361-9209. doi: https://doi.org/10.1016/j.trd.2018.01.028.

E. von Schneidemesser, F. Kuik, K. A. Mar, and T. Butler. Potential reductions in ambient NO 2 concentrations from meeting diesel vehicle emissions standards. *Environmental Research Letters*, 12(11):114025, nov 2017. doi: 10.1088/1748-9326/aa8c84. URL https://doi.org/10.1088/1748-9326/aa8c84.

J. G. Wardrop and J. I. Whitehead. Some theoretical aspects of road traffic research. *Proceedings of the Institution of Civil Engineers*, 1(5):767–768, 1952. doi: 10.1680/ipeds.1952.11362. URL https://doi.org/10.1680/ipeds.1952.11362.

WHO. Review of evidence on health aspects of air pollution – REVIHAAP project: final technical report. Technical report, World Health Organisation, 2013. URL https://www.euro.who.int/__data/assets/pdf_file/0004/193108/REVIHAAP-Final-technical-report-final-version.pdf. Last Access: May 2021.

WHO. Ambient (outdoor) air pollution, 2018. URL https://www.who.int/en/news-room/fact-sheets/detail/ambient-(outdoor)-air-quality-and-health. Last access: May 2021.

WHO. Who global air quality guidelines: Particulate matter (pm2.5 and pm10), ozone, nitrogen dioxide, sulfur dioxide and carbon monoxide, 2021. Last Access: October 2021.

M. Williams. *Chapter 7 The Policy Response to Improving Urban Air Quality*, volume 28. The Royal Society of Chemistry, 2009. ISBN 978-1-84755-907-

4. doi: 10.1039/9781847559654-00129. URL http://dx.doi.org/10.1039/9781847559654-00129.

L. Wismans, R. van den Brink, L. Brederode, K. Zantema, and E. van Berkum. Comparison of estimation of emissions based on static and dynamic traffic assignment models. In *92th Annual Meeting of the Transportation Research Board*, pages 1689–1699, Washington, 2013. ISBN 9788578110796. doi: 10.1017/CBO9781107415324.004.

D. W. Wyatt, H. Li, and J. E. Tate. The impact of road grade on carbon dioxide (CO2) emission of a passenger vehicle in real-world driving. *Transportation Research Part D: Transport and Environment*, 32:160–170, 2014. ISSN 13619209. doi: 10.1016/j.trd.2014.07.015.

S. Zegeye, B. De Schutter, J. Hellendoorn, and E. Breunesse. Integrated macroscopic traffic flow and emission model based on METANET and VT-micro. In G. Fusco, editor, *Models and Technologies for Intelligent Transportation Systems* (Proceedings of the International Conference on Models and Technologies for Intelligent Transportation Systems, Rome, Italy, June 2009), pages 86–89. Aracne Editrice, Rome, Italy, 2010. URL https://www.dcsc.tudelft.nl/~bdeschutter/pub/rep/09_017.pdf. Last Access: March 2019.

K. Zhang, S. Batterman, and F. Dion. Vehicle emissions in congestion: Comparison of work zone, rush hour and free-flow conditions. *Atmospheric Environment*, 45 (11):1929–1939, 2011. ISSN 13522310. doi: 10.1016/j.atmosenv.2011.01.030. URL http://dx.doi.org/10.1016/j.atmosenv.2011.01.030.

Y. Zhang and P. A. Ioannou. Environmental impact of combined variable speed limit and lane change control: A comparison of moves and cmem model. *IFAC-PapersOnLine*, 49(3):323–328, 2016. ISSN 2405-8963. doi: https://doi.org/10.1016/j.ifacol.2016.07.054. 14th IFAC Symposium on Control in Transportation SystemsCTS 2016.

X. Zhou, S. Tanvir, H. Lei, J. Taylor, B. Liu, N. M. Rouphail, and H. C. Frey. Integrating a simplified emission estimation model and mesoscopic dynamic traffic simulator to efficiently evaluate emission impacts of traffic management strategies. *Transportation Research Part D: Transport and Environ-*

ment, 37:123–136, 2015. ISSN 13619209. doi: 10.1016/j.trd.2015.04.013. URL http://dx.doi.org/10.1016/j.trd.2015.04.013.

Appendices

A. Model evaluation in urban background sites

We complement the evaluation of the system considering all the monitoring sites measuring NO_2 in Barcelona for the period of study (Fig. A.1). Table A.1 shows the performance statistics for CALIOPE-Urban (20m) and CALIOPE (1km) and Fig. A.2 shows the average daily cycle. We find that both models behave similarly at the urban background stations and tend to slightly underestimate NO_2 concentrations, mostly at the valley hours (e.g., 12:00) consistently with the two traffic representative stations shown in Chapter 5.

Table A.1: NO_2 model evaluation statistics calculated at the urban background sites measuring NO_2 not shown in the manuscript during the study period for CALIOPE (1km) and CALIOPE-Urban (20m).

Site	Model	FAC2	MB	RMSE	r
Palau Reial	CALIOPE	0,60	-13,92	29,87	0,53
	CALIOPE-Urban	0,65	-7,87	27,27	0,54
Valll d'Hebrón	CALIOPE	0,65	-15,67	27,98	0,58
	CALIOPE -Urban	0,63	-17,06	29,5	0,55
Ciudatella	CALIOPE	0,85	0,79	23,49	0,59
	CALIOPE -Urban	0,83	-3,46	23,8	0,59
Sants	CALIOPE	0,75	-11,3	27,86	0,58
	CALIOPE -Urban	0,69	-13,07	29,44	0,54
Poblenou	CALIOPE	0,81	-13,5	26,19	0,69
	CALIOPE -Urban	0,79	-14,14	26,56	0,69

Figure A.1: Location of the official air quality monitoring network in Barcelona. The map represents traffic (red), suburban background (orange) and urban background (green) stations. The boxes in purple represent the stations that measure NO_2. Adapted from ASPB (2020).

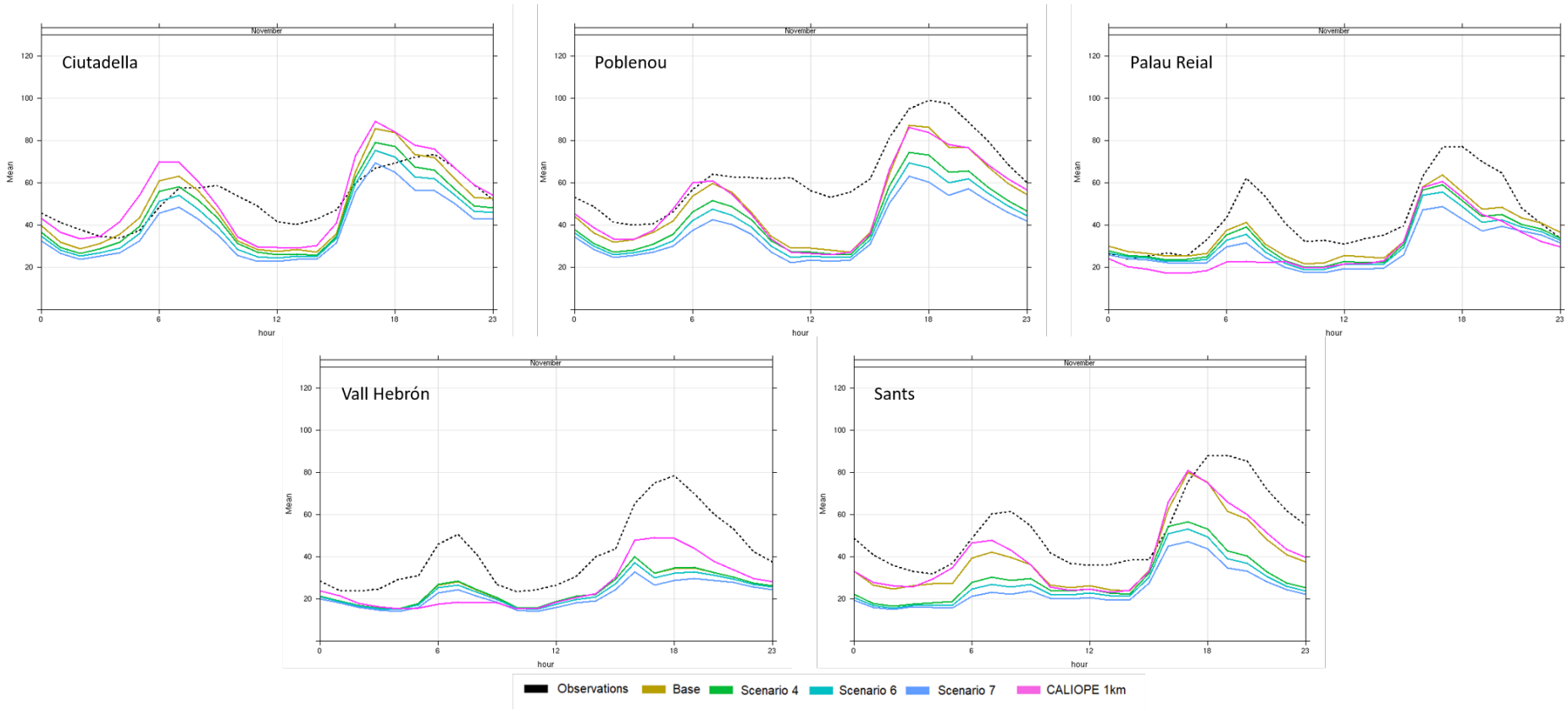

Figure A.2: NO_2 average daily cycle at the urban background sites measuring NO_2 not shown in the manuscript during the study period (7-25th November 2017). Observations are represented as dotted back lines, CALIOPE-Urban (20m) and CALIOPE (1km) for the Base Case scenario are represented in brown and pink, respectively. The simulated scenario 4, scenario 6 and scenario 7 are represented in green, sky blue and blue, respectively.

B. Description of measures applied for the Tactical Urban Planning (TUP) scenario

We describe here all the modifications performed on the network for the Tactical Urban Planning scenario (TUP). We describe the affected street, the specific segments modified and the number of lanes and speed limit modifications.

- Sants and Creu Coberta: reduction of 1 lane per direction. Speed limit from 50km/h to 30km/h.
- Via Laietana: Reduction from several to 1 lane.
- Rocafort (from Gran via to Av. Roma): reduction of 1 lane. Speed limit from 50km/h to 30km/h.
- Girona (from Gran Via to Diagonal): reduction of 1 lane. Speed limit from 50km/h to 30km/h.
- Consell de Cent (from Rocafort to Urgell): reduction of 1. Speed limit from 50km/h to 30km/h.
- Consell de Cent (from Urgell to Girona): reduction of 2 lanes. Speed limit from 50km/h to 30km/h.
- València (from Meridiana to Tarragona): reduction of 1 lane.
- Roger de Llúria (from Diagonal to pl. Urquinaona): reduction of 1 lane.
- Pau Clarís (from Diagonal to pl. Urquinaona): reduction of 1 lane.
- Castillejos (from Consell de Cent to St Antoni Maria Claret): reduction of 1 lane.
- Indústria (from Bailén to Castillejos): reduction of 1 lane.
- Aragó (from Meridiana to Tarragona): reduction of 1 lane.

- Aragó (from Sicília to Muntaner): reduction of 1 lane (total lanes reduced on this section: 2).
- Pssg. Zona Franca (from pl. Cerdà to Motors): reduction of 1 lane per direction.
- Pelai (from Balmes to Rambla Catalunya): reduction of 2 lanes.
- Gran Via (from pssg. De Gràcia to Marina): reduction of 1 lane.
- Ronda Universitat: reduction of 2 lanes.

Modifications based on:

Ajuntament de Barcelona, Una Mobilitat sostenible en un nou Espai Públic. (2020b)

Ajuntament de Barcelona, Una Mobilitat sostenible en un nou Espai Públic - Fase 2. (2020c).

C. Description of measures applied for the Superblocks (SPB) scenario

In this section we show the eight superblocks applied in the network: Girona, Poblenou, St. Antoni, Consell de Cent, Les Corts, Sants, St. Gervasi and Horta. The green dotted line segments on the Fig. C.1 were modified with a speed limit of 10 km/h and a vehicle capacity of 300 vehicles/hour. Additionally, specific turnings were applied were needed.

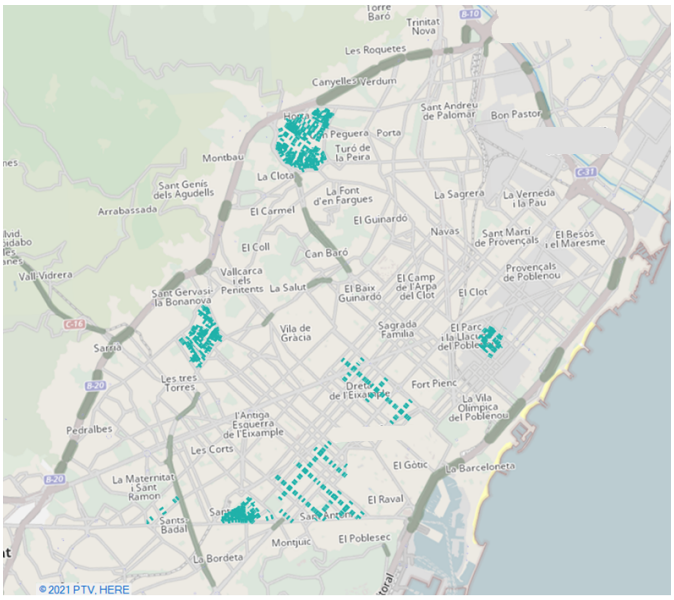

Figure C.1: Screenshot of the VISUM traffic simulator with the Superblocks implemented shown as green lines.